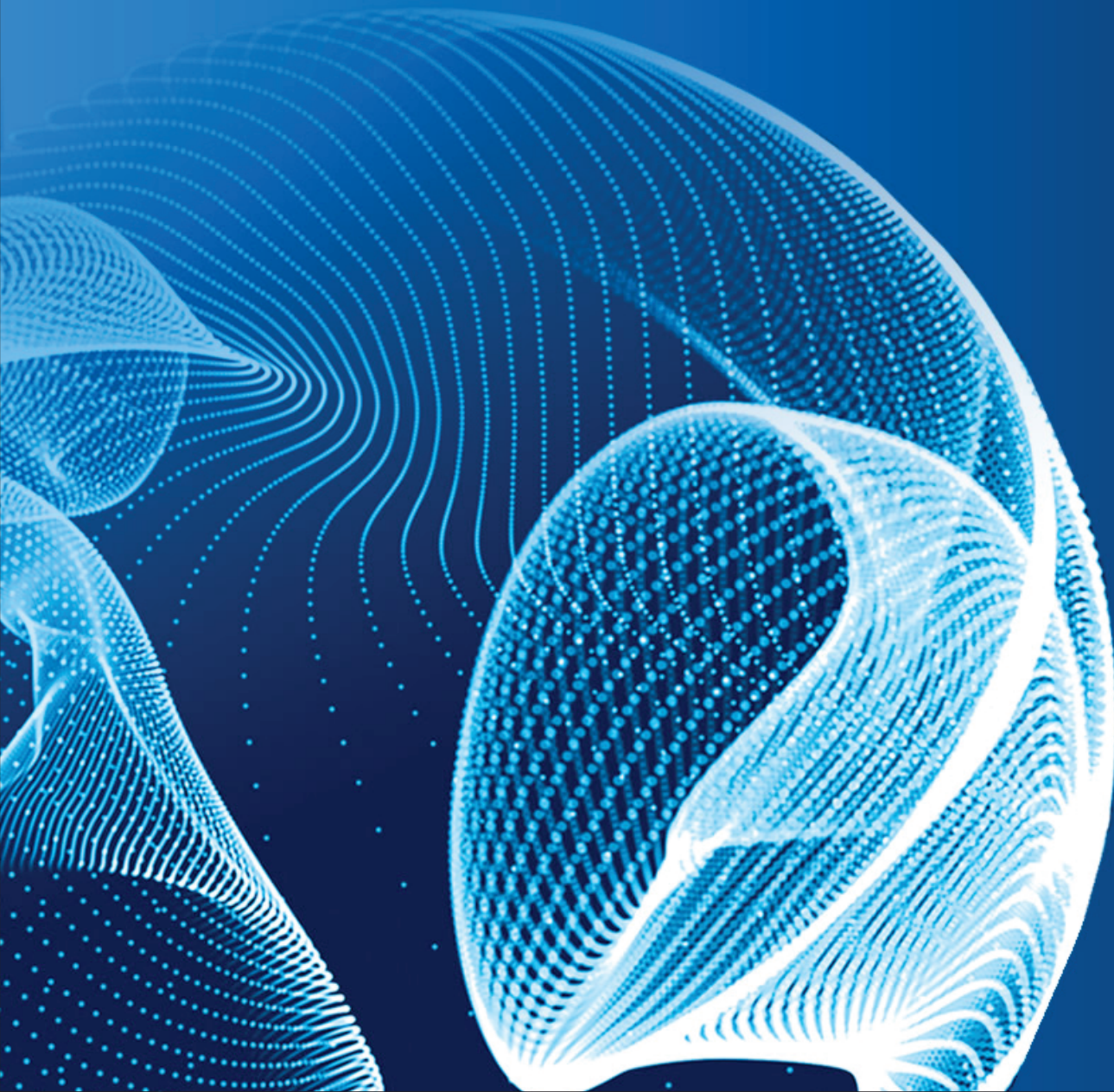


# ENGINEERING JOURNAL of Satbayev University

Volume 147 (Issue 1)  
February 2025



**EDITOR-IN-CHIEF**

**Alma Bekbotayeva**, PhD, associate professor, Geology and Petroleum Engineering Institute of Satbayev University, Kazakhstan

**DEPUTY EDITOR-IN-CHIEF**

**Kanai Rysbekov**, candidate of technical sciences, associate professor, Mining and Metallurgical Institute of Satbayev University, Kazakhstan

**Vasyl Lozinskyi**, PhD, associate professor, National TU Dnipro Polytechnic, Ukraine

**MANAGING EDITOR**

**Gulziya Burshukova**, PhD, associate professor, Satbayev University, Kazakhstan

**MEMBERS OF THE EDITORIAL BOARD**

**Ata Utku Akçil**, PhD, professor, Suleyman Demirel University, Turkey

**Adilkhan Baibatsha**, doctor of geological and mineralogical sciences, professor, Geology and Petroleum Engineering Institute of Satbayev University, Kazakhstan

**Atac Bascetin**, PhD, professor, Istanbul Technical University, Turkey

**Madina Barmenshinova**, candidate of technical sciences, associate professor, Mining and Metallurgical Institute of Satbayev University, Kazakhstan

**Omirsirik Baigenzhanov**, PhD, associate professor, Mining and Metallurgical Institute of Satbayev University, Kazakhstan

**Tatiana Chepushtanova**, PhD, associate professor, Mining and Metallurgical Institute of Satbayev University, Kazakhstan

**Agata Duczmal-Czernikiewicz**, PhD, habilit.doctor, professor, Adam Mickiewicz University, Poland

**Serik Moldabaev**, doctor of technical sciences, professor, Mining and Metallurgical Institute of Satbayev University, Kazakhstan

**Brajendra Mishra**, PhD, professor, Worcester Polytechnic Institute, USA

**Suping Peng**, professor, academician, Chinese Mining University, China

**Reimar Seltsmann**, PhD, professor, The Earth Sciences Department, Center for Russian and Central Asian Mineral Research (CERCAMS), Great Britain

**Atsushi Shibayama**, PhD, professor, Akita University, Japan

**Olena Sdvyzhkova**, doctor of technical sciences, professor, National TU Dnipro Polytechnic, Ukraine

**Khalidilla Yusupov**, doctor of technical sciences, professor, Mining and Metallurgical Institute of Satbayev University, Kazakhstan

## БАС ҒЫЛЫМИ РЕДАКТОР

**Алма Бекботаева**, PhD, қауымдастырылған профессор, Satbayev University Геология және мұнай-газ ісі институты, Қазақстан

## БАС ҒЫЛЫМИ РЕДАКТОРДЫҢ ОРЫНБАСАРЛАРЫ

**Қанай Рысбеков**, т.ғ.к., қауымдастырылған профессор, Satbayev University Тау-кен-металлургия институты, Қазақстан

**Василий Лозинский**, PhD, қауымдастырылған профессор, «Днепр политехникасы» Ұлттық техникалық университеті, Украина

## ЖАУАПТЫ ХАТШЫ

**Гулзия Буршукова**, PhD, қауымдастырылған профессор, Satbayev University, Қазақстан

## РЕДАКЦИЯЛЫҚ АЛҚА МҮШЕЛЕРІ

**Ata Utku Akçil**, PhD, профессор, Сүлейман Демирел Университеті, Түркия

**Әділхан Байбатша**, г-м.ғ.д., профессор, Satbayev University Геология және мұнай-газ ісі институты, Қазақстан

**Atac Bascetin**, PhD, профессор, Ыстамбұл техникалық университеті, Түркия

**Мадина Барменшинова**, т.ғ.к., қауымдастырылған профессор, Satbayev University Тау-кен-металлургия институты, Қазақстан

**Өмірсерік Байгенженов**, PhD, қауымдастырылған профессор, Satbayev University Тау-кен-металлургия институты, Қазақстан

**Татьяна Чепуштанова**, PhD, қауымдастырылған профессор, Satbayev University Тау-кен-металлургия институты, Қазақстан

**Agata Duczmal-Czernikiewicz**, PhD, хабилит.доктор, профессор, Адам Мицкевич Университеті, Польша

**Серік Молдабаев**, т.ғ.д., профессор, Satbayev University Тау-кен-металлургия институты, Қазақстан

**Brajendra Mishra**, PhD, профессор, Вустер политехникалық институты, АҚШ

**Suping Peng**, профессор, академик, Қытай тау-кен университеті, ҚХР

**Reimar Seltmann**, PhD, профессор, Жер туралы ғылымдар бөлімі, Ресей және Орта Азия минералды зерттеулер орталығы (CERCAMS), Ұлыбритания

**Atsushi Shibayama**, PhD, профессор, Akita University, Жапония

**Олена Сдвижкова**, т.ғ.д., профессор, «Днепр политехникасы» Ұлттық техникалық университеті, Украина

**Халидилла Юсупов**, т.ғ.д., профессор, Satbayev University Тау-кен-металлургия институты, Қазақстан

## ГЛАВНЫЙ НАУЧНЫЙ РЕДАКТОР

**Алма Бекботаева**, PhD, асоц.профессор, Институт геологии и нефтегазового дела Satbayev University, Казахстан

## ЗАМЕСТИТЕЛИ ГЛАВНОГО НАУЧНОГО РЕДАКТОРА

**Канай Рысбеков**, к.т.н., асоц.профессор, Горно-металлургический институт Satbayev University, Казахстан

**Василий Лозинский**, PhD, асоц.профессор, Национальный технический университет «Днепровская политехника», Украина

## ОТВЕТСТВЕННЫЙ СЕКРЕТАРЬ

**Гулзия Буршукова**, PhD, асоц.профессор, Satbayev University, Казахстан

## ЧЛЕНЫ РЕДАКЦИОННОЙ КОЛЛЕГИИ

**Ata Utku Akçil**, PhD, профессор, Университет Сулеймана Демиреля, Турция

**Адилхан Байбатша**, д.г-м.н., профессор, Институт геологии и нефтегазового дела Satbayev University, Казахстан

**Atac Bascetin**, PhD, профессор, Стамбульский технический университет, Турция

**Мадина Барменшинова**, к.т.н., Горно-металлургический институт Satbayev University, Казахстан

**Омирсерик Байгенженов**, PhD, асоц.профессор, Горно-металлургический институт Satbayev University, Казахстан

**Татьяна Чепуштанова**, PhD, асоц.профессор, Горно-металлургический институт Satbayev University, Казахстан

**Agata Duczmal-Czernikiewicz**, PhD, хабилит.доктор, профессор, Университет Адама Мицкевича, Польша

**Серик Молдабаев**, д.т.н., профессор, Горно-металлургический институт Satbayev University, Казахстан

**Brajendra Mishra**, PhD, профессор, Вустерский политехнический институт, США

**Suping Peng**, профессор, академик, Китайский горнопромышленный университет, КНР

**Reimar Selmann**, PhD, профессор, Отдел Наук о Земле, Центр Российских и Среднеазиатских Минеральных Исследований (CERCAMS), Великобритания

**Atsushi Shibayama**, PhD, профессор, Akita University, Япония

**Олена Сдвижкова**, д.т.н., профессор, Национальный технический университет «Днепровская политехника», Украина

**Халидилла Юсупов**, д.т.н., профессор, Горно-металлургический институт Satbayev University, Казахстан

<https://doi.org/10.51301/ejsu.2025.i1.01>

## Economic analysis of the processing of various titanium-containing raw materials to obtain titanium, vanadium, and niobium

T.K. Sarsembekov, T.A. Chepushtanova, E.S. Merkitabeyev\*

Satbayev University, Almaty, Kazakhstan

\*Corresponding author: [y.merkibayev@satbayev.university](mailto:y.merkibayev@satbayev.university)

**Abstract.** This work presents an economic analysis of processing various titanium-containing raw materials-titanium slag and synthetic rutile-through chlorination in a molten salt medium in the presence of carbon. The processing of titanium-containing raw materials is carried out using a chlorination technology in molten alkali metal salts ( $MgCl_2$ ,  $NaCl$ ,  $KCl$ ) with high-concentration gaseous chlorine in the presence of a carbon-containing reducing agent. Anthracite is used as the reducing agent, while waste sludge from magnesium electrolysis is used as the molten medium. The processing takes place in cylindrical chlorination furnaces lined with fireclay bricks at temperatures of 720-800°C. The chlorination products are directed to a condensation system. The work provides a description of the Satpayev ilmenite deposit in East Kazakhstan and presents the chemical composition of Satpayev ilmenite concentrate, titanium slag, and synthetic rutile obtained through various processes. A correlation is established between the vanadium, niobium, and tantalum content in ilmenite concentrates and their prevalence in the Earth's crust. Based on this correlation, the order of transition metals in Group V of the periodic table is determined according to their decreasing concentration in the concentrates. Technological challenges associated with processing titanium-containing raw materials with elevated levels of certain components are described, along with some methods for producing synthetic rutile. A cost comparison is provided for the production of titanium slag and synthetic rutile. Material balance calculations for the chlorination process of titanium slag and synthetic rutile from different production methods are performed to assess raw material costs and waste disposal expenses. The study concludes that producing synthetic rutile from Satpayev ilmenite concentrate is economically feasible.

**Keywords:** *slag, rutile, costs, processing, chlorination, waste.*

Received: 06 November 2024

Accepted: 14 February 2025

Available online: 28 February 2025

### 1. Introduction

Ilmenite is the most important raw material source for the global titanium industry. Large ilmenite deposits are found in India (Kerala, Ceylon), the USA (Florida), Brazil, Russia, Ukraine, and other countries [1]. The physicochemical and mineralogical properties of ilmenite are well studied [2,3]. Various methods exist for enriching and processing ilmenite, including direct reduction methods [4]. However, the most common method is reductive ore-thermal smelting, which produces a titanium-enriched product-titanium slag and pig iron, which is used in industrial enterprises. An alternative method for processing ilmenite concentrate is thermochemical treatment to produce synthetic rutile. Examples include the sulfiding process and carbothermal reduction [5].

In the Republic of Kazakhstan, three titanium-zirconium sand deposits have been developed in the Aktobe (Shokash), Akmola (Obukhov), and East Kazakhstan (Satpayev-Bektimir) regions [6]. The Satpayev deposit has been prioritized as the most promising and the closest to the processing plant. This deposit is located 200 km from Ust-Kamenogorsk.

The Satpayev ilmenite placer was discovered in 1989 during preliminary geophysical and geochemical studies. It was formed by the reworking of the ore-bearing weathering crust of the Karaotkel deposit [7]. The placer is located in the southwestern frame of the Preobrazhensky granitoid massif of the Buransky complex. Subordinate rock formations include the Maksut gabbroids and the Kunush granites, with fragmentary outcrops of the Bukon and Maitubin suites also noted [8].

The placer is of alluvial origin, with a productive sand-clay horizon of presumed pre-Neogene age lying on weathered crusts or bedrock [8]. The deposit consists of three alluvial (buried) placers of Oligocene age [7]. The channel width varies from 100 to 650 meters, the total explored length is 7,250 meters, and the thickness of ore sands ranges from 4 to 11 meters. The ore minerals are primarily ilmenite (90-97%) and zircon, with occasional occurrences of rutile, anatase, and leucoxene. The average ilmenite content in ore-bearing horizons is 151 kg/m<sup>3</sup>. The balance reserves of the placer are as follows: ore sands – 12,053 thousand m<sup>3</sup>, ilmenite-1,821 thousand tons [8].

## 2. Materials and methods

The ilmenite concentrates from the Satpayev deposit, as a raw material for titanium slag production with subsequent processing using chloride technology, has several significant drawbacks, including high levels of iron and silicon oxides. However, one advantage of this raw material is its relatively low vanadium content and the presence of rare-earth elements (vanadium, scandium, niobium) that can be extracted as by-products.

A comparison of ilmenite compositions from different sources revealed that the most significant difference between the Vilnohirska (Ukraine) ilmenite concentrate and the one from Kazakhstan is the higher degree of weathering of the Ukrainian ores, as indicated by the almost complete absence of Fe<sup>2+</sup>. This is likely the reason for the lower vanadium and niobium content, indirectly suggesting that niobium and tantalum were initially associated with Fe<sup>2+</sup> but were lost during geological transformations.

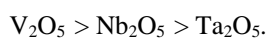
Spectral analysis of the chemical composition of the initial titanium-containing materials showed that the Vilnohirska ilmenite concentrate contains nearly 1.7 times more vanadium pentoxide and 1.6 times more niobium pentoxide than the Kazakhstani concentrate.

A correlation has been established between the content of vanadium, niobium, and tantalum in ilmenite concentrates and their abundance in the Earth's crust, in weight percent:

- V –  $2.0 \times 10^{-2}$ ;
- Nb –  $3.2 \times 10^{-5}$ ;
- Ta –  $2.4 \times 10^{-5}$

It should be noted that vanadium group elements form the most stable compounds in the pentavalent state, as they achieve a stable electron configuration with eight electrons after losing five from their outermost and penultimate orbitals. As the atomic number increases, the tendency of these elements to exhibit valency lower than five decreases.

According to the identified pattern, the transition metals of Group V (secondary subgroup) in the periodic table are arranged in the following order based on their decreasing concentration in the ilmenite concentrates:



Vanadium, niobium, and tantalum, considering their fractional percentage content, are present in ilmenite concentrates as isomorphous impurities in titanium minerals.

Scanning electron microscopy (SEM) of localized surface areas of polished sections from the Obukhov ilmenite concentrate has provided micrographs that illustrate the morphology, association characteristics, and elemental composition

of mineral aggregates and individual mineral grains. These micrographs reveal isomorphous vanadium impurities in rutile and leucosene grains, where vanadium replaces trivalent iron ions during the natural decomposition of ilmenite.

Isomorphous impurities of niobium and tantalum in titanium minerals, as well as rare-earth elements from the cesium and yttrium groups present in the Obukhov ilmenite concentrate (OIC), were not detected due to their low concentration and the insufficient resolution of our JEOL JXA-8230 scanning electron microanalyzer from the Japanese company JEOL.

## 3. Results and discussion

Below are micrographs of rutile and leucosene grains from the Obukhov ilmenite concentrate with isomorphous vanadium impurities (Figure 1). Further below, Table 1 presents the results of the balance distribution and extraction analysis of titanium, iron, vanadium, and niobium in the products of reductive electro-smelting of charge mixtures from the Vilnohirska and Satpayev ilmenite concentrates with anthracite. Table 2 provides the chemical composition of the Satpayev ilmenite concentrate.

Due to the high content of iron oxides in the pyrometallurgical smelting of the Satpayev ilmenite concentrate, the following challenges arise:

- increased cost of titanium slag due to higher consumption of electrical energy, carbon-containing reductant, and electrodes;
- furnace clogging with accretions, leading to a reduction in the furnace bath volume and decreased productivity;
- exposure of the furnace lining in the upper part of the bath.

As a result of these challenges, titanium slag production is carried out using a mixture of ilmenite concentrates from the Satpayev (Kazakhstan) and Vilnohirska (Ukraine) deposits in various proportions. The most technologically and economically optimal ratios are Vilnohirska/Satpayev – 60/40% and 65/35%.

At the same time, several technologies for producing synthetic rutile from ilmenite concentrate have been developed and are mainly applied abroad: Becher process (Australia), Oceanic process (Canada), Chlorine process (Australia), NewGenSR process (Finland-Australia), Mintek process (South Africa), Murso process (Australia-Japan), Tiomin (TSR) process (Canada), Heubach process (Germany), Austpac ERMS/EARS process (Australia) [4], Mitsubishi process (Japan), SREP process (Australia), Western Titanium process (Australia), Dhrangadhra process (India), Benilite process (USA), Ishihara Sangyo process (Japan) [10].

**Table 1. Distribution of titanium, iron, vanadium, and niobium among the products of ilmenite concentrate processing**

Product names	Content, %				Extraction, %			
	TiO <sub>2</sub>	FeO	V <sub>2</sub> O <sub>5</sub>	Nb <sub>2</sub> O <sub>5</sub>	TiO <sub>2</sub>	FeO	V <sub>2</sub> O <sub>5</sub>	Nb <sub>2</sub> O <sub>5</sub>
Titanium slag	86.214	6.355	0.383	0.0438	97.803	16.166	84.891	99.984
Gas cleaning dust	43.40	36.00	0.275	0.0325	1.968	2.506	2.436	3.373
Flue gas dust	36.90	24.65	0.11	0.02	0.014	0.030	0.007	0.016
Master alloy	Ti	Fe	V	Nb	Ti	Fe	V	Nb
	0.012	96.98	0.02	-	0.005	69.50	1.734	-
Work-in-Progress (WIP) Product	-	-	-	-	2.178	14.304	13.368	-
Total:	-	-	-	-	100	100	100	100

**Table 2. Chemical composition of the Satpayev ilmenite concentrate**

Component	SiO <sub>2</sub>	TiO <sub>2</sub>	Fe <sub>2</sub> O <sub>3</sub>	Al <sub>2</sub> O <sub>3</sub>	Cr <sub>2</sub> O <sub>3</sub>	CaO	MgO	MnO	V <sub>2</sub> O <sub>5</sub>	P <sub>2</sub> O <sub>5</sub>	S	ZrO <sub>2</sub>	Sc <sub>2</sub> O <sub>3</sub>	Ta <sub>2</sub> O <sub>5</sub>	Nb <sub>2</sub> O <sub>5</sub>	Act. (Bq/kg)
%	0.91	52.98	41.87	0.33	0.31	0.27	0.41	2.9	0.2	0.17	0.035	0.16	0.002	0.002	0.02	1236.5

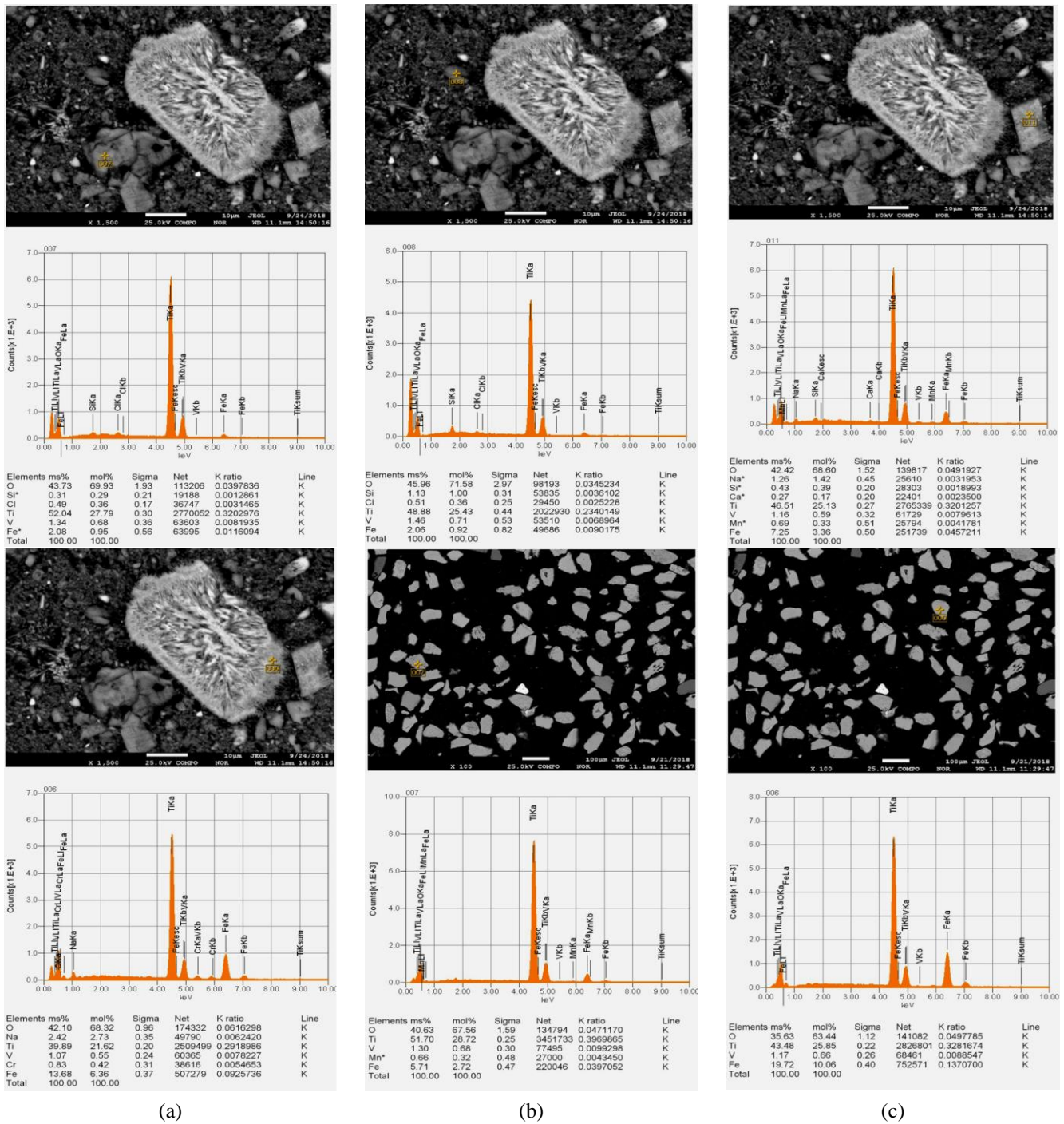


Figure 1. Micrographs of rutile and leucoxene grains from the Obukhov ilmenite concentrate with isomorphous vanadium impurities: (a) – associates of leucoxene grains; (b) – rutile grain; (c) – leucoxene grain

There are several industrial methods for obtaining synthetic rutile or high-quality titanium slag from ilmenite as a raw material for chloride processes [11]. These processes involve a combination of thermal oxidation and reduction through roasting, leaching, and physical separation. Iron is converted into soluble divalent or elemental forms by reduction at high temperatures, followed by acid leaching to obtain synthetic rutile (TiO<sub>2</sub>).

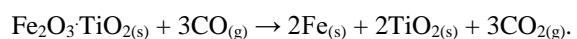
The industrial method of processing ilmenite into synthetic rutile is typically represented by the Becher process. Ilmenite contains 40-65% titanium in the form of TiO<sub>2</sub>, with the remaining portion consisting of iron oxide. In the Becher process, iron oxide is removed, leaving behind synthetic rutile containing more than 90% TiO<sub>2</sub>. The technological

scheme includes four main stages: oxidation, reduction, aeration, and acid leaching.

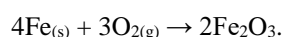
Oxidation involves heating ilmenite in a rotary kiln with air to convert the iron in ilmenite into iron oxides:



This allows for the utilization of a wide range of ilmenite materials with various forms of iron (II) and iron (III) for further processing. The reduction process is carried out in a rotary kiln with pseudobrookite (Fe<sub>2</sub>O<sub>3</sub>·TiO<sub>2</sub>), a mixture of coal and sulfur at temperatures above 1200°C to reduce iron oxide to metallic iron:



Metallic iron is oxidized and precipitates from the solution as sludge during the aeration stage, known as «rust removal», in large tanks containing a 1% ammonium chloride solution at a temperature of 80°C. Then, the finer iron oxide is separated from the larger synthetic rutile particles.

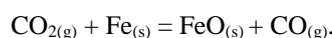


After the majority of iron oxide is removed, the residual iron oxide is leached using 0.5 M sulfuric acid and separated from the synthetic rutile.

In another industrial process, the Benelite process, thermal reduction with carbon is used to convert other forms of iron into divalent iron, which is then separated through leaching with an 18–20% HCl solution.

The Murso process employs fluidized beds for thermal transformations, where ilmenite undergoes pre-oxidation in a fluidized bed at 900–950°C. The hot oxidized ore is then transferred to another fluidized bed, where iron ions are reduced using a reductant (such as gaseous H<sub>2</sub>). The product from the second fluidized bed is subsequently leached with approximately 20% HCl at 108–110°C. The remaining hydrochloric acid is regenerated after the magnetic separation of solid synthetic rutile from the leach solution.

In the Laporte process, the ore is pre-oxidized in a fluidized bed at around 950°C, followed by reduction roasting in a rotary kiln using coal as the reductant. Incomplete reduction of iron to the divalent state without metallization is achieved through proper selection of equipment, temperature, and reductant. The partial pressure of CO<sub>2</sub> generated during the reaction is sufficient to prevent the formation of metallic iron.



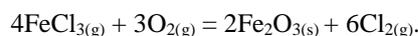
The reactivity of the roasted ore is so high that a single-stage leaching with an 18% HCl solution at atmospheric pressure for 3.5 hours is sufficient to produce a product with the same overall particle size distribution as the original ore. A contact filter is used during leaching to prevent the formation of very fine particles from the soft material. It is claimed that the discharged ore does not contain fine TiO<sub>2</sub> particles.

Reduction roasting, in which the iron content in ilmenite is reduced to divalent forms followed by sulfuric acid leaching, is used in the Kataoka process in Japan. In this process, hydrated titanium dioxide is added to the leach solution as seeds to increase the rate of titanium salt precipitation and improve the leaching efficiency and iron removal. This also allows iron to be extracted from the ore at lower temperatures and lower sulfuric acid concentrations, making the reactor design more economical. More than 95% of the TiO<sub>2</sub> content in ilmenite can be recovered.

While most synthetic rutile processes yield products containing 93% TiO<sub>2</sub>, the Austpac process produces synthetic rutile with 97% TiO<sub>2</sub>. Ilmenite ore is roasted at 800–1000°C to selectively magnetize ilmenite so that gangue minerals can be easily removed through magnetic separation. Roasting also activates the iron-bearing component of ilmenite, enhancing iron leaching. Iron and other impurities are removed by leaching with 25% (by mass) HCl. The resulting solids are then filtered, washed, and calcined. The product undergoes magnetic separation at the final stage, yielding synthetic rutile containing 97% TiO<sub>2</sub>.

In the Dunn process, an alternative thermal conversion method has been proposed. The principle of the selective chlorination process is that iron in ilmenite chlorinates more

easily than titanium. The excess ilmenite in the fluidized bed prevents titanium chlorination since any chlorinated titanium reacts with iron oxide to form titanium dioxide. The gaseous iron chloride exiting the fluidized bed reacts with oxygen to form Fe<sub>2</sub>O<sub>3</sub> and Cl<sub>2</sub> gas for reuse, as described in the following equation:



The reactivity of ilmenite ore during hydrochloric acid leaching was significantly enhanced by the reduction of metallic iron in the solution. It was proven that adding a small amount of iron powder (0.1 kg of iron powder per 1 kg of ilmenite ore) significantly increased the leaching rate of both iron and titanium. When the solid-to-liquid ratio was increased from 1/20 to 1/8, complete dissolution of iron and titanium was achieved in 1.5 hours with the addition of iron powder, compared to 2.5 hours under similar leaching conditions without iron powder.

The direct leaching process for upgrading Rosetta ilmenite concentrate (40–47% TiO<sub>2</sub>) into synthetic rutile without a thermal treatment stage was investigated by Lashin (2005). A high acid concentration (a high molar ratio of ilmenite to acid) and reduction by metallic iron facilitated the removal of iron from the mineral lattice while preventing titanium dissolution. Without the addition of a reducing agent, the iron leaching efficiency did not exceed approximately 55% when using concentrated HCl (12 M) with a solid-to-liquid ratio of 1:5 at 90°C for 8 hours, while titanium remained almost completely undissolved. The addition of metallic iron increased the titanium recovery to 89% TiO<sub>2</sub>. Clearly, a reducing agent is necessary to convert Fe(III) into the more soluble Fe(II) form. The remaining total iron content of less than 7% Fe<sub>2</sub>O<sub>3</sub> is likely due to the complex mineralogical composition, influenced by the presence of three main groups of solid solutions in the FeO–Fe<sub>2</sub>O<sub>3</sub>–TiO<sub>2</sub> ternary system:

- FeO·Fe<sub>2</sub>O<sub>3</sub>–Fe<sub>2</sub>TiO<sub>4</sub>: magnetite–ulvospinel series;
- Fe<sub>2</sub>O<sub>3</sub>·FeTiO<sub>3</sub>: hematite–ilmenite series;
- Fe<sub>2</sub>TiO<sub>5</sub>–FeTi<sub>2</sub>O<sub>5</sub>: pseudobrookite series.

As seen in Table 3, synthetic rutile obtained by any of the processes surpasses titanium slag in TiO<sub>2</sub> content and has a lower Fe content while retaining V<sub>2</sub>O<sub>5</sub> and Nb<sub>2</sub>O<sub>5</sub> for further by-product extraction.

Literature [9] provides data comparing the production costs of synthetic rutile and titanium slag using various technologies (Table 4). From Table 4, it can be seen that the costs and production expenses for titanium slags are higher compared to synthetic rutile production processes.

In this work, an attempt is made to further analyze the economic feasibility of processing synthetic rutile and titanium slag using chloride technology. The analysis is based on calculating the material balance of the chlorination process when processing different raw materials (with varying TiO<sub>2</sub> and FeO content), determining the consumption of raw materials, main reagents, and waste generation volumes. Accordingly, the economic costs of processing each type of titanium-containing raw material are compared.

The calculation of material balances was performed in MS Excel using the methodology presented in the literature [11]. In the calculations, finely ground anthracite with the following composition (%) is used as a reducing agent: 93.45 C; 3.52 volatiles; 2.33 ash; 0.7 S; 0.1 H<sub>2</sub>O. Chlorination is carried out using anodic chlorine gas with the addition of evaporated chlorine, with a total mass concentration of ~96%.

**Table 3. Chemical composition of synthetic rutile obtained by different processes [10] compared to titanium slag (60/40% Vilnohirsk / Satpayev)**

Process / Component	Titanium slag 60/40 Vilnohirsk / Satpayev	Ishihara Sangyo process	Bemilite process	Dhrangadhra process	Western titanium process	Becher process	SREP process	Mitsubishi process	Summit process	Murso process	Chlorine technology process
TiO <sub>2</sub>	86.0	96.1	93.0	90-92	92.0	92.5	92-95	96.7	94.0	96.2	97.5
Fe(total)	-	-	2.0	3.0	3.6	2.4	1.0-3.0	-	-	-	0.46
FeO	6.6	-	-	-	-	-	-	-	2.0	-	-
Fe <sub>2</sub> O <sub>3</sub>	-	1.3	-	-	-	-	-	0.4	-	1.5	0.66
Cr <sub>2</sub> O <sub>3</sub>	0.7	0.15	0.04	0.2	-	0.10	0.2-0.3	-	0.10	0.15	0.11
Al <sub>2</sub> O <sub>3</sub>	2.3	0.46	0.42	1.0	0.7	1.1	0.5-0.8	0.7	1.7	0.2	0.49
V <sub>2</sub> O <sub>5</sub>	0.3	0.20	0.06	0.25	0.12	0.22	0.25	-	0.15	0.04	0.04
Nb <sub>2</sub> O <sub>5</sub>	0.1	0.25	0.6	-	-	0.25	0.3	-	-	-	0.07
Ta <sub>2</sub> O <sub>5</sub>	0.02	-	-	-	-	-	-	-	-	-	-
Sc <sub>2</sub> O <sub>3</sub>	0.02	-	-	-	-	-	-	-	-	-	-
P <sub>2</sub> O <sub>5</sub>	-	0.17	-	0.2	-	0.03	0.01	-	0.1	-	0.072
MnO	2.0	0.03	0.22	0.1	2.0	1.1	0.8-1.2	0.06	1.7	0.05	<0.01
MgO	0.9	0.07	0.05	0.05	0.15	0.30	0.3	-	-	0.04	0.027
CaO	0.5	0.01	-	0.05	0.03	0.03	0.07-0.15	-	0.7	-	0.065
ZrO <sub>2</sub>	0.2	0.15	0.12	1.0	-	0.2	0.1	-	0.2	-	0.19
SiO <sub>2</sub>	3.0	0.5	1.6	1.5	0.7	0.9	0.8-1.2	0.1	0.5	-	0.46
SnO <sub>2</sub>	-	-	0.14	-	-	-	-	-	-	-	0.003
As	-	-	-	-	-	-	-	-	-	-	-
S	0.02	0.01	0.01	-	0.15	0.2	0.03	-	0.02	-	0.006
C	-	-	-	-	0.15	-	-	-	-	-	0.09
U	-	-	-	-	-	~10 ppm	10 ppm	-	-	-	-
Th	-	-	-	-	-	80-450 ppm	80-90 ppm	-	-	-	-

**Table 4. Comparative analysis of the production cost of synthetic rutile and titanium slags using different technologies**

Processes	TiO <sub>2</sub> , %	Capital costs, \$/t	Operating cost, \$/t	Product price, \$/t
ERMS	>97	450	140	420
Becher	>90	550	150	350
Benilite	>93	750	280	380
Titania Slag	>85	970	190	300
Ti-slag 60/40 Voln./Satp	>85	-	-	801.6

To maintain an acceptable viscosity of the working melt in the chlorinator, spent electrolyte with the following composition (%) is used: 76 KCl; 15.5 NaCl; 2.7 CaCl<sub>2</sub>; 5.5 MgCl<sub>2</sub>; 0.02 MgO; 0.04 Fe<sub>2</sub>O<sub>3</sub>; 0.07 Al<sub>2</sub>O<sub>3</sub>; 0.07 SiO<sub>2</sub>; 0.1 others. The electrolyte feed depends on the FeO content in the titanium-containing raw material and is as follows:

- for 7-9% FeO – 120 kg/t TiCl<sub>4</sub>;
- for 4-5% FeO – 110 kg/t TiCl<sub>4</sub>;
- for 2-3% FeO – 100 kg/t TiCl<sub>4</sub>.

The results of the calculation are shown in Table 5.

**Table 5. Results of material balance calculations for chlorination**

Material	TiO <sub>2</sub> , %	FeO, %	Specific consumption per 1 ton of TiCl <sub>4</sub> , kg				Specific formation per 1 ton of TiCl <sub>4</sub> , kg		Specific material costs, \$/t	Specific costs for waste utilization, \$/t
			Slag/rutile	Reduc. agent	Cl	Elect.	TiCl <sub>4</sub> slag waste	Waste gases		
Ti-slag 60/40 Voln./Satp.	86	6.6	537.6	96	975.3	120	92.7	324.3	99 476	21 597
Syn. rutile Becher process	92.5	3.65	496.8	87.9	891.6	110	56.1	296.9	90 966	17 609
Syn. Rutile Western Titanium Process	92	4.13	499.6	87.9	891.4	110	62.8	296.8	90 949	18 108
Syn. Rutile Dhrangadhra Process	92	5.04	500	88.9	900.5	110	47.7	300.4	91 870	17 135
Syn. Rutile Ishihara Sangyo Process	96.1	2.62	477.4	85.7	863.2	100	37.5	289.2	88 028	15 863
Syn. Rutile Summit Process	94	2	488.9	88	885.4	100	58.1	296.9	90 256	17 759
Syn. Rutile SREP Process	93.5	3.11	491.4	87.6	884.3	100	51.9	295.9	90 103	17 248
Syn. Rutile Chlorine Technology Process	97.5	1.4	470.3	84.9	852.7	100	34.9	286.4	87 018	15 541

The calculation is based on 1000 kg of processed titanium slag or synthetic rutile, with results presented per 1 ton of produced TiCl<sub>4</sub>. The obtained results indicate that the specific costs of the chlorination process directly depend on the quality of the processed titanium-containing raw material. The higher the TiO<sub>2</sub> content and the lower the FeO content, the lower the processing costs.

It should be noted that the results of the material balance calculations are theoretical in nature and slightly underestimated

compared to practical data, as the calculations are based on 1 ton of TiCl<sub>4</sub> obtained in a vapor-gas mixture, without accounting for TiCl<sub>4</sub> losses during condensation. According to the author's estimates, the error does not exceed 4%. However, in the author's opinion, the obtained results make it possible to conduct an economic analysis of processing various titanium-containing raw materials using chlorination in a molten alkali metal salt medium in the presence of carbon.

#### 4. Conclusions

Thus, from an economic standpoint, the processing of synthetic rutile compared to titanium slag is more feasible and retains the possibility of extracting rare earth elements such as vanadium and niobium as by-products. This analysis allows for considering the possibility of establishing a production stage for synthetic rutile from the Satpayev ilmenite concentrate at titanium manufacturing enterprises.

#### Author contributions

Conceptualization: T.K.S., T.A.C.; Data curation: E.S.M.; Formal analysis: T.K.S., E.S.M.; Funding acquisition: T.K.S., T.A.C.; Investigation: T.K.S., T.A.C.; Methodology: E.S.M.; Project administration: T.K.S., E.S.M.; Resources: E.S.M.; Software: E.S.M.; Supervision: T.K.S., T.A.C.; Validation: E.S.M.; Visualization: E.S.M.; Writing – original draft: T.K.S., E.S.M.; Writing – review & editing: T.A.C. All authors have read and agreed to the published version of the manuscript.

#### Funding

This research was funded by the Science Committee of the Ministry of Education and Science of the Republic of Kazakhstan (Grant No. AP22686490).

#### Conflicts of interests

The authors declare no conflict of interest.

#### Data availability statement

The original contributions presented in this study are included in the article. Further inquiries can be directed to the corresponding author.

#### References

[1] Zwierynski, A.J., Zlotkowski, A., Solecki, M. L., Balicki, R., Binkowska, W., Janiak, A., Edelmüller, H., Gardynik, A. &

- Leśniowska M. (2022). Ilmenite, the raw material of the future. *Mathematical methods and terminology in geology*, 69-74
- [2] Mehdilo, A., Irannajad, M. & Rezaei B. (2015). Chemical and mineralogical composition of ilmenite: Effects on physical and surface properties. *Minerals Engineering*, (70), 64-76. <https://doi.org/10.1016/j.mineng.2014.09.002>
- [3] Schmidt, R. (2019). Magnetic properties of ilmenite  $Mn_2FeSbO_6$ . *Journal of Magnetism and Magnetic Materials*, (480), 58-63. <https://doi.org/10.1016/j.jmmm.2019.02.047>
- [4] Wei, Lu, Xuwei, Lu, Junyi, Xiang, Kai, Hu, Shiqing, Zhao, Jie, Dang, Kexi, Han & Bing, Song. (2019). Effect of preoxidation on the reduction of ilmenite concentrate powder by hydrogen. *International Journal of Hydrogen Energy*, 44(2) 4031-4040. <https://doi.org/10.1016/j.ijhydene.2018.12.139>
- [5] Subasinghe, H.C.S., Ratnayake, A.S. (2021). Processing of ilmenite into synthetic rutile using ball milling induced sulphurisation and carbothermic reduction. *Minerals Engineering*, (173), 107197. <https://doi.org/10.1016/j.mineng.2021.107197>
- [6] Kurmangaliyev, A.A. (2005). Current state and development trends of the raw material base of the titanium-magnesium industry in the Republic of Kazakhstan. *Geology, Mining, Metallurgy. Bulletin of VKGTU*, (4), 13-20.
- [7] Dyachkov, B.A., Mochalkina, L.N., Kuzmina, O.N., Bochkova, O.I. & Kravchenko M.M. (2005). Types of weathering crust deposits in Eastern Kazakhstan. *Geology, Mining, Metallurgy. Bulletin of VKGTU*, (4), 6-12.
- [8] Kravchenko, M.M., Dyachkov, A.A., Suiyepaev, E.S., Sapargaliyev, E.M., Azelkhanov, A.Zh., Oitseva, T.A. (2016). Prospects for strengthening and developing the raw material base of titanium production in Eastern Kazakhstan. *Geology. Bulletin of Perm University*, (1), 82-90.
- [9] Zabolotskaya, Y.V. (2014). Autoclave de-siliconization of leucocene concentrate with calcium hydroxide to obtain synthetic rutile (doctoral dissertation). *Moscow*
- [10] Harald Elsner. (2010). Heavy Minerals of Economic Importance. *BGR, Hannover, Germany*
- [11] Zhang, W., Zhu, Zh. & Cheng, Ch.Y. (2011). A literature review of titanium metallurgical processes. *Hydrometallurgy*, (108), 177-188. <https://doi.org/10.1016/j.hydromet.2011.04.005>
- [12] Nadolsky, A.P. (1980). Calculation of processes and apparatus for refractory metal production. *Moscow: Metallurgy*.

## Титан, ванадий және ниобий алу арқылы құрамында титан бар әр түрлі шикізатты өңдеудің экономикалық талдауы

Т.К. Сарсембеков, Т.А. Чепуштанова, Е.С. Меркибаев\*

Satbayev University, Алматы, Қазақстан

\*Корреспонденция үшін автор: [y.merkibayev@satbayev.university](mailto:y.merkibayev@satbayev.university)

**Андатпа.** Жұмыста әртүрлі титан бар шикізатты-титан қожын және синтетикалық рутил – көміртектің қатысуымен балқытылған тұзды ортада хлорлау әдісімен өңдеудің экономикалық талдауы ұсынылған. Құрамында титан бар шикізатты қайта өңдеу құрамында көміртегі бар тотықсыздандырғыштың қатысуымен жоғары концентрацияланған хлор газымен балқытылған сілтілі металл тұздарында ( $MgCl_2$ ,  $NaCl$ ,  $KCl$ ) хлорлау технологиясы бойынша жүзеге асырылады. Тотықсыздандырғыш ретінде антрацит, балқытылған орта ретінде магний электролизінің үйінді шламы қолданылады. Қайта өңдеу шамот кірпішпен қапталған цилиндрлік хлорлау пештерінде  $720-800^{\circ}C$  температурада жүзеге асырылады. Жұмыста Шығыс Қазақстандағы Сәтбаев ильменит кен орнының сипаттамасы берілген, әртүрлі тәсілдермен алынған Сәтбаев ильменит концентратының, титан қожының және синтетикалық рутил химиялық құрамы ұсынылған. Ильменит концентраттарындағы ванадий, ниобий және тантал құрамы мен олардың жер қыртысында таралуы арасында корреляция орнатылған. Осы корреляция негізінде элементтердің периодтық жүйесінің V тобындағы өтпелі металдардың реті олардың концентраттардағы концентрациясы төмендеген сайын анықталады. Құрамында титан бар шикізатты кейбір компоненттердің жоғарылауымен өңдеуге байланысты

технологиялық қиындықтар, сондай-ақ синтетикалық рутил алудың кейбір әдістері сипатталған. Титан қожы мен синтетикалық рутил өндірісінің құнын салыстыру келтірілген. Шикізат шығындары мен қалдықтарды кәдеге жарату шығындарын бағалау үшін титан қожын хлорлау процесінің материалдық балансы мен өндірістің әртүрлі әдістерінің синтетикалық рутил есептеулері жүргізілді. Зерттеуде Сәтбаев кен орнының ильменит концентрат синтетикалық рутил өндірісі экономикалық тұрғыдан тиімді деген қорытындыға келді.

**Негізгі сөздер:** қож, рутил, шығындар, қайта өңдеу, хлорлау, қалдықтар.

## Экономический анализ переработки различного титансодержащего сырья с получением титана, ванадия и ниобия

Т.К. Сарсембеков, Т.А. Чепуштанова, Е.С. Меркибаев\*

Satbayev University, Алматы, Казахстан

\*Автор для корреспонденции: [y.merkibayev@satbayev.university](mailto:y.merkibayev@satbayev.university)

**Аннотация.** В работе представлен экономический анализ переработки различного титансодержащего сырья – титанового шлака и синтетического рутила – методом хлорирования в расплавленной солевой среде в присутствии углерода. Переработка титансодержащего сырья осуществляется по технологии хлорирования в расплавленных солях щелочных металлов ( $MgCl_2$ ,  $NaCl$ ,  $KCl$ ) высококонцентрированным газообразным хлором в присутствии углеродсодержащего восстановителя. В качестве восстановителя используется антрацит, в качестве расплавленной среды – отвальный шлак электролиза магния. Переработка осуществляется в цилиндрических печах хлорирования, футерованных шамотным кирпичом, при температурах 720-800°C. Продукты хлорирования направляются в конденсационную систему. В работе дано описание Сатпаевского месторождения ильменита в Восточном Казахстане, представлен химический состав Сатпаевского ильменитового концентрата, титанового шлака и синтетического рутила, полученных различными способами. Установлена корреляция между содержанием ванадия, ниобия и тантала в ильменитовых концентратах и их распространенностью в земной коре. На основании этой корреляции определен порядок переходных металлов в V группе периодической системы элементов по мере убывания их концентрации в концентратах. Описаны технологические сложности, связанные с переработкой титансодержащего сырья с повышенным содержанием некоторых компонентов, а также некоторые способы получения синтетического рутила. Приведено сравнение себестоимости производства титанового шлака и синтетического рутила. Проведены расчеты материального баланса процесса хлорирования титанового шлака и синтетического рутила различных способов производства для оценки затрат на сырье и затрат на утилизацию отходов. В исследовании сделан вывод о том, что производство синтетического рутила из концентрата ильменита Сатпаевского месторождения экономически целесообразно.

**Ключевые слова:** шлак, рутил, затраты, переработка, хлорирование, отходы.

### Publisher's note

All claims expressed in this manuscript are solely those of the authors and do not necessarily represent those of their affiliated organizations, or those of the publisher, the editors and the reviewers.

<https://doi.org/10.51301/ejsu.2025.i1.02>

## Production of iron oxide pigment from the metallic component of ilmenite smelting

B.K. Kenzhaliyev, A.A. Ultarakova\*, N.G. Lokhova, K.K. Kassymzhanov, A.O. Mukangaliyeva

*Institute of Metallurgy and Ore Beneficiation, Almaty, Kazakhstan*

\*Corresponding author: [ult.alma@mail.ru](mailto:ult.alma@mail.ru)

**Abstract.** The smelting of off-grade ilmenite concentrates from the Obukhovskoye deposit results in the generation of significant quantities of reduced iron, which presents an opportunity for its utilization in the production of iron oxide pigments. The transformation of industrial waste into value-added materials aligns with contemporary trends in sustainable materials science. This study investigates the precipitation of divalent iron from sulfuric and hydrochloric acid solutions using ammonia to form goethite, focusing on the influence of magnesium impurities on the precipitation process. The presence of magnesium was found to inhibit the formation of goethite, leading to a significant reduction in pigment yield and quality. A ferrous solution was prepared by dissolving finely divided reduced iron in sulfuric acid, followed by the precipitation of iron oxides using a 25% ammonia solution. The synthesized iron oxide pigment was further refined through hydrogen peroxide treatment, ensuring a more uniform pigment composition and improved color stability. This approach offers a viable method for the recycling of industrial by-products while simultaneously addressing environmental concerns related to waste disposal. The findings contribute to the advancement of resource-efficient pigment synthesis techniques, demonstrating the potential for utilizing metallurgical waste as a precursor for high-quality iron oxide pigments suitable for various industrial applications.

**Keywords:** iron alloy, sulfuric acid, ferrous sulfate, precipitation, goethite, pigment.

Received: 11 November 2024

Accepted: 14 February 2025

Available online: 28 February 2025

### 1. Introduction

Iron oxide-based pigments play a crucial role across various industries and scientific fields due to their unique physicochemical properties, high stability, and broad color spectrum, which can be derived from both natural and synthetic sources. However, synthetic pigments, particularly those based on iron oxides, offer several advantages that significantly expand their applications while ensuring consistent product quality [1,2].

Yellow iron oxide ( $\alpha$ -FeOOH), also known as goethite, is one of the most significant pigments in industrial applications. Its distinctive properties provide a stable yellow color, making it highly sought after in the production of paints, coatings, plastics, and even cosmetics [3]. An essential aspect of goethite's application is its thermal stability and chemical inertness, which render it preferable for use in environments exposed to external factors such as ultraviolet radiation and atmospheric conditions. In the construction industry, yellow iron oxide is extensively used for coloring concrete and bricks, owing to its superior resistance to fading and color stability under aggressive environmental conditions [4].

Red iron oxide ( $\alpha$ -Fe<sub>2</sub>O<sub>3</sub>), commonly known as hematite, is one of the most widespread and in-demand pigments due to its vibrant red hue. In industrial applications, hematite serves not only as a pigment but also as a catalyst in chemical reactions and an active material in energy storage sys-

tems, including lithium-ion batteries and supercapacitors. From a chemical standpoint,  $\alpha$ -Fe<sub>2</sub>O<sub>3</sub> exhibits exceptional chemical stability, making it indispensable in the production of durable coatings and construction materials [5,6]. Furthermore, its use in cosmetics and pharmaceuticals is attributed to its non-toxicity and safety, which is particularly critical when developing products that come into direct contact with human skin.

Black iron oxide (Fe<sub>3</sub>O<sub>4</sub>), commonly known as magnetite, stands out among iron oxide-based pigments due to its intrinsic magnetic properties. This characteristic expands its potential applications in high-tech industries, including the production of magnetic data storage devices, such as magnetic tapes and hard drives [7-10]. Additionally, Fe<sub>3</sub>O<sub>4</sub> is widely used in the manufacturing of toners for printing devices, attributed to its ability to achieve uniform pigment particle distribution on surfaces.

Magnetite has also found extensive applications in medicine, particularly in magnetic resonance imaging (MRI), where it serves as a contrast agent. Moreover, it is utilized in targeted drug delivery systems, where its high biocompatibility and surface functionalization capabilities enable its integration into nanomedicine, opening new prospects for diagnostics and therapy [11-13].

Synthetic iron oxide pigments offer distinct advantages over their natural counterparts [14]. Firstly, they ensure color

purity and stable, reproducible quality, which is particularly crucial for manufacturing processes requiring precise color control. Secondly, the ability to fine-tune the physicochemical properties of synthetic pigments allows for the development of materials with tailored characteristics, including high-temperature stability, chemical resistance, and fade resistance. This makes synthetic pigments highly preferable in industries such as high-performance paint and coating production, especially for applications under extreme operating conditions [15-18].

The incorporation of iron oxides into construction materials is driven by their high resistance to atmospheric factors and ultraviolet radiation. Concrete, bricks, and building mortars pigmented with iron oxides exhibit long-lasting durability and color retention over extended periods. This aspect is particularly important in architectural projects and urban infrastructure development, where both longevity and aesthetic appeal are critical factors [19].

In pharmaceutical and cosmetic industries, iron oxide pigments are employed due to their non-toxicity and safety for human health. These pigments are widely used in decorative cosmetics, such as eyeshadows, blushes, and lipsticks, where high purity and color stability are essential. In pharmaceuticals, iron oxides are used for tablet and capsule coloring, facilitating medication identification and enhancing consumer appeal [20-24].

Particular attention should be given to the use of iron oxides in specialized fields, such as ceramics, magnetic coatings, and toners. In ceramic manufacturing, iron oxide pigments are employed to create durable-colored glazes and enamels that retain their hues even after high-temperature firing [25,26]. In the production of magnetic coatings, iron oxides play a key role due to their ferromagnetic properties, making them indispensable for hard drives and magnetic tapes. Furthermore, in toner production for laser printers and copiers, iron oxides are utilized for their uniform distribution properties and strong adhesion to paper surfaces.

In summary, iron oxide-based pigments, both natural and synthetic, have a vast range of applications across multiple industries, including construction, chemical, pharmaceutical, and cosmetic sectors [27]. However, synthetic pigments, due to their high purity, stability, and reproducibility, open new avenues for the development of high-performance materials. Future research on iron oxide pigments will focus on the development of novel functional materials with enhanced properties, ensuring even broader applications in science and technology [28,29].

Investigating and developing new methods for obtaining iron-containing pigments from chemical and metallurgical waste is a highly relevant and pressing challenge for modern science and industry. In recent years, significant attention has been given to utilizing industrial waste as raw materials for the synthesis of high-quality pigments, which not only reduces production costs but also addresses waste disposal and recycling issues, contributing to environmental sustainability. Iron-containing pigments, such as hematite ( $\alpha\text{-Fe}_2\text{O}_3$ ) and other iron oxides, exhibit high stability, corrosion resistance, and a broad spectrum of applications, making them indispensable across multiple industrial sectors [30].

The utilization of ferrous sulfate ( $\text{FeSO}_4$ ) waste, accumulated during chemical and metallurgical processes, for the synthesis of iron-containing pigments is a promising research direction. It is well established that the two-stage synthesis

method for iron red pigment from long-term stored ferrous sulfate waste involves the stages of purification and precipitation [31]. The first stage-purification of ferrous sulfate waste is a crucial procedure to obtain high-quality raw materials suitable for further use. Modern purification methods, including the application of microwave reactors, significantly accelerate and enhance the efficiency of iron salt purification, representing a key step in achieving high-purity final products.

The use of a microwave reactor for the synthesis of iron oxide-based pigments allows for a substantial reduction in the phase transition temperature of goethite ( $\alpha\text{-FeOOH}$ ) to hematite ( $\alpha\text{-Fe}_2\text{O}_3$ ). While traditional methods require temperatures of approximately  $500^\circ\text{C}$ , the microwave method reduces this threshold to  $170^\circ\text{C}$ , thereby eliminating the need for additional thermal processing or calcination. This represents a significant breakthrough not only in terms of energy efficiency but also in improving the physicochemical properties of the synthesized materials. Lowering the synthesis temperature reduces the formation of pigment agglomerates, directly influencing its quality and coloration ability. As a result, the synthesized materials exhibit more stable and homogeneous characteristics compared to commercial analogs, as confirmed by several studies [32].

The synthesis of pigments from ferrous sulfate waste has proven to be highly efficient and serves as an effective solution for industrial waste recycling. This approach offers broad prospects for the industrial-scale production of iron-based pigments, which can be applied in construction materials, paint and coating industries, and several other sectors. Laboratory studies indicate that synthesized pigments exhibit notable advantages over commercial products, making their utilization highly attractive from both technological and economic standpoints [33].

Another important development is the production of anti-corrosion pigments based on hematite derived from steel industry waste. A specific method has been developed for obtaining pigments from powdered residues formed during the rolling of reinforcement steel, including the use of rust and mill scale [34]. These waste materials typically contain a high percentage of iron oxides, primarily  $\text{Fe}_2\text{O}_3$ , along with other oxide impurities such as  $\text{SiO}_2$ ,  $\text{CaO}$ ,  $\text{Al}_2\text{O}_3$ , and  $\text{MnO}$ , which may influence the final pigment properties. Notably, the initial waste material contains various crystalline phases of iron oxides, including magnetite, maghemite, lepidocrocite, wüstite, goethite, and hematite. The presence of these phases highlights the complex structure and rich composition of the raw materials, necessitating precise control over temperature conditions and retention time during calcination to produce a homogeneous pigment with high hematite content.

The pigment synthesis process involves calcining the raw material at different temperatures, allowing for the regulation of hematite content in the final product. The highest hematite concentration ( $\alpha\text{-Fe}_2\text{O}_3$ ) is achieved by calcination at  $850^\circ\text{C}$  for 1 hour, emphasizing the need to optimize processing conditions to obtain the highest-quality pigment. This method is highly efficient, enabling the production of anticorrosion pigments with enhanced properties. This is particularly critical for applications in aggressive environments where corrosion resistance is essential.

Thus, modern methods for producing iron-containing pigments from industrial waste represent a critical advancement in the development of recycling technologies and the utilization of secondary resources. These methods not only address

waste disposal issues but also contribute to the creation of new materials with superior performance characteristics, making them highly valuable across various scientific and industrial fields. The implementation of such methods can significantly reduce production costs, improve product quality, and minimize environmental impact, making these innovations highly promising for future industrial applications.

## 2. Materials and methods

### 2.1. Precipitation of pure components from iron-containing acidic solutions

Currently, the processing of titanium-containing concentrates (titanomagnetite, ilmenite, rutile) with high chromium, vanadium, and manganese content is gaining increasing relevance in global industrial practice [14].

The object of this study was model iron-containing acidic solutions.

Analysis Methods: X-ray phase analysis of the sludge was performed using a D8 Advance diffractometer (BRUKER) with Cu-K $\alpha$  radiation. The obtained diffraction data were processed and interplanar spacing calculations were carried out using EVA software. Sample decoding and phase identification were performed using the Search/Match program with the ASTM Card Database.

X-ray fluorescence analysis was conducted using a wavelength-dispersive spectrometer Venus 200 (PANalytical B.V., Netherlands).

The chemical composition of the samples was determined by optical emission spectrometry with inductively coupled plasma (ICP-OES) using an Optima 2000 DV spectrometer (Perkin Elmer, USA).

Experimental Procedure: The following equipment was used for the experiments: pH meter Mark 901 (Russia), Laboratory hot plate Arc Velp (Italy), Magnetic stirrer Stirrer ES Velp (Italy). Model solutions of 0.1N hydrochloric acid (pH 1.2) and 0.1N sulfuric acid (pH 1.34) were prepared. Ferrous sulfate heptahydrate (FeSO $_4$ ×7H $_2$ O) was added to the solutions in the required quantity to achieve an iron concentration of 50 g/L. After the addition of ferrous sulfate heptahydrate, the pH of the hydrochloric acid solution increased to 1.61, while the sulfuric acid solution reached 1.7. The hydrochloric acid solution was acidified to pH -1.0 using 10% HCl, and the sulfuric acid solution was adjusted to pH -1.0 with 10% H $_2$ SO $_4$ .

The precipitation of iron oxides from these solutions was carried out by the gradual addition of a 25% ammonia solution at temperatures ranging from 25°C to 55°C. A 250 mL heat-resistant beaker containing the prepared model solution was heated to the required temperature using a laboratory hot plate, while stirring at 200 rpm. Ammonia was added dropwise using a glass pipette until the pH reached 3. The resulting solution with the precipitate was filtered, and the solid residue (cake) was dried at 105°C for 2 hours.

## 3. Results and discussion

The results of precipitation experiments from hydrochloric acid solutions are presented in Table 1. Fe $^{3+}$ O(OH). When the temperature was increased to 55°C, somalnokite (syn.  $\epsilon$ -Fe $_2$ O $_3$ , iron (III) oxide) was formed. Similar precipitation experiments were conducted using sulfuric acid solutions, adjusting the pH to 4.5. The results of iron oxide precipitation using a 25% ammonia solution from sulfuric acid solutions in the temperature range of 25-55°C are presented in Table 2.

According to the X-ray phase analysis results, the precipitates obtained over the entire temperature range were identified as bernallite Fe $^{3+}$ (OH) $_3$ .

The third series of experiments involved the precipitation of iron oxides from an iron-hydrochloric acid solution, in which MgCl $_2$  was added to obtain a magnesium concentration of 10.1 g/dm $^3$ , with an initial solution pH of -1. The precipitation process was conducted at temperatures ranging from 25 to 55°C, with the addition of a 25% ammonia solution to adjust the pH to 4.5. The experiment lasted for 4 hours. The solution containing the precipitate was filtered, and the precipitate was dried at 105°C for 2 hours. The results of these experiments are presented in Table 3.

Table 4 shows the changes in X-ray phase analysis as the temperature of iron oxide precipitation increases.

Due to the high content of the amorphous component, X-ray fluorescence analysis could not be performed on the precipitates obtained at 25°C and 35°C. In the precipitate obtained at 45°C, goethite Fe $^{3+}$ O(OH) and magnesium sulfate hydrate MgSO $_4$ ×2H $_2$ O were identified. The precipitate obtained at 55°C contained goethite Fe $^{3+}$ O(OH) and iron oxide Fe $_2$ O $_3$ , with traces of MgSO $_4$ ×1.25H $_2$ O also detected. The presence of magnesium sulfate hydrate is attributed to insufficient washing of the precipitate and the presence of an amorphous phase.

Table 1. Results of iron oxide precipitation from hydrochloric acid solutions

Name	Temperature, °C	Cake weight, g	Volume, ml	Fe		Mg	
				g/dm $^3$	wt.%	g/dm $^3$	wt.%
Initial Solution			1000	50	100	0.11	100
25% Ammonia Solution	25		36				
Obtained							
Precipitate		3.28		36.1	2.4	0.03	0.9
Solution			1000	48.8	97.6	0.107	99.1
25% Ammonia Solution	35		36				
Obtained							
Precipitate		3.48		42.12	2.9	0.028	0.9
Solution			1000	48.53	97.1	1.07	99.1
25% Ammonia Solution	45		36				
Obtained							
Precipitate		3.24		40.8	2.6	0.019	0.6
Solution			1000	48.68	97.4	0.1073	99.4
25% Ammonia Solution	55		36				
Obtained							
Precipitate		3.2		43.83	2.8	0.014	0.4
Solution			1000	48.6	97.2	1.075	99.6

**Table 2. Results of iron oxide precipitation from sulfuric acid solutions**

Name	Temperature, °C	Cake weight, g	Volume, ml	Fe		Mg	
				g/dm <sup>3</sup>	wt.%	g/dm <sup>3</sup>	wt.%
Initial solution			1000	50	100	0.128	100
25% ammonia solution	25		30				
Obtained							
Precipitate		3.72		32.94	2.5	0.018	0.5
Solution			1000	48.8	97.5	0.128	99.5
25% ammonia solution	35		30				
Obtained							
Precipitate		3.44		34.7	2.4	0.023	0.6
Solution			1000	48.8	97.6	0.131	99.4
25% ammonia solution	45		30				
Obtained							
Precipitate		6.64		33.22	4.4	0.014	0.12
Solution			1000	47.8	95.6	0.192	99.88
25% ammonia solution	55		30				
Obtained							
Precipitate		4.44		31.6	2.81	0.142	0.7
Solution			1000	48.6	97.19	0.054	99.3

**Table 3. Results of iron oxide precipitation from hydrochloric acid solutions in the presence of magnesium chloride**

Name	Precipitation, temperature, °C	Precipitate weight g	Volume, ml	Fe		Mg	
				g/dm <sup>3</sup>	wt.%	g/dm <sup>3</sup>	wt.%
Initial solution			10000	50	100	10.1	100
25% ammonia solution	25	14	-	-	-	-	-
MgCl <sub>2</sub>	40	-	-	-	-	-	-
Obtained	-	-	-	-	-	-	-
Precipitate	-	3.28	-	27.35	1.9	2.60	0.9
Solution	-	10000	-	49.0	97.1	10.3	99.1
25% ammonia solution	35	14	-	-	-	-	-
MgCl <sub>2</sub>	40	-	-	-	-	-	-
Obtained	-	-	-	-	-	-	-
Precipitate	-	3.48	-	34.3	2.7	2.96	1.2
Solution	-	10000	-	48.6	97.3	10.08	98.8
25% Ammonia solution	45	14	-	-	-	-	-
MgCl <sub>2</sub>	40	-	-	-	-	-	-
Obtained	-	-	-	-	-	-	-
Precipitate	-	3.24	-	25.9	1.3	3.87	2.25
Solution	-	10000	-	48.5	96.9	9.89	97.75
Initial solution	-	-	10000	50.0	100%	10.1	100%
25% ammonia solution	25	14	-	-	-	-	-
MgCl <sub>2</sub>	40	-	-	-	-	-	-
Obtained	-	-	-	-	-	-	-
Precipitate (wt.%)	-	3.28	-	27.35	1.9	2.60	0.9

The precipitation process was carried out within the temperature range of 25-55°C, with the addition of ammonia to adjust the solution pH to 4.5. The duration of the experiment was 4 hours. The solution containing the precipitate was filtered by gravity, and the precipitate was dried at 100°C for two hours. The results of these experiments are presented in Table 5.

**Table 4. Results of X-ray phase analysis of precipitates in the presence of magnesium chloride in the temperature range of 25-55°C**

Precipitation temperature, °C	Amorphous phase content, %	Crystalline phase content, %
25	78.6	21.6
35	74.7	25.3
45	50.9	49.1
55	58.8	41.2

**Table 5. Results of iron oxide precipitation from sulfuric acid solutions in the presence of magnesium sulfate**

Name	Precipitation temperature, °C	Precipitate weight, g	Volume, ml	Fe		Mg	
				g/dm <sup>3</sup>	wt.%	g/dm <sup>3</sup>	wt.%
Initial solution			10000	50.0	100	10.0	100
25% ammonia solution	25	50	-	-	-	-	-
MgSO <sub>4</sub>	50	-	-	-	-	-	-
Obtained	-	-	-	-	-	-	-
Precipitate	-	3.24	-	30.7	2.0	1.27	0.9
Solution	-	10000	-	48.08	96.2	9.89	98.1
25% ammonia solution	35	50	-	-	-	-	-
MgSO <sub>4</sub>	50	-	-	-	-	-	-
Obtained	-	-	-	-	-	-	-
Precipitate	-	3.08	-	34.5	2.3	0.97	0.7
Solution	-	10000	-	47.9	97.8	9.86	99.3
25% ammonia solution	45	50	-	-	-	-	-
MgSO <sub>4</sub>	50	-	-	-	-	-	-
Obtained	-	-	-	-	-	-	-
Precipitate	-	3.24	-	28.6	2.0	1.27	0.9
Solution	-	10000	-	47.90	97.3	9.99	99.2
25% ammonia solution	55	50	-	-	-	-	-
MgSO <sub>4</sub>	50	-	-	-	-	-	-
Obtained	-	-	-	-	-	-	-
Precipitate	-	4.32	-	30.6	2.2	0.95	0.6
Solution	-	10000	-	47.7	97.3	9.94	99.8

Table 6 shows the changes in X-ray phase analysis as the temperature of iron oxide precipitation increases. The precipitates obtained within the temperature range of 25-55°C contain goethite  $Fe^{3+}O(OH)$  with an admixture of magnesium sulfate hydrate  $MgSO_4 \times 1.25H_2O$ .

**Table 6. Results of X-ray phase analysis of precipitates in the presence of magnesium sulfate in the temperature range of 25-55°C**

Precipitation temperature, °C	Amorphous phase content, %	Crystalline phase content, %
25	64.5	35.4
35	63.0	37.0
45	52.2	47.8
55	50.5	49.5

Thus, from pure model acidic iron-containing solutions, within the temperature range of 25-55°C, crystalline goethite and iron oxide is precipitated. However, in the presence of magnesium ions, the precipitation process results in a significant portion of amorphous precipitate, while the crystalline fraction consists of goethite and iron oxide.

### 3.1. Production of iron oxide pigment from the magnetic fraction of roasted titanium-containing product

To investigate the possibility of obtaining pigment, a batch of reduced iron obtained through the pyrometallurgical processing of ilmenite concentrate was selected. Table 7 presents the X-ray fluorescence composition of the metal. The material consisted of variously shaped droplet-like iron ingots, which were crushed and sieved through four meshes with apertures of 2 mm, 1 mm, 0.5 mm, and 0.1 mm. The results of the fractional analysis are shown in Table 8.

**Table 7. X-ray fluorescence composition of reduced iron**

Element	Content, %	Error Margin, $\pm 3\sigma$
Fe	95.74	0.14
Cr	0.17	0.086
P	0.329	0.043
Si	0.192	0.063
Mn	0.162	0.071
Cu	0.064	0.021
V	0.039	0.023
Nb	0.024	0.004
Sn	0.021	0.02

**Table 8. Fractional analysis of crushed metal**

Class	Content, %
+2 mm	3.6
-2+1 mm	4.9
-1+0,5 mm	18.0
-0,5+0,1 mm	73.5
Total:	100.0

The fine fraction was retained for pH adjustment, while the coarse fraction (+1–0.5 mm, 20 g) was placed in a beaker, and 200 mL of 15% sulfuric acid solution was added. The mixture was leached at room temperature until the complete dissolution of metallic iron. Throughout the mixing process, pH measurements were conducted and maintained at 1. If the pH increased, sulfuric acid was added dropwise, whereas if the pH dropped to 0, fine iron fraction was supplemented.

The total sulfuric acid consumption amounted to 12 mL. The solution was filtered, yielding 2.52 g of solid residue (cake) and 250 mL of solution with an iron content of 67.3 g/L. From this solution, 3.12 g of iron was precipitated using

6 mL of ammonia. A light brown goethite was obtained with impurities, and the composition of its main components is provided in Table 9. Figure 1 presents a photograph of hematite derived from the dried goethite.

**Table 9. Chemical composition of goethite, wt. %**

Component wt. %	Fe	Mg	Al	Si	Mn	V	Cr	Co	Ga	As	O
	43.4	0.033	0.013	0.06	0.05	0.13	0.1	0.083	0.012	0.007	56.11



**Figure 1. Light brown hematite**

Thus, goethite with impurities was obtained, serving as a precursor for pigment production.

The practical synthesis procedure for yellow iron oxyhydroxide pigment from hematite using hydrogen peroxide involves several critical stages. First, 30 g of hematite powder is suspended in 600 mL of distilled water and heated to 35-40°C. Maintaining a precise temperature range is crucial for optimal reaction kinetics. Subsequently, 60 mL of 30% hydrogen peroxide is slowly added over 10-15 minutes under continuous stirring to ensure uniform oxidation and prevent rapid gas evolution. The mixture is then held at the target temperature for 30-60 minutes, allowing for the formation of iron oxyhydroxide, indicated by the gradual yellowing of the suspension. Upon completion of the reaction, the mixture is slightly cooled, and the solid pigment is separated from the liquid phase by filtration. The collected yellow pigment is dried at 120°C for two hours to remove residual moisture and stabilize its structure. This controlled drying process is essential to achieve the desired crystalline and chemical stability of the final product.

To ensure the scientific validity of the procedure, the dried pigment undergoes X-ray diffraction (XRD) analysis to confirm its crystalline phases, verifying the successful formation of iron oxyhydroxide. The results of the X-ray structural analysis of the iron oxide pigment are presented in Figure 2, while Figure 3 provides a photograph of the obtained pigment.

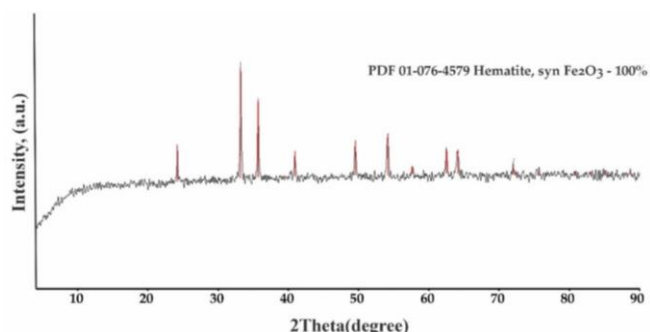


**Figure 2. X-ray diffraction pattern of hematite pigment**

Currently, the primary consumers of iron oxide pigments are the construction materials industry. Established production processes include bulk-colored paving tiles manufactured using the «Besser» technology, colored wall blocks, colored bricks, colored chalk, gypsum, plasters, and other related products.



Figure 3. Yellow iron oxide pigment

Considering that classical methods of pigment production are energy-intensive due to the high cost of reagents and the complex processing schemes for iron oxides, there is an increasing demand for simplified technologies. These alternative methods facilitate the production of pigments with a diverse color palette by utilizing various industrial waste streams as raw materials, making them highly relevant in the current industrial landscape.

#### 4. Conclusions

The results of X-ray fluorescence analysis of the precipitates obtained during iron oxide precipitation from hydrochloric acid solutions in the temperature range of 25-45°C indicate that the precipitate consists of goethite  $\text{Fe}^{3+}\text{O}(\text{OH})$ . With an increase in temperature to 55°C, somalnokite ( $\epsilon\text{-Fe}_2\text{O}_3$ , iron(III) oxide) is formed.

According to the X-ray phase analysis of the precipitates obtained from sulfuric acid solutions, bernallite  $\text{Fe}^{3+}(\text{OH})_3$  was the dominant phase throughout the entire temperature range.

During iron oxide precipitation from hydrochloric acid solutions in the presence of magnesium chloride, an increase in temperature led to a decrease in the amorphous fraction and an increase in the crystalline phase content.

Due to the high amorphous content, X-ray fluorescence analysis could not be performed on precipitates obtained at 25°C and 35°C. The precipitate obtained at 45°C was identified as goethite  $\text{Fe}^{3+}\text{O}(\text{OH})$  and magnesium sulfate hydrate  $\text{MgSO}_4 \times 2\text{H}_2\text{O}$ . The precipitate obtained at 55°C contained goethite  $\text{Fe}^{3+}\text{O}(\text{OH})$  and iron oxide  $\text{Fe}_2\text{O}_3$ , with traces of  $\text{MgSO}_4 \times 1.25\text{H}_2\text{O}$  also detected. The presence of magnesium sulfate hydrate is attributed to insufficient washing of the precipitate and the presence of an amorphous phase.

In iron oxide precipitation from sulfuric acid solutions in the presence of magnesium sulfate, a temperature increase also led to a decrease in the amorphous fraction and an increase in the crystalline phase content. The precipitates obtained in the temperature range of 25-55°C contained goethite  $\text{Fe}^{3+}\text{O}(\text{OH})$  with an admixture of magnesium sulfate hydrate  $\text{MgSO}_4 \times 1.25\text{H}_2\text{O}$ .

From pure model acidic iron-containing solutions in the temperature range of 25-55°C, crystalline goethite and iron oxide was precipitated. However, in the presence of magnesium ions, a significant portion of the precipitate was amorphous, while the crystalline fraction consisted of goethite and iron oxide.

The dissolution of the +1–0.5 mm fraction of reduced iron in a 15% sulfuric acid solution at room temperature and pH 1 was followed by iron oxide precipitation using a 25% ammonia solution. The resulting product was goethite with impurities, serving as a precursor for pigment production.

To obtain yellow iron oxide pigment, hematite powder was suspended in distilled water and heated to 35-40°C. Once the target temperature was reached, 30% hydrogen peroxide was slowly added under constant stirring, followed by a 30-60-minute reaction period. The precipitate was then separated by filtration and dried at 120°C for two hours.

#### Author contributions

Conceptualization: B.K.K., A.A.U.; Data curation: B.K.K., A.A.U.; Formal analysis: A.A.U., A.O.M., N.G.L.; Funding acquisition: B.K.K., A.A.U.; Investigation: A.A.U., N.G.L.; Methodology: A.A.U., A.O.M.; Project administration: B.K.K., A.A.U.; Resources: K.K.K., A.O.M.; Software: K.K.K., A.O.M.; Supervision: B.K.K., A.A.U.; Validation: B.K.K., A.A.U.; Visualization: K.K.K., A.O.M.; Writing – original draft: B.K.K., A.A.U.; Writing – review & editing: B.K.K., A.A.U. All authors have read and agreed to the published version of the manuscript.

#### Funding

This research was funded by the Science Committee of the Ministry of Science and Higher Education of the Republic of Kazakhstan (Program-Targeted Funding BR21882140 on the theme: ‘Creation of new technological solutions for complex processing of complex metallurgical raw materials in accordance with the concept of Industry 4.0 and Digital Twin’).

#### Conflicts of interests

The authors declare no conflict of interest.

#### Data availability statement

The original contributions presented in this study are included in the article. Further inquiries can be directed to the corresponding author.

#### References

- [1] Lu, Y., Dong, W., Wang, W., Ding, J., Wang, Q., Hui, A. & Wang, A. (2018). Optimal Synthesis of Environment-Friendly Iron Red Pigment from Natural Nanostructured Clay Minerals. *Nanomaterials*, (8), 925. <https://doi.org/10.3390/nano8110925>
- [2] Belenky, E.F., Riskin, I.V. (1974). *Chemistry and Technology of Pigments*. 4th ed., revised and supplemented. Leningrad: Khimiya
- [3] Khodakov, G.S. (1972). *Fine Grinding of Building Materials*. Moscow: Stroyizdat
- [4] Brindley, G.W., Brown, G. (Eds.). (1980). *Crystal Structures of Clay Minerals and Their X-ray Identification*. Mineralogical Society, London. <https://doi.org/10.1180/mono-5>

- [5] Sverguzova, S.V., Tarasova, G.I. (2008). Pigment-Filler from Wet Separation Waste of Ferruginous Quartzites. *Construction Materials*, (6), 72–74.
- [6] Chetfield, H.V. (Eds.). (1999). *Paint Coatings*. Moscow: Khimiya
- [7] Akhnazarova, S.L., Kafarov, V.V. (1985). *Optimization Methods for Experiments in Chemical Technology* (2nd edition). Moscow: Khimiya
- [8] Fedoseeva, E.N., Zorin, A.D., Zanozina, V.F., Samsonova, L.E., Markova, M.L. & Goryacheva, N.M. (2013). Iron Oxide Pigment from Metallurgical Waste for Silicate Brick Production. *Construction Materials. Scientific-Technical and Industrial Journal*, (14), 21–24
- [9] Sverguzova, S.V., Tarasova, G.I. (2005). Production of Pigment Fillers from Ferruginous Quartzite Beneficiation Tailings. *Construction Materials*, (7), 13–15
- [10] Splinter, K., Moszyński, D. & Lenzion-Bieluń, Z. (2023). Microwave-Reactor-Based Preparation of Red Iron Oxide Pigment from Waste Iron Sulfate. *Materials*, (16), 3242. <https://doi.org/10.3390/ma16083242>
- [11] Kanykina, O.N., Chetverikova, A.G. & Mezhuyeva, L.V. (2021). Method for Producing Goethite. Patent RF No. 2748801
- [12] Larin, V.K., Bikbaev, L.Sh. & Bibik, E.G. (2018). Method for Producing Iron Oxide Pigments. Patent RF No. 2656047
- [13] Anoja, Kawsihan, D., Dissanayake, Nadeesha, Rathuwadu, H., Perera, K.E.D.Y.T., Dayananda, K.R., Koswattage, R., Mahadeva, Arnab, Ganguly, G., Das, Mantilaka, Mudiyansele, M.G.P.G., Mantilaka. (2023). Synthesis of an Eco-Inspired Anticorrosive Composite for Mild Steel Applications. *RSC Advances*, (13), 28852-28860. <https://doi.org/10.1039/d3ra02857g>
- [14] Zhao, L., Wang, L., Qi, T., China, D., Zhao, H. & Liu, Y. (2014). A Novel Method to Extract Iron, Titanium, Vanadium, and Chromium from High-Chromium Vanadium-Bearing Titanomagnetite Concentrates. *Hydrometallurgy*, (149), 106–109. <https://doi.org/10.1016/j.hydromet.2014.07.014>
- [15] Li, X., Wang, C., Zeng, Y., Li, P., Xie, T. & Zhang, Y. (2016). Bacteria-assisted preparation of nano  $\alpha$ -Fe<sub>2</sub>O<sub>3</sub> red pigment powders from waste ferrous sulfate. *Journal of Hazardous Materials*, (317), 563-569. <https://doi.org/10.1016/j.jhazmat.2016.06.021>
- [16] Daenzer, R., Feldmann, T. & Demopoulos, G. (2015). Oxidation of Ferrous Sulfate Hydrolyzed Slurry-Kinetic Aspects and Impact on As(V) Removal. *Industrial & Engineering Chemistry Research*, (54), 1738-1747. <https://doi.org/10.1021/IE503976K>
- [17] Chen, M., Lu, G., Guo, C., Yang, C., Wu, J., Huang, W., Yee, N. & Dang, Z. (2015). Sulfate migration in a river affected by acid mine drainage from the Dabaoshan mining area, *South China. Chemosphere*, (119), 734-743. <https://doi.org/10.1016/j.chemosphere.2014.07.094>
- [18] Deng, L., Ma, G., & Chen, Q. (2023). Preparation of Iron Phosphate Battery Materials from Industrial Ferrous Sulfate Waste by Liquid Phase Method. *Integrated Ferroelectrics*, (234), 67-78. <https://doi.org/10.1080/10584587.2023.2191550>
- [19] Li, C., Zhigan, D., Wei, C., Fan, G., Xingbin, L., Minting, L. & Wang, Y. (2018). Production of low-sulfur hematite by hydrothermal oxydrolisis of ferrous sulfate. *Hydrometallurgy*, (178), 294-300. <https://doi.org/10.1016/j.hydromet.2018.05.012>
- [20] Gázquez, M., Contreras, M., Pérez-Moreno, S., Guerrero, J., Casas-Ruiz, M. & Bolívar, J. (2021). A Review of the Commercial Uses of Sulphate Minerals from the Titanium Dioxide Pigment Industry: The Case of Huelva (Spain). *Minerals*, (11), 575. <https://doi.org/10.3390/MIN11060575>
- [21] Lavrynenko, O. & Shchukin, Y. (2015). Development of the Hydroxysulfate Green Rust on the Steel Surface Contacting with Water Ferric and Ferrous Salt Solutions. *Mineralogical Journal*, 37(2), 23-36. <https://doi.org/10.15407/mineraljournal.37.02.023>
- [22] Ke, P., Liu, Z. & Li, L. (2018). Synthesis, characterization, and property test of crystalline polyferric sulfate adsorbent used in treatment of contaminated water with a high As(III) content. *International Journal of Minerals, Metallurgy, and Materials*, (25), 1217-1225. <https://doi.org/10.1007/s12613-018-1674-8>
- [23] Thibault, Y., McEvoy, J. G. & Beauchemin, S. (2020). Iron and sulphur management options during Ni recovery from (bio)leaching of pyrrhotite tailings, Part 1: Mechanisms of low-temperature transformation from goethite and jarosite to magnetic spinel. *Minerals Engineering*, (150), 106265. <https://doi.org/10.1016/j.mineng.2020.106265>
- [24] Zhang, C., Wang, A., Jiang, H. & Deng, Y. (2019). Magnetic Seed-Assisted Iron Recovery from the Reductive Leaching Solution in Hydrometallurgical Process. *Transactions of the Indian Institute of Metals*, 1-7. <https://doi.org/10.1007/s12666-019-01728-7>
- [25] Ouyang, B., Lu, X., Liu, H., Li, J., Zhu, T., Zhu, X., Lou, J. & Wang, R. (2014). Reduction of jarosite by *Shewanella oneidensis* MR-1 and secondary mineralization. *Geochimica et Cosmochimica Acta*, (124), 54-71. <https://doi.org/10.1016/J.GCA.2013.09.020>
- [26] Liu, J., Hu, G., Du, K., Peng, Z., Wang, W. & Cao, Y. (2014). The new technique on separation of Cr and Fe as well as Ni-Co-Mn impurity in leaching sulfate solution of ferrochrome alloy. *Russian Journal of Non-Ferrous Metals*, (55), 533-537. <https://doi.org/10.3103/S1067821214060157>
- [27] Maia, L. C., dos Santos, G. R., Gurgel, L. V. A. & Carvalho, C. F. (2020). Iron recovery from the coarse fraction of basic oxygen furnace sludge. *Environmental Science and Pollution Research*, 1-13. <https://doi.org/10.1007/s11356-020-09910-x>
- [28] Tikhonov, R. D., Polomoshnov, S., & Kostuk, D.V. (2020). Spectrophotometric Monitoring of Chloride Electrolyte for the Electrochemical Deposition of Permalloy. *Russian Microelectronics*, (49), 467-471. <https://doi.org/10.1134/S1063739720070136>
- [29] De, E.R. (2017). United States Patent Office 1. Retrieved from: <https://consensus.app/papers/united-states-patent-office-1-de/69d038e1bc5650a5b7ccee1e46db3bd5/>
- [30] Sklute, E., Jensen, B., Rogers, A. D. & Reeder, R. (2014). Visible and Infrared Spectral Characteristics and Morphology of Amorphous Iron Sulfates. Conference Paper. Retrieved from: <https://consensus.app/papers/visible-and-infrared-spectral-characteristics-and-sklute/h/e421afe08b36528990db412ff36c5f34>
- [31] Johnston, S., Morgan, B. & Burton, E. (2016). Legacy impacts of acid sulfate soil runoff on mangrove sediments. *Chemical Geology*, (427), 43-53. <https://doi.org/10.1016/J.CHEMGEO.2016.02.013>
- [32] Shi, Z., Wang, M., Zhang, G.K. & Zhang, L. (2014). Leaching and Kinetic Modeling of Pyrite Cinder in Sulphuric Acid. *Asian Journal of Chemistry*, 25(1), 105-109. <https://doi.org/10.14233/ajchem.2013.12810>
- [33] Jiang, S. & Wang, Z. (2014). Method for precipitating iron from goethite containing ferro-nickel mixed solution.
- [34] Splinter, K., Moszyński, D. & Lenzion-Bieluń, Z. (2023). Microwave-Reactor-Based Preparation of Red Iron Oxide Pigment from Waste Iron Sulfate. *Materials*, 16(8), 3242. <https://doi.org/10.3390/ma16083242>

## Ильменит балқымасының металл құрамдас бөлігінен темір оксидті пигмент алу

Б.К. Кенжалиев, А.А.Ультаракова\*, Н.Г. Лохова, К.К. Касымжанов, А.Ө. Мұқанғалиева

Металлургия және қен байыту институты, Алматы, Қазақстан

\*Корреспонденция үшін автор: [ult.alma@mail.ru](mailto:ult.alma@mail.ru)

**Андатпа.** Обухов кен орнының кондициялық емес ильменит концентраттарын балқыту қалпына келтірілген Темірдің едәуір мөлшерінің пайда болуына әкеледі, бұл оны темір оксиді пигменттерін өндіруде қолдануға мүмкіндік береді. Өнеркәсіптік қалдықтарды қосылған құны бар материалдарға айналдыру тұрақты материалтану саласындағы қазіргі тенденцияларға сәйкес келеді. Бұл зерттеу магний қоспаларының тұндыру процесіне әсеріне ерекше назар аудара отырып, гетит түзу үшін аммиакты қолдана отырып, күкірт және тұз қышқылдарының ерітінділерінен екі валентті Темірдің тұндырылуын зерттейді. Магнийдің болуы гетиттің түзілуін тежейтіні анықталды, бұл пигменттің өнімділігі мен сапасының айтарлықтай төмендеуіне әкеледі. Құрамында темір бар ерітінді күкірт қышқылында ұсақ ұнтақталған қалпына келтірілген темірді еріту арқылы, содан кейін 25% аммиак ерітіндісін пайдаланып темір оксидтерін тұндыру арқылы дайындалды. Синтезделген темір оксиді пигменті сутегі асқын тотығымен өңдеу арқылы одан әрі тазартылды, бұл пигменттің біртекті құрамын және түс тұрақтылығын жақсартты. Бұл тәсіл қалдықтарды жоюға қатысты экологиялық мәселелерді шеше отырып, өнеркәсіптік жанама өнімдерді қайта өңдеудің өміршең әдісін ұсынады. Нәтижелер металлургиялық қалдықтарды әртүрлі өнеркәсіптік қолданбаларға жарамды жоғары сапалы темір оксиді пигменттері үшін прекурсор ретінде пайдалану әлеуетін көрсете отырып, пигментті синтездеудің ресурс тиімді әдістерін дамытуға ықпал етеді.

**Негізгі сөздер:** темір қоспасы, күкірт қышқылы, темір купоросы, тұндыру, гетит, пигмент.

## Получение железооксидного пигмента из металлической составляющей плавки ильменита

Б.К. Кенжалиев, А.А. Ультаракова\*, Н.Г. Лохова, К.К. Касымжанов, А.О. Муканғалиева

Институт металлургии и обогащения, Алматы, Казахстан

\*Автор для корреспонденции: [ult.alma@mail.ru](mailto:ult.alma@mail.ru)

**Аннотация.** Плавка некондиционных ильменитовых концентратов Обуховского месторождения приводит к образованию значительных количеств восстановленного железа, что открывает возможность его использования в производстве железооксидных пигментов. Трансформация промышленных отходов в материалы с добавленной стоимостью соответствует современным тенденциям в области устойчивого материаловедения. В данном исследовании изучается осаждение двухвалентного железа из растворов серной и соляной кислот с использованием аммиака для образования гетита, при этом особое внимание уделяется влиянию примесей магния на процесс осаждения. Было обнаружено, что присутствие магния ингибирует образование гетита, что приводит к значительному снижению выхода и качества пигмента. Железосодержащий раствор готовили путем растворения тонкоизмельченного восстановленного железа в серной кислоте с последующим осаждением оксидов железа с использованием 25%-ного раствора аммиака. Синтезированный железооксидный пигмент дополнительно очищали путем обработки перекисью водорода, что обеспечивало более однородный состав пигмента и улучшенную стабильность цвета. Этот подход предлагает жизнеспособный метод переработки промышленных побочных продуктов, одновременно решая экологические проблемы, связанные с утилизацией отходов. Результаты способствуют развитию ресурсоэффективных методов синтеза пигментов, демонстрируя потенциал использования металлургических отходов в качестве прекурсора для высококачественных пигментов оксида железа, подходящих для различных промышленных применений.

**Ключевые слова:** сплав железа, серная кислота, железный купорос, осаждение, гетит, пигмент.

### Publisher's note

All claims expressed in this manuscript are solely those of the authors and do not necessarily represent those of their affiliated organizations, or those of the publisher, the editors and the reviewers.

<https://doi.org/10.51301/ejsu.2025.i1.03>

## Investigation of self-propagating high-temperature synthesis based on TiB+Ti composite powders

A. Myrzakhan<sup>1</sup>, E. Korosteleva<sup>2</sup>, G. Smailova<sup>1\*</sup>, A. Uderbaeva<sup>1</sup>

<sup>1</sup>Satbayev University, Almaty, Kazakhstan

<sup>2</sup>National Research Tomsk Polytechnic University, Tomsk, Russia

\*Corresponding author: [g.smailova@satbayev.university](mailto:g.smailova@satbayev.university)

**Abstract.** This article considers modern methods of increasing wear resistance and reliability of machine parts using composite materials, especially in the field of powder surfacing and synthesis of metal-matrix composites. One of the effective methods is self-propagating high-temperature synthesis (SHS), which allows obtaining composite coatings with improved mechanical and thermal properties. Powder surfacing methods, such as electron beam surfacing (EBF), provide wear-resistant, heat-resistant and hardening coatings on a titanium base. Powders of titanium and its alloys are obtained by reduction of oxides with calcium hydride, which contributes to the formation of materials with high strength and good flowability. Special attention is paid to titanium boride as a strengthening phase for composites. The use of these technologies contributes to a significant increase in the durability and reliability of machines and mechanisms, which leads to resource saving and reduction of operating costs. The studies include the analysis of structural characteristics of the obtained powders and coatings, as well as the determination of their physical and mechanical properties. The variations in these properties as a function of the titanium binder content in the composite powder are analyzed. The description of the microstructure of powders and coatings, as well as the influence of composition on their characteristics, allows us to draw conclusions about the possibility of using these materials to create functional coatings with improved performance characteristics, such as increased wear resistance and heat resistance. The results of the study can be useful for the development of new materials with improved operational properties for use in various industries.

**Keywords:** composite powder, titanium boride, titanium, electron-beam coatings, powder surfacing, self-propagating high-temperature synthesis.

Received: 24 October 2024

Accepted: 14 February 2025

Available online: 28 February 2025

### 1. Introduction

In modern manufacturing, the introduction of highly efficient technological processes is a key factor in advancing the engineering industry. The primary objective of the mechanical engineering sector today is to ensure high product quality at minimal cost and within tight deadlines. At the same time, the requirements for finished products remain stringent: materials must combine reliability, precision in manufacturing, and an optimal balance between low specific weight and high strength while providing sufficient hardness, wear resistance, and (or) chemical resistance of the surface layer of parts. Enhancing the operational efficiency of dynamic structures (aerospace, energy, construction, and others) is possible through the use of materials with specialized properties. One such group of materials is composite materials (CMs), which consist of a combination of two or more chemically and structurally different components distributed throughout the volume of the part. This allows the development of materials with tailored properties. Composite materials outperform individual components in strength, thermal resistance, and especially reliability. They exhibit unique properties not

found in their individual constituents and demonstrate 50-100% greater resistance to transient loads and fatigue limits compared to conventional alloys. They also have a higher modulus of elasticity and specific strength and are less prone to crack formation.

Powder metallurgy is one of the most promising areas of modern manufacturing. This approach enables the production of high-volume structural elements for general applications as well as specialized materials such as antifriction, friction, electrical contact, highly porous, hard, and refractory materials. The use of powder technology allows for the enhancement of useful properties in existing materials, for example, increasing material utilization efficiency up to 80-96% by influencing their structural characteristics. Powders differ in chemical properties (content of base metal, impurities, contaminants, and toxicity), physical properties (shape, size, specific surface area, true density, particle microhardness), and technological properties (bulk density, flowability, compactability, formability, and pressability). The main advantage of powder metallurgy lies in the ability to produce components with diverse compositions. This method allows easy fabrication of products from refractory materials (e.g.,

© 2025. A. Myrzakhan, E. Korosteleva, G. Smailova, A. Uderbaeva

[Myrzakhan.Akbota@stud.satbayev.university](mailto:Myrzakhan.Akbota@stud.satbayev.university); [elenak@tpu.ru](mailto:elenak@tpu.ru); [g.smailova@satbayev.university](mailto:g.smailova@satbayev.university); [a.uderbaeva@satbayev.university](mailto:a.uderbaeva@satbayev.university)

Engineering Journal of Satbayev University. eISSN 2959-2348. Published by Satbayev University

This is an Open Access article distributed under the terms of the Creative Commons Attribution License (<http://creativecommons.org/licenses/by/4.0/>), which permits unrestricted reuse, distribution, and reproduction in any medium, provided the original work is properly cited.

ceramics) and from mixtures of metallic powders and refractory compounds, such as metal-ceramic composites. Additionally, powder metallurgy enables the production of components from metals that cannot form alloys in the molten state due to significant differences in melting temperatures (e.g., tungsten and copper). This method is also effective for producing metal-nonmetal composites, such as copper-graphite or aluminum-aluminum oxide.

Another advantage of powder material is their structural homogeneity. During the manufacturing of products using powder metallurgy, powders are thoroughly mixed in advance to achieve uniform particle distribution in the charge. As a result, products made from such powders exhibit a consistent distribution of components throughout their entire volume. Practice has shown that using pure powders allows for the production of materials with lower impurity content compared to cast materials. This is because sintering occurs in an inert environment or vacuum, preventing the formation of oxides, nitrides, and other undesirable chemical compounds. Thus, it is crucial that the composition and distribution of elements in the final product, obtained through powder metallurgy, remain the same as during the initial powder mixing and charge preparation stages. Powder metallurgy technology enables the production of precision components and is also used to create materials with special properties or specified characteristics that cannot be achieved by any other method.

The process of obtaining metallic powder is the first and one of the key operations in powder metallurgy. The chemical composition, structure, and other characteristics of powders depend both on the production method and the properties of the metal used.

Powder production methods vary depending on the required dispersion and volume and include the following main techniques:

1. Mechanical grinding;
2. Atomization of melts with compressed air;
3. Reduction of ore or scale;
4. Electrolytic deposition
5. Explosion of a conductor with an electric current

From an economic standpoint, the most efficient methods are ore or scale reduction and atomization of melts with compressed air. Conductor explosion is used to obtain powders from electrically conductive materials, while mechanical grinding of certain powders requires consideration of their separation tendencies. In industry, other specialized methods are also employed, such as thermal decomposition of volatile compounds, precipitation, carburization, and other advanced techniques.

## 2. Materials and methods

The technological process of obtaining a product begins with the preparation of a powder mixture that includes several different powder components. First, the powders are weighed and then thoroughly mixed in rotating drums, mills, mixers, or other mechanical devices. This results in a homogeneous powder mixture with uniformly distributed particles of various types. The prepared charge is then shaped into a powder blank with specified form, dimensions, and density. During this stage, the initial powder volume decreases as consolidation occurs. Powder compaction is achieved by pressing it in a metal die under pressure, resulting in a solid pressed part that closely resembles the final product in shape and size.

However, since the process of powder compaction is quite complex, predicting the exact outcome of pressing is difficult, as different powders behave differently, and even slight changes in composition or substitution of powder grades can alter the result. Therefore, the pressing load must be selected individually for each mixture. Some powder mixtures do not compact properly, even under high loads, leading to crumbling or cracking of the products. In most cases, cold pressing is used, but it does not always provide the necessary mechanical strength for the blanks, and under low loads, such blanks may break apart. To prevent this, plasticizers or other additives are introduced into the powder mixture before pressing to improve particle adhesion without taking up much volume or affecting the final properties of the products. After pressing, the powder blanks undergo sintering to achieve the required mechanical properties and impart the necessary physical and chemical characteristics. Sintering is one of the key processes in powder metallurgy, largely determining the final properties of materials and products. This process involves a complex combination of various physicochemical phenomena occurring simultaneously or sequentially during the heating of the compact or free powder.

Some of these phenomena are associated with the typical effects of high temperature on polycrystalline materials, while others are specific to porous powder bodies. The primary goal of sintering is to achieve the desired material properties that develop during the heating of the initial powder body. In the process of heating to high temperatures, two main types of sintering can occur: solid-phase sintering, in which no liquid phase is formed, and liquid-phase sintering, in which low-melting components of the powder mixture partially melt. When examining the sintering processes of multicomponent powder systems, it is necessary to consider several characteristics unique to this process. First, the reduction of free energy depends not only on factors typical of single-component powders and heterodiffusion, which facilitates concentration equalization in the system, but also on the formation of interphase surfaces, whose energy is usually lower than the surface energy at the boundary between a substance and a void. The progress of the sintering process is largely determined by the phase diagrams of the components in the multicomponent system. The kinetics of densification and changes in the physical and mechanical properties of the material depend on the extent of alloy formation during the process. Unlike single-component systems, where diffusion processes typically promote densification, in multicomponent systems, heterodiffusion can slow down shrinkage. After sintering is completed, the product undergoes additional processing, such as finishing, calibration, and heat treatment.

Among the various physicochemical and physico-mechanical processes occurring in the powder medium during processing, one of the key factors is interparticle contact interaction. Depending on the type of impact (electron-beam surfacing, selective laser melting, plasma sintering, vacuum sintering, self-propagating high-temperature synthesis (SHS), etc.), this interaction may be solid-phase or occur in the presence of a liquid phase. As a result, even when using the same initial components, different processes may take place, such as shrinkage or volumetric growth with the formation of a large number of pores.

Each powder system has its own specific features, which are determined by equilibrium phase diagrams for the selected elements. Although powder technological processes are inherently non-equilibrium, primary parameters (concentrations, temperature regimes) are typically determined based on equilibrium diagrams while considering possible chemical reactions [1].

In this study, the main focus is on self-propagating high-temperature synthesis (SHS) of metal-matrix composite materials [2,3]. SHS is one of the promising methods for obtaining composite materials, based on the interaction of two or more elements in an exothermic reaction, which occurs in the form of layer-by-layer combustion or a thermal explosion. This synthesis method relies on localized exothermic reactions that release heat, allowing the exothermic reaction wave to propagate throughout the entire volume of the material [4]. This method has several advantages, such as reduced energy consumption, increased process efficiency, and improved product purity. The primary method of initiating an SHS reaction involves the local application of a thermal impulse to the surface of the system (e.g., using an electric coil, spark discharge, laser beam, etc.), which leads to the formation of a combustion wave that then propagates through the unheated starting material [5].

The SHS process can be carried out in three ways: gasless combustion, filtration combustion, and hybrid combustion. Gasless combustion is used in «solid-solid» systems, filtration combustion in «metal-gas» systems, while hybrid combustion combines both previous methods. In filtration combustion, gas filtration can be either spontaneous or forced, depending on the gas supply, and is classified based on the direction of the combustion front relative to the filtering gas flow as either co-current or counter-current. For weakly exothermic reactions or mixtures with a high content of inert fillers, preheating of the charge in a furnace is required to initiate the synthesis reaction. In SHS processes, the charge can be located in a vacuum, in open air, or in an inert or reactive gas under pressure. Figure 1 presents a schematic representation of the SHS technology for powder production.

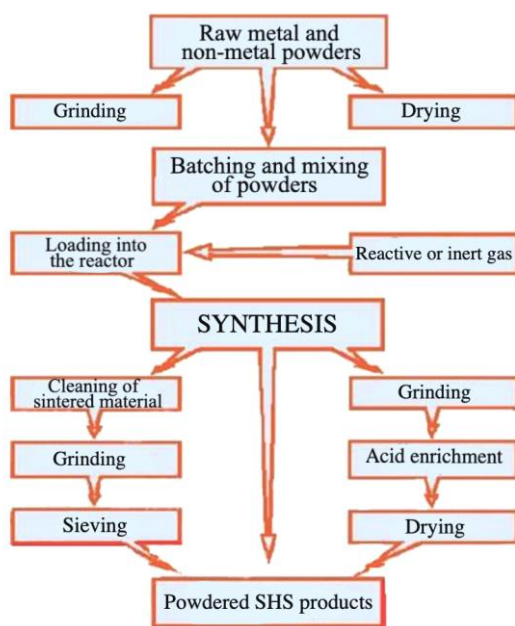


Figure 1. Schematic representation of the SHS technology for powder production

The SHS method enables an increase in productivity at significantly lower costs compared to vacuum sintering of powder mixtures, offering significant advantages in the following aspects:

- product output per unit time;
- energy consumption for batch production;
- equipment and maintenance costs.

When using the SHS method, certain challenges arise related to production characteristics such as controlling the composite structure and matrix properties. In the process of vacuum sintering of powder mixtures, it is possible to flexibly regulate the heating rate and isothermal holding temperature, allowing for adjustments in phase composition, structural dispersion, and sintered material strength. In SHS technology, parameters that influence the phase composition and properties of the final product include the composition, degree of compaction, and volume of the reaction mixture, the dispersion of powder reactants, and the initial temperature at which the synthesis reaction begins [6-10]. Thus, the process proceeds based on predefined parameters that determine the course of the reaction.

The task of improving the reliability and durability of machine and mechanism components is often directly related to the wear resistance of their friction surfaces. Enhancing the wear resistance of parts extends the service life of machines, leading to significant savings in financial resources, labor, and materials.

One of the most effective ways to improve the reliability of machine components and mechanisms in mechanical engineering is the application of various coatings to the working surfaces of parts. Wear-resistant coatings for titanium alloys provide high wear resistance due to their bonding with metallic materials. Powder surfacing is widely used as a method for obtaining wear-resistant coatings for titanium and its alloys. To significantly enhance wear resistance and restore the dimensions of worn-out parts, surfacing is performed on the surfaces that experience continuous wear. Pre-prepared surfacing alloys in the form of rods or tubes are applied. Surfacing is the process of depositing a layer of metal onto a part's surface to modify its dimensions or impart specific properties such as hardness, corrosion resistance, and wear resistance. The composition of the powder filler material is selected to create composite coatings with a matrix structure containing dispersed particles of refractory compounds, such as carbides, borides, and nitrides. Reinforcing phases may include TiC, TiB, TiN, and TiB<sub>2</sub>.

Special attention is given to titanium boride as a hard and refractory strengthening phase in titanium-based metal-matrix composites. The formation of «titanium boride + titanium» composites can be achieved through the «titanium + B<sub>4</sub>C» reaction [11-12], as well as by synthesizing pure powders [13-14]. The study of composite powders and coatings derived from them has significant practical importance. To produce titanium boride coatings, electron beam surfacing is used, in which an electron beam is employed to create coatings with specified shapes and properties on the surface of a part. This technology enables the creation of both single-layer and multilayer coatings for various applications, including wear-resistant, heat-resistant, and strengthening coatings. Electron beam surfacing is performed using powders with a particle size range of 50 to 350 μm. Depending on the shape of the part and coating requirements, different application schemes may be used. For example, an electron beam with a

power of several kilowatts can be focused into a spot less than a millimeter in diameter. When directed at the surface of a part, the metal in the beam's impact area instantly melts while the rest of the part remains cool. Once the beam is removed, the molten metal immediately solidifies. The principle of electron beam surfacing is illustrated in Figure 2. The electron beam creates a molten metal pool on the surface of the part. Powder is fed into this molten pool via a dosing system, and the particles form a coating with the required properties on the surface. The workpiece being surfaced moves within a vacuum chamber relative to a stationary electron gun and powder feeder, or the electron gun and powder feeder move relative to a stationary workpiece.

The technology of multi-pass electron beam surfacing is based on the phenomenon of «freezing» the powder into the liquid-metal melt pool. With each successive pass, a new portion of powder is incorporated into the melt while the previously deposited layer is remelted. The powder fed into the molten metal pool accelerates the crystallization process, promoting the formation of a fine-grained structure and reducing residual stresses in the deposited coating. The required thickness of the deposited layer is achieved by adjusting the powder feed rate or increasing the number of passes. A higher crystallization rate contributes to the formation of a uniform, fine-dispersed structure in the deposited layer [6-7].

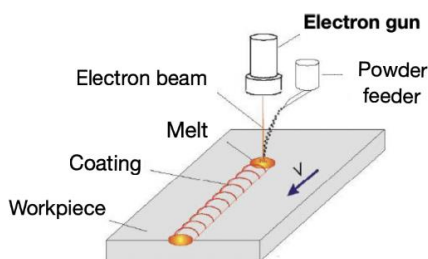


Figure 2. Principle of electron beam surfacing

Powders with particle sizes smaller than 50  $\mu\text{m}$  have insufficient flowability in a vacuum, making it difficult to feed them into the molten pool. Powders larger than 350  $\mu\text{m}$  require higher energy input for melting, which can lead to excessive penetration of the base material and increased residual stresses. The key parameters characterizing the surfacing process include the energy and current of the electron beam, its diameter, the size and shape of the beam scan on the surface of the part, the movement speed of the workpiece, and the powder feed rate. A distinctive feature of electron beam surfacing is the presence of a prolonged transition zone between the base material and the coating. Since the powder melts directly on the surface of the part, the material properties gradually change from the base to the coating.

Titanium and titanium alloy powders are obtained by reducing metal oxides with calcium hydride, a method developed in the 1950s. The choice of calcium hydride as a reducing agent is due to its high reactivity, which allows it to reduce almost all metal and non-metal oxides regardless of their thermodynamic activity. At the same time, no solid solutions or chemical compounds of calcium with the «reduced» metals are formed. The reduced titanium and alloy powders have an irregular shape and a highly developed particle surface, which allows them to be easily compacted at relatively low pressing pressures in rigid molds, as well as by hydrostatic pressing in flexible casings. These powders can

be easily rolled into strips and sintered in a vacuum or a neutral atmosphere. Titanium and titanium-based alloy powders are used in the production of corrosion-resistant filters for fine purification of technical liquids in the form of porous rolled sheets. Titanium powders have also found applications in medicine for the manufacture of implants, in the food industry for producing regenerative filters in purification systems for drinking and mineral water, juices, and beverages, in the production of highly reliable pyrotechnic devices, and in non-dispersible porous getters (gas absorbers) with high sorption capacity and absorption rate. Additionally, these powders are used for manufacturing aluminum and other metal composites, watch mechanism components, and acid-resistant equipment. They are also employed for plasma and microplasma coating applications [7].

The first attempts to obtain titanium boride through surfacing or sintering of compressed powder compacts were made by Moissan [15-16] and Wedekind [17]. Titanium boride has gained widespread use in many modern industries due to its numerous technical advantages relevant to different fields. Figure 3 presents the phase diagram of B-Ti composites.

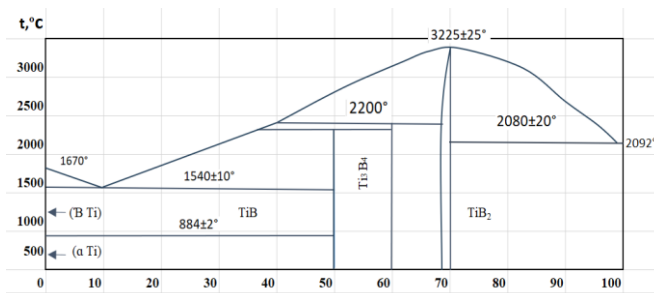


Figure 3. Phase diagram of B-Ti composites

In metallurgy and mechanical engineering, titanium diboride is primarily used as a component of powder mixtures for coating and surfacing applications. Additionally, titanium boride powder is utilized in the production of heat-resistant, refractory, and wear-resistant alloys, as well as a base material for high-temperature cutting tools, in cermets for nuclear technology, for manufacturing thermocouple sheathings, and in the tool industry as an abrasive material and a filler in diamond wheels and pastes for processing various materials.

Matrix and reinforcing materials are typically selected based on the following criteria [18]:

- both materials should have low density.
- the modulus of elasticity of the reinforcing material should be significantly higher than that of the matrix material (considering the relatively low modulus of elasticity of Ti alloys);
- the matrix and reinforcing materials should have similar coefficients of thermal expansion;
- the materials must be chemically stable relative to each other to prevent the formation of unfavorable regions along the boundaries between the matrix and the reinforcing material.

In our research, the TiB + Ti metal-matrix composite was synthesized using the SHS method.

### 3. Results and discussion

In this study, composite powders were obtained using the self-propagating high-temperature synthesis (SHS) method from powder mixtures of titanium grade TPP-8 with a parti-

cle size of 50-100 μm and amorphous technical boron grade «A» with varying titanium binder content (20 vol.%, 30 vol.%, 40 vol.%, 50 vol.%, 60 vol.%). To prepare the powder mixtures, the powders were blended, and their chemical composition, along with the volumetric percentage of each component, is presented in Table 1. Composite powders with 50 vol.% and 60 vol.% metallic matrixes were prepared by mixing in a gravity mixer of the «drunken barrel» type with steel balls for 3-4 hours to achieve a homogeneous structure.

**Table 1. Batching for SHS composites TiB+%Ti (20 vol.% – 60 vol.%)**

Vol. % Ti	Batching, wt. %		Theoretical density, g/cm <sup>3</sup>
	Ti	B	
TiB + 20 vol.% Ti	84.86	15.14	3.9675
TiB + 30 vol.% Ti	86.57	13.43	4.022
TiB + 40 vol.% Ti	88.33	11.67	4.079
TiB + 50 vol.% Ti	90.14	9.86	4.141
TiB + 60 vol.% Ti	91.99	8.01	4.206

Samples for synthesis were obtained using the cold double-sided pressing method in a cylindrical mold MS-500 (Figure 4). The pressure was selected to achieve an initial porosity of 40-45%. As a result, the samples had a cylindrical shape with a diameter of 25 mm and a height of up to 10 mm.

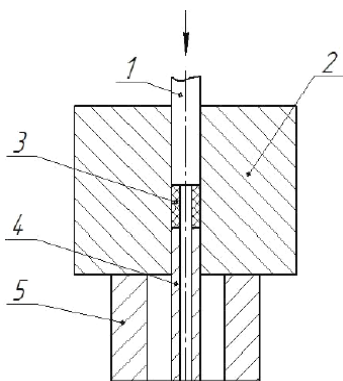


**Figure 4. Diagram of double-sided pressing: 1 - upper punch; 2 - die; 3 - pressed charge; 4 - lower punch; 5 - backing plate**

SHS composite powders were synthesized from pre-pressed tablets without preliminary heating, in an argon atmosphere with an excess pressure of about 0.5 atm, followed by slow cooling in the reactor (Figure 5). To ignite the powder and initiate the combustion wave, a small layer of Ti+Si powder mixture was sprinkled onto the Ti+B tablets.

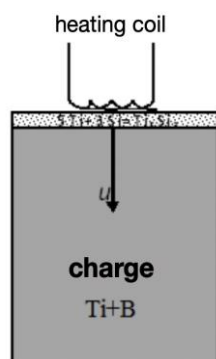
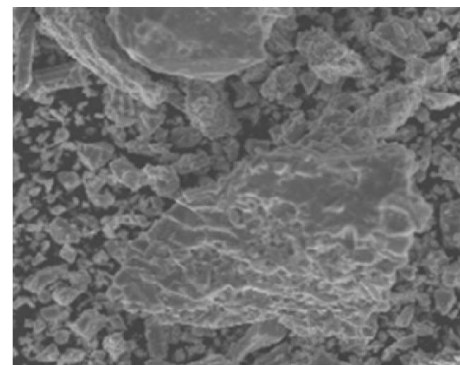


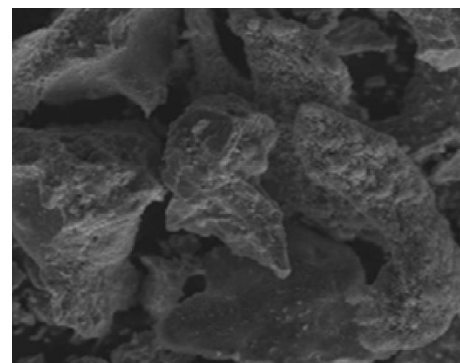
**Figure 5. Implementation of SHS composite powders without preliminary charge preheating**

The obtained porous SHS compacts were crushed, and a sieving process was used to isolate the fraction suitable for surfacing, ranging from 56 to 200 μm. The synthesized powders initially had different metallic binder contents (20 vol.%, 30 vol.%, 40 vol.%, 50 vol.%, 60 vol.%). To achieve high-quality coatings and improve the weldability of the powders during electron beam surfacing (EBS), the SHS powders were diluted with titanium powder up to 80 vol.% Ti. Electron beam coatings made from composite powders of «titanium boride + 20% and 50% titanium» were applied in a vacuum using an EBS setup at the Institute of Solid-State Chemistry and Mechanochemistry of the Siberian Branch of the Russian Academy of Sciences (ISSCM SB RAS). This setup consisted of an electron source, a scanning electron beam control system, a powder feeder, and a manipulator for moving the substrate relative to the scanning electron beam. Composite powders were obtained through layer-by-layer combustion of cylindrical compacts made from powder mixtures of titanium grade TPP-8 and amorphous technical boron grade «A» in an argon atmosphere.

The combustion was initiated by heating an ignition tablet using a molybdenum coil. The synthesis was carried out in a sealed reactor under an argon atmosphere with an excess pressure of approximately 0.5 atm, followed by slow cooling in the reactor. The porous SHS compacts were crushed, and a sieving process was used to isolate the fraction suitable for surfacing, ranging from 56 to 200 μm. The structure and phase composition of the SHS powders and coatings were analyzed using equipment from the «Nanotech» Shared Research Facility at ISSCM SB RAS. The methods included X-ray phase analysis (DRON-7 diffractometer, Burevestnik, Russia, CuKα radiation) and optical metallography (AXIOVERT-200MAT, Zeiss, Germany). After crushing, the SHS composite powder predominantly had a fragmented shape (Figure 6).



(a)



(b)

**Figure 6. Morphology of SHS powder: (a) – TiB + 20% Ti; (b) – TiB + 50% Ti**

The typical microstructure of the composite powder is shown in Figure 7a. The powder product synthesized with a low titanium binder content (20-40%) consists of titanium boride agglomerates or individual large needle-like structures. The structure of SHS products with a higher titanium content (50-60%) and prior mechanical activation is more dispersed (Figure 7b).

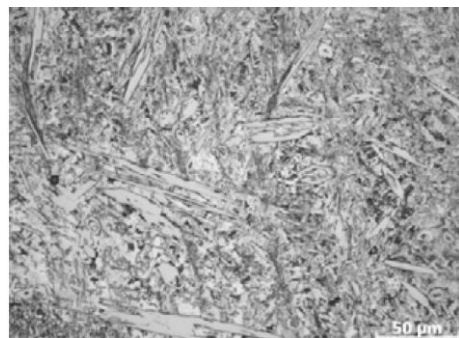


(a)

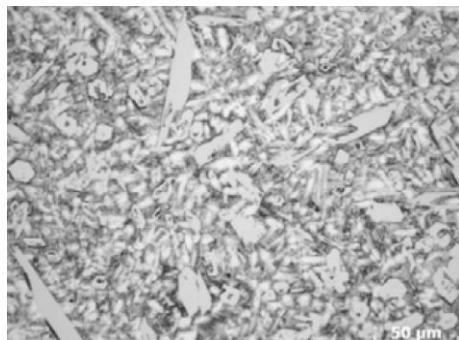


(b)

**Figure 7. Microstructure of SHS powder: (a) – TiB + 20% Ti; (b) – TiB + 50% Ti**



(a)



(b)

**Figure 8. Microstructure of the surfacing: (a) – TiB + 20 → 80% Ti; (b) – TiB + 50 → 80% Ti**

X-ray phase analysis of SHS powders revealed that in all cases of «titanium-boron» synthesis, a multiphase material was obtained, with titanium monoboride as the primary phase. To improve the weldability, titanium powder was added to the composite powders with different titanium binder contents (20% and 50%) in amounts sufficient to achieve powder mixtures with an integral binder content of 80%. The microstructure of the coatings deposited using powder mixtures containing composite powders of the two studied compositions is shown in Figure 8.

#### 4. Conclusions

Composite powders of «titanium monoboride + titanium» were obtained and studied using the self-propagating high-temperature synthesis (SHS) method.

Electron beam coatings deposited using composite powders exhibited hardness and abrasive wear resistance that were 2.2 and 3.7 times higher, respectively, than those of the titanium alloy VT-1-0.

#### Author contributions

Conceptualization: A.M., A.U.; Data curation: E.K, G.S., A.U.; Formal analysis: A.M., E.K., G.S.; Funding acquisition: E.K.; Investigation: A.M., E.K.; Methodology: A.M., E.K., A.U.; Project administration: A.M., A.U.; Resources: E.K, G.S.; Software: E.K., A.U.; Supervision: E.K, G.S., A.U.; Validation: G.S., A.U.; Visualization: E.K, G.S., A.U.; Writing – original draft: A.M.; Writing – review & editing: A.M., G.S., A.U. All authors have read and agreed to the published version of the manuscript.

#### Funding

This research was funded by Russian Foundation for Basic Research (grant No. 16-48-700381).

#### Conflicts of interests

The authors declare no conflict of interest.

#### Data availability statement

The original contributions presented in this study are included in the article. Further inquiries can be directed to the corresponding author.

#### References

- [1] Korosteleva, E.N. & Korzhova, V.V. (2020). Structure and phase composition of metal-matrix composites (TiB) – Ti obtained by SHS and vacuum sintering. *Russian Physics Journal*, (63), 1195-1201. <https://doi.org/10.1007/s11182-020-02159-4>
- [2] Liang, Y.H., Wang, H.Y., Yang, Y.F., Zhao, R.Y. & Jiang, Q.C. (2008). Effect of Cu content on the reaction behaviors of self-propagating high-temperature synthesis in Cu–Ti–B<sub>4</sub>C system. *Journal of Alloys and Compounds*, 462(1–2), 113-118. <https://doi.org/10.1016/j.jallcom.2007.08.033>
- [3] Zhang, L., Wang, H.Y., Li, S.T., Liu, C. & Jiang, Q.C. (2009). Influence of reactant particle size on products of self-propagating high-temperature synthesis in 30 wt.% Cr–Ti–B<sub>4</sub>C system. *Journal of Alloys and Compounds*, 468(1–2), 143-149. <https://doi.org/10.1016/j.jallcom.2008.01.007>
- [4] Levashov, E.A., Mukasyan, A.S., Rogachev, A.S. & Shtansky, D.V. (2016). Self-propagating high-temperature synthesis of

- modern materials and coatings. *International Materials Reviews*, 62(4), 203–239. <https://doi.org/10.1080/09506608.2016.1243291>
- [5] Sahay, S.S., Ravi Chandran, K.S. & Atri, R. (1999). Evolution of microstructure and phases in situ processed Ti–TiB composites containing high volume fractions of TiB whiskers. *Journal of Materials Research*, (14), 4214–4223.
- [6] Panin, V.E., Belyuk, S.I., Durakov, V.G., Pribytkov, G.A. & Rempe, N.G. (2000). Electron beam surfacing in vacuum: equipment, technology, and coating properties. *Welding Production*, (2), 34–38. <https://doi.org/10.1080/09507110009549234>
- [7] Panin, V.E., Durakov, V.G., Pribytkov, G.A., Polev, I.V. & Belyuk, S.I. (1998). Electron beam surfacing of powder carbide steels. *Physics and Chemistry of Material Processing*, (6), 53–59
- [8] Chandran, K.S.R., Panda, K.B. & Sahay, S.S. (2004). TiBw-reinforced Ti composites: Processing, properties, application prospects, and research needs. *JOM*, (56), 42–48. <https://doi.org/10.1007/s11837-004-0127-1>
- [9] Saito, T. (2004). The automotive application of discontinuously reinforced TiB–Ti composites. *JOM*, (56), 33–36. <https://doi.org/10.1007/s11837-004-0125-3>
- [10] Huang, L.J., Geng, L., Peng, H.X. & Zhang, J. (2011). Room temperature tensile fracture characteristics of in situ TiBw/Ti6Al4V composites with a quasi-continuous network architecture. *Scripta Materialia*, 64(9), 844–847. <https://doi.org/10.1016/j.scriptamat.2011.01.011>
- [11] Novikov, N.P., Borovinskaya, I.P. & Merzhanov, A.G. (1974). Dependence of the composition of products and combustion speed in metal-boron systems on the ratio of reactants. *Combustion and Explosion Physics*, 10(2), 201–206. <https://doi.org/10.1007/BF01464173>
- [12] Azatyan, T.S. & Maltsev, V.M. (1980). On the mechanism of combustion wave propagation in titanium-boron mixtures. *Combustion and Explosion Physics*, 16(2), 37–42. <https://doi.org/10.1007/BF00740195>
- [13] Attar, H., Lober, L., Funk, A., et al. (2015). Mechanical behavior of porous commercially pure Ti and Ti-TiB composite materials manufactured by selective laser melting. *Materials Science & Engineering A*, (625), 350–356. <https://doi.org/10.1016/j.msea.2014.12.036>
- [14] Moissan, A. (1895). Comptes Rendus, 70, 290. Crochard (Paris)
- [15] Moissan, A. (1896). Préparation et propriétés du titane. *Annales de Chimie et de Physique*, (7), 229
- [16] Wedekind, E. (1913). Synthese von Boriden im elektrischen Vakuumofen. *Berichte der Deutschen Chemischen Gesellschaft*, (46), 1198. <https://doi.org/10.1002/cber.191304601155>
- [17] Kusakina, Ju., Levashov, E., Livanov, D. & Karabasov, Ju. (2002). *New Materials*. MISIS, Moscow

## TiB+Ti композициялық ұнтақтарына негізделген өздігінен таралатын жоғары температуралы синтезді зерттеу

А. Мырзахан<sup>1</sup>, Е. Коростелева<sup>2</sup>, Г. Смаилова<sup>1\*</sup>, А. Удербаева<sup>1</sup>

<sup>1</sup>Satbayev University, Алматы, Қазақстан

<sup>2</sup>Ұлттық зерттеу Томск политехникалық университеті, Томск, Ресей

\*Корреспонденция үшін автор: [g.smailova@satbayev.university](mailto:g.smailova@satbayev.university)

**Аңдатпа.** Бұл мақалада Композициялық материалдарды қолдана отырып, машина бөлшектерінің тозуға төзімділігі мен сенімділігін арттырудың заманауи әдістері, әсіресе ұнтақты балқыту және металломатиялық композиттерді синтездеу саласында қарастырылады. Тиімді әдістердің бірі-механикалық және термиялық қасиеттері жақсартылған композициялық жабындарды алуға мүмкіндік беретін өздігінен таралатын жоғары температуралы синтез (ӨТЖТС). Электронды сәулелік қаптау (ЭСҚ) сияқты ұнтақты қаптау әдістері титан негізіндегі тозуға төзімді, ыстыққа төзімді және қатайтатын жабындарды қамтамасыз етеді. Титан және оның қорытпаларының ұнтақтары кальций гидридіден оксидтерді тотықсыздандыру әдісімен алынады, бұл жоғары беріктігі мен жақсы ағындылығы бар аналардың пайда болуына ықпал етеді. Титан боридіне композиттер үшін қатайтатын фаза ретінде ерекше назар аударылады. Бұл технологияларды пайдалану машиналар мен механизмдердің беріктігі мен сенімділігінің едәуір артуына ықпал етеді, бұл ресурстарды үнемдеуге және пайдалану шығындарының төмендеуіне әкеледі. Жүргізілген зерттеулерге алынған ұнтақтар мен жабындардың құрылымдық сипаттамаларын талдау және олардың физикалық және механикалық қасиеттерін анықтау кіреді. Бұл қасиеттердің өзгеруі композициялық ұнтақтағы титан байламының көлемдік құрамына байланысты қарастырылады. Ұнтақтар мен жабындардың микроқұрылымының сипаттамасы, сондай-ақ композицияның олардың сипаттамаларына әсері тозуға төзімділік пен ыстыққа төзімділіктің жоғарылауы сияқты жақсартылған пайдалану сипаттамалары бар функционалды жабындарды жасау үшін осы материалдарды қолдану мүмкіндігі туралы қорытынды жасауға мүмкіндік береді. Зерттеу нәтижелері әртүрлі салаларда пайдалану үшін жақсартылған өнімділігі бар жаңа материалдарды әзірлеу үшін пайдалы болуы мүмкін.

**Негізгі сөздер:** композициялық ұнтақ, титан бориді, титан, катодты сәулелік жабындар, ұнтақты қаптау, өздігінен таралатын жоғары температуралы синтез.

## Исследование самораспространяющегося высокотемпературного синтеза на основе композиционных порошков TiB+Ti

А. Мырзахан<sup>1</sup>, Е. Коростелева<sup>2</sup>, Г. Смаилова<sup>1\*</sup>, А. Удербоева<sup>1</sup>

<sup>1</sup>Satbayev University, Алматы, Казахстан

<sup>2</sup>Национальный исследовательский Томский политехнический университет, Томск, Россия

\*Автор для корреспонденции: [g.smailova@satbayev.university](mailto:g.smailova@satbayev.university)

**Аннотация.** В данной статье рассматриваются современные методы повышения износостойкости и надежности деталей машин с использованием композиционных материалов, особенно в области порошковой наплавки и синтеза металломатричных композитов. Одним из эффективных способов является самораспространяющийся высокотемпературный синтез (СВС), который позволяет получать композиционные покрытия с улучшенными механическими и термическими свойствами. Методы порошковой наплавки, такие как электронно-лучевая наплавка (ЭЛН), обеспечивают создание износостойких, жаропрочных и упрочняющих покрытий на титановом основании. Порошки титана и его сплавов получают методом восстановления оксидов гидридом кальция, что способствует формированию материалов с высокой прочностью и хорошей сыпучестью. Особое внимание уделяется бориду титана как упрочняющей фазе для композитов. Использование данных технологий способствует значительному увеличению долговечности и надежности машин и механизмов, что приводит к экономии ресурсов и снижению эксплуатационных затрат. Проведенные исследования включают анализ структурных характеристик полученных порошков и покрытий, а также определение их физических и механических свойств. Рассматриваются изменения этих свойств в зависимости от объемного содержания титановой связки в композиционном порошке. Описание микроструктуры порошков и покрытия, а также влияние состава на их характеристики, позволяет сделать выводы о возможности применения данных материалов для создания функциональных покрытий с улучшенными эксплуатационными характеристиками, таких как повышенная износостойкость и термостойкость. Результаты исследования могут быть полезны для разработки новых материалов с улучшенными эксплуатационными свойствами для использования в различных отраслях промышленности.

**Ключевые слова:** композиционный порошок, борид титана, титан, электронно-лучевые покрытия, порошковая наплавка, самораспространяющийся высокотемпературный синтез.

### Publisher's note

All claims expressed in this manuscript are solely those of the authors and do not necessarily represent those of their affiliated organizations, or those of the publisher, the editors and the reviewers.

# Investigation of the physico-mechanical properties of cohesive soils in deluvial-proluvial (QII-III) and alluvial (QIII-IV) deposits of the Alakol Depression

M.M. Alzhigitova\*, M.R. Zapparov, E.S. Auelkhan, E.M. Kuldeyeva

*Satbayev University, Almaty, Kazakhstan*

\*Corresponding author: [m.alzhigitova@satbayev.university](mailto:m.alzhigitova@satbayev.university)

**Abstract.** When conducting engineering and geological surveys, one of the main tasks is to determine the physical and mechanical properties of soils. The physical properties of soils are necessary for accurate soil classification, while the mechanical properties are essential for calculating the stability of foundations, as well as the foundations of buildings and structures. This article presents the results of a study on the physico-mechanical properties of cohesive soils in deluvial-proluvial and alluvial deposits of the Alakol depression. Modern geological processes and phenomena in this region are mainly influenced by human engineering and economic activities, particularly land reclamation and construction. Until the 1960s, the development of certain UCPs (Unified Classification Points) was sporadic. The erosion activity of water flows was primarily observed during spring floods and heavy rains, leading to the washout and collapse of riverbanks. Deflation was evident in the Aeolian reworking of alluvial-lacustrine deposits, resulting in the formation of blow basins, sand dunes, wind ripples, and other microrelief features. Additionally, salinization and waterlogging led to the widespread development of salt marshes and puffin formations in areas with shallow groundwater levels.

**Keywords:** absolute marks, depression, complex, alluvial, deluvial, physical and mechanical properties.

Received: 06 November 2024

Accepted: 14 February 2025

Available online: 28 February 2025

## 1. Introduction

The natural boundaries of the region include Lake Balkhash to the north, the Tarbagatai Ranges to the northeast, the Chu-Ili Mountains to the southwest, and the spurs of the Dzungarian Mountains to the south. The absolute elevation of the plain surface varies from 600 m in the south to 340 m in the north.

Most of the region is covered with extensive sandy massifs. In the west, deeply dissected Taukum sands dominate, while the center is characterized by the Saryesik-Atyrau and Muyunkum sands. To the east, the Mokkum and Zhamanzhal sands are prevalent, and between Lake Balkhash and Lake Sasykkol lie the Karakum and Sarykum sands. All sand massifs exhibit narrow, elongated ridges aligned with seasonally alternating northwesterly and northeasterly winds. The elevations of dunes and sand ridges range from 3 to 30 m, reaching up to 50 m in the Taukum massifs (Figure 1).

The valley of the Ili River, the largest river in the region, is situated between the Taukum and Saryesik-Atyrau sands. The modern and Late Quaternary river deltas of the Ili River (covering an area of 8 000 km<sup>2</sup>) are dissected by a dense network of meandering channels and dry branches known as bakanas, some of which are partially covered with sand. The entire region is composed of a thick (up to 2 000 m) sequence of loose, weakly lithified Cenozoic deposits [1, 2].



**Figure 1.** Map of the Alakol depression

The formation of the Alakol depression in the Upper Triassic period was accompanied by the accumulation of a terrigenous coal-bearing formation (TT3-JJ1), consisting of interbedded sandstones, conglomerates, and siltstones with coal interlayers. During the Paleogene-Neogene period, lacustrine and lacustrine-alluvial sediments of the terrigenous red-colored formation were deposited under hot, arid climatic conditions. These include montmorillonite-rich, red-colored

carbonate clays, pinkish-gray Eocene marls, and light-toned bentonite clays, which are overlain by brick-red sandy clays with lenses and interlayers of red-colored clay sands (P3-N1). These deposits occur at significant depths and are, therefore, poorly studied from an engineering and geological perspective.

**2. Materials and methods**

Under conditions of intensified mountain-building tectonic movements in the border areas of the region, Pliocene-Quaternary red-colored molassic formations were deposited alongside the subsidence of depressions. The geotechnical assessment of Quaternary deposits is based on geological-genetic complexes and their geomorphological association with the corresponding geotechnical zones.

Within the basement plains on the Paleozoic folded foundation of the region's northeastern part, cover eluvial-deluvial and deluvial-proluvial accumulations have developed. These are distinguished as stratigraphic-genetic complexes of Quaternary eluvial-deluvial and deluvial-proluvial

deposits (pl.1). The modulus of deformation of loams ranges from 17.6 to 50 MPa, while the degree of corrosion varies from 1.5 to 2.3 g/m<sup>2</sup> (the uniform corrosion rate of carbon steel is 2.55 mm/year) [3]. The physical and mechanical properties of cohesive soils in deluvial-proluvial (QII-III) and alluvial (QIII-IV) deposits of the Alakol Depression are summarized in Table 1.

Rocks of the alluvial-proluvial and alluvial complexes are mainly distributed on submountain inclined accumulative plains. Quaternary alluvial-proluvial deposits form sediment cones and fans at the base of mountains. The structure of these cones distinctly exhibits two accumulative cycles, beginning with gravel-pebble deposits containing individual boulders and sand-clay aggregates, and ending with variously grained sands and dense loams containing small pebbles and gravel. The thickness of the Lower Quaternary deposits ranges from 5 to 20 m, while Middle and Upper Quaternary deposits reach thicknesses of 80 to 140 m. The properties of cohesive soils in these complexes are presented in Table 2.

**Table 1. Physical and mechanical properties of cohesive soils in deluvial-proluvial (QII-III) and alluvial (QIII-IV) deposits of the Alakol Depression**

Indicators	Loam		Loam		Loam	
	dp QII-III	dp QII-III	aQIII	aQIV	aQIII	aQIV
Particle density, g/cm <sup>3</sup>	2.68-2.75 2.72 (15)	2.70-2.74 2.72 (36)	2.66-2.75 2.71 (29)	2.70-2.82 2.72 (35)	2.65-2.72 2.68 (63)	2.66-2.73 2.69 (31)
Density, g/cm <sup>3</sup>	1.49-1.88 1.67 (15)	1.41-1.93 1.68 (36)	1.40-2.10 1.75 (28)	1.34-2.03 1.74 (35)	1.43-2.01 1.71 (63)	1.30-2.19 1.67 (31)
Skeletal density, g/cm <sup>3</sup>	1.32-1.64 1.48 (15)	1.28-1.59 1.48 (36)	1.37-1.65 1.50 (12)	1.30-1.85 1.49 (35)	1.31-1.71 1.52 (63)	1.20-1.85 1.51 (31)
Porosity, %	40.3-51.5 45.8 (15)	41.8-59.2 45.5 (36)	-	34.4-52.3 47.6 (25)	-	42.7-54.3 48.4 (6)
Porosity coefficient, %	0.66-1.06 0.85 (15)	0.72-1.12 0.84 (36)	0.56-0.98 0.76 (28)	0.47-1.098 0.81 (35)	0.495-1.061 0.75 (63)	0.438-0.921 0.66 (25)
Yield point humidity, %	22-31 26 (15)	18.5-25 23.1 (36)	22-38 26.7 (30)	15.7-41 28 (14)	17-33 23 (63)	17-30 24.3 (31)
Plasticity number, %	7-11.7 8.9 (15)	3.2-6.9 5.6 (15)	5-17 9.4 (30)	5-16 11 (14)	1-7 4.6 (63)	1-7 4.8 (31)
Internal friction angle, degree: at natural humidity	17-30 24 (7)	19-29 26 (11)	-	12-46 28 (13)	-	22-45 36 (15)
Adhesion at natural humidity, 10 <sup>5</sup> Pa	0.15-0.8 0.5 (7)	0.2-0.9 0.7 (11)	-	0.3-2.1 1.09 (13)	-	0.03-0.88 0.43 (15)
Relative drawdown coefficient at P = 0.3 MPa	0.017-0.11 0.07 (7)	0.006-0.113 0.04 (27)	0.002-0.1 0.033 (9)	-	-	-

**Table 2. Physical and mechanical properties of cohesive soils in the quaternary alluvial-proluvial deposits**

Indicators	Sandy loam			Sandy loam		
	apQ	apQII-III	apQIII-IV	apQ	apQII-III	apQIII-IV
Particle density, g/cm <sup>3</sup>	2.65-2.73 2.88 (89)	2.65-2.73 2.88 (44)	2.68-2.74 2.72 (18)	2.6-2.81 2.71 (65)	2.68-2.82 2.72 (62)	2.70-2.75 2.73 (9)
Density, g/cm <sup>3</sup>	1.36-2.09 1.75 (89)	1.41-1.93 1.67 (44)	1.25-1.99 1.64 (18)	1.17-2.09 1.64 (62)	1.40-2.01 1.55 (62)	1.54-1.76 1.61 (9)
Skeleton density, g/cm <sup>3</sup>	1.38-1.77 1.55 (72)	1.28-1.75 1.49 (44)	1.28-1.75 1.54 (15)	1.07-1.77 1.46 (34)	1.31-1.72 1.49 (62)	-
Porosity coefficient	0.29-0.98 0.70 (89)	0.59-1.13 0.84 (44)	0.58- 1.17 0.76 (18)	0.29-1.38 0.79 (63)	0.58-1.05 0.87 (62)	0.63-0.85 0.75 (9)
Yield point humidity, %	16-30 23 (89)	18.5-26.8 23 (38)	21-25 22.5 (10)	22-51 27 (65)	19.6-25.9 23.5 (10)	22.6-30.7 27.7 (9)
Plasticity number, %	1-7 4.6 (90)	3.2-6.9 5.6 (38)	2.2-6.6 5.1 (10)	7-17.3 9.1 (65)	12.1-18.8 17.1 (10)	9.0-11.7 10.7 (9)
Internal friction angle, degree: at natural humidity	20-37 26 (27)	14-46 26 (16)	14-46 28 (8)	21-48 27 (14)	11-46 28 (18)	-
when soaking with water	-	11-17 16 (5)	11-17 15.8 (5)	-	11-37 18 (44)	-
Coupling, 10 <sup>5</sup> Pa: at natural humidity	0.08-2.7 0.37 (36)	0.2-1.9 0.86 (16)	0.7-1.9 1.03 (5)	0.10-3.8 0.64 (40)	0.4-1.7 0.98 (18)	-
hen soaking with water	-	0.3-0.9 0.5 (5)	--	-	0.1-0.7 0.43 (44)	-
Module deformations, MPa	3.9-19 12 (3)	--	-	2.6-10 5.9 (9)	--	-
Relative drawdown coefficient at P = 0.3 MPa	0.001-0.150 0.045 (11)	0.006-0.113 0.04 (27)	0.001-0.06 0.02 (3)	0.002-0.20 0.065 (9)	--	-

Loamy alluvial-proluvial deposits exhibit subsidence characteristics [4]. The amount of subsidence varies as follows: apQII loam thickness ranges from 5.4 to 72.8 cm, apQII-III from 16.5 to 16.8 cm, and apQIII-IV up to 5 cm. The most subsident deposits are the Lower and Middle Quaternary alluvial-proluvial loams of ancient sediment cones.

Channel facies are represented by gravel-pebble deposits with a sand aggregate, frequent interlayers, and lenses of different-grained sands. The clastic material is well-rounded and differentiated by strike and section. Boulders and gravel-pebble deposits with a sand-clay aggregate form the base of the section. Sand and gravel formations with lenses and interlayers of different-grained sands and loamy rocks usually lie above. Near the surface, coarse-grained rocks are overlain by gray loams and sandy loams.

The soil properties are very similar, despite testing being carried out in different river valleys of the northern and northeastern slopes of the Dzungarian Alatau. The loams of the first above-floodplain terraces (aQIII) are saline in some areas, and the soils exhibit increased corrosivity. Single determinations showed a degree of corrosion of 2.2-12 g/m<sup>2</sup> (the corrosion rate of carbon steel is 2.5-13.3 mm/year). Loam is slightly shrunken in some areas, and its subsidence under household loads is less than 5 cm [5].

The characterization of engineering and geological conditions and map construction is based on the principle of geological-genetic (formation) analysis. The territory is divided into geological bodies-the primary objects of mapping. These bodies represent parts of geological formations, including stratigraphic-genetic and lithological-facies complexes of rocks and their characteristic combinations. The sediments were studied for the depth of development of lithified rocks capable of supporting structural loads. Neogene clay deposits were taken as a regional water barrier.

### 3. Results and discussion

Quaternary deposits are widespread from the surface throughout the entire research area, where most hazardous geological processes occur. Based on the conducted studies, the following first-to-surface stratigraphic-genetic complexes were identified within the study area. These differ in genesis, geological age, and lithology.

Stratigraphic-genetic complex of modern alluvial deposits (aQIV). Deposits of this complex are confined to floodplains and low terraces (up to 5 m) of nearly all major rivers in the region. They also form the extensive deltas of the Yrgaity, Terekty, Takyu, and Chindaly rivers, among others. Riverbed and floodplain terrace deposits are composed of loam and sandy loam with gravel and small pebbles, boulder-pebble aggregates with sand-gravel inclusions, and low-power lenses of different-grained sands and clays (Table 3).

Boulders ranging in size from 30-40 cm to 1.0-1.5 m in diameter are observed in the beds and floodplains of mountain rivers. All detrital material is well-rounded. In contrast, the flat part of the area is characterized by finer-grained alluvial deposits, primarily sandy-clay material with gravel and small, well-rounded pebbles. The thickness of alluvial deposits in mountain valleys reaches 10-12 m, whereas, within the flat plain, it does not exceed 3-5 m [6].

According to previous studies, groundwater is encountered at depths of 2-5 m, occasionally reaching 10-15 m. The water is fresh, with a mineralization of 0.1-0.2 g/dm<sup>3</sup>. Due to the limited development area, this complex is considered unsuitable for construction purposes.

**Table 3. Physical and mechanical properties of gravel-pebble deposits with sand aggregate (aQIV)**

N	Physical and mechanical properties	Minimum value	Maximum value	Arithmetic mean
1.	Soil density, g/cm <sup>3</sup>			
2.	Volume density of soil, g /cm <sup>3</sup> :			
	Loose	1.10	2.18	1.67
	Compacted	1.12	1.94	1.63
3.	Clay fraction, %			0.73
4.	Dust fraction, %			2.16
5.	Sand fraction, %			31.68
6.	Gravel fraction, %			65.43
7.	Natural humidity, %	0.60	4.20	1.93
8.	Filtration coefficient, m /day	30.70	77.40	77.40
9.	Natural slope angle, deg:			
	dry	37.0	53.0	46.47
	underwater	35.0	49.0	42.87

Figure 2 shows a typical granulometric composition graph for gravel-pebble deposits with sand aggregate. The filtration coefficient, determined using the Boldyrev method in experimental pit infusions, ranges from 9.18 to 31.10 m/day.

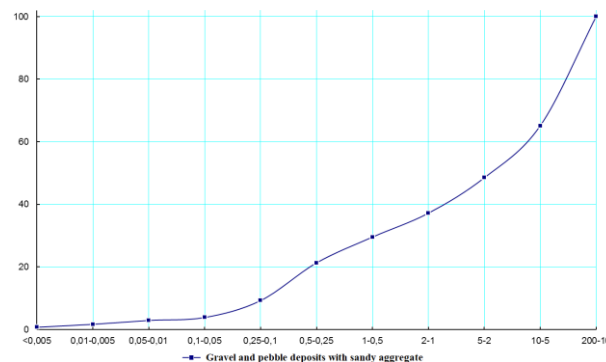


**Figure 2. Integral curve of the granulometric composition of modern alluvial deposits**

Coarse-grained sand is rarely found as interlayers. Two samples were taken (w-5/1, 0 and 2.0 m). The composition of these deposits includes 63.6-78.0% sand and 22.0-36.4% gravel. The compacted soil's volume weight ranges from 1.57 to 1.60 g/cm<sup>3</sup>, while the soil skeleton's density is 1.74-1.89 g/cm<sup>3</sup>. Natural moisture content varies between 1.0-1.2%. The natural slope angle is 40-42° for dry ground and 39-42° under water [7,8]. Loam is widely developed in the area, overlying boulder and pebble deposits.

Figure 3 presents a typical graph illustrating the granulometric composition of loam. Additionally, five monoliths were extracted from these loams (M-6/2.0 m, M-7/2.5 m, M-8/2.0 m, M-9/2.5 m, and M-10/1.0 m).

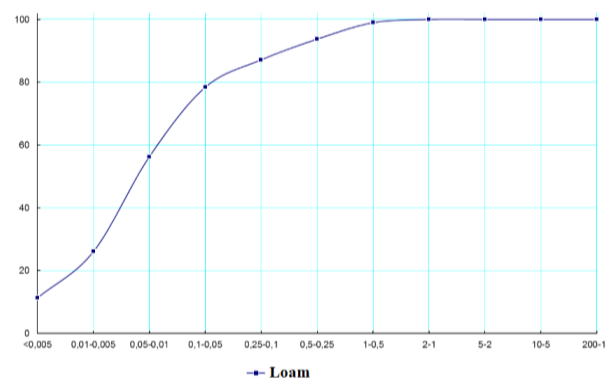


**Figure 3. Granulometric Composition of Gravel-Pebble Deposits with Sand Aggregate**

The soil density is 2.70 g/cm<sup>3</sup>. The volume weight of dense soils ranges from 1.43 to 1.54 g/cm<sup>3</sup>, whereas loose soils range from 1.34 to 1.47 g/cm<sup>3</sup>. Natural moisture content varies between 5.0% and 13.5% (Table 4).

**Table 4. Physical and mechanical properties of loam aQIV**

N	Physical and mechanical properties	Minimum value	Maximum value	Arithmetic mean
1.	Soil density, g/cm <sup>3</sup>	2.70	2.70	2.70
2.	Volume density of soil, g/cm <sup>3</sup> :			
	Loose	0.65	1.65	1.26
	Compacted	0.82	1.69	1.36
3.	Clay fraction, %			11.29
4.	Dust fraction, %			44.98
5.	Sand fraction, %			55.02
6.	Gravel fraction, %			-7
7.	Natural humidity, %	2.90	26.80	9.91
8.	Yield point	22.20	46.40	35.54
9.	Rolling border	15.20	29.30	21.84
10.	Plasticity index	7.0	17.70	10.70
11.	Turnover rate	-1.46	-0.48	-1.12
12.	Water saturation coefficient	0.15	0.36	0.24
13.	Filtration coefficient, m/day	0.04	0.08	0.06

According to compression test results, these loams are classified as medium compressible, with a compressibility coefficient (m<sub>0</sub>) of 0.015-0.068 kg/cm<sup>3</sup>. The soil is highly compacted, with a skeleton density of 1.35-1.47 g/cm<sup>3</sup>. The yield index ranges from 0.48 to 1.64, indicating solid and plastic properties, while the total deformation modulus reaches 24.1-123.2 kg/cm<sup>3</sup>. The soil's porosity ranges from 45.6% to 50.3%, and the natural state porosity coefficient (e) is 0.713-1.015.

Stratigraphic-genetic complex of modern lake sediments (IQIV). This complex is prevalent along the southern coasts of Lakes Alakol and Zhalanashkol. The lake plain is generally flat and smoothed, with a slight (<1°) slope toward the northeast. Lake deposits consist of dense loams, clays, clay loams, and sands, interspersed with well-rounded pebbles and gravel, with a thickness varying from 1-3 m to 6 m.

According to previous studies, underground water is found at depths of 0.5-1.5 m, with a significant portion of the surface swampy. The water quality is fresh, with a salinity of 0.2-0.5 g/cm<sup>3</sup>. Gravel and pebble deposits with a loamy aggregate have developed from the surface (Figure 4).

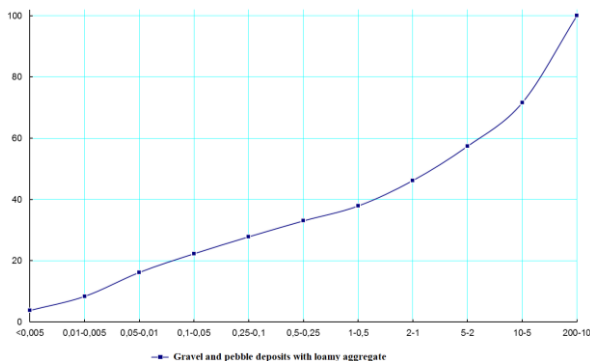


**Figure 4. Integral curve of the granulometric composition of modern lake sediments**

Experimental data from pit infusions using the Boldyrev method indicate a filtration coefficient ranging from 9.18 to 31.10 m/day (Table 5).

**Table 5. Physical and mechanical properties of gravel-pebble deposits with loam aggregate (IQIV)**

N	Physical and mechanical properties	Minimum value	Maximum value	Arithmetic mean
1.	Soil density, g / cm <sup>3</sup>	-	-	-
2.	Volume density of soil, g /cm <sup>3</sup> : Loose/compacted	-	-	-
3.	Clay fraction, %			3.77
4.	Dust fraction, %			12.40
5.	Sand fraction, %			30.0
6.	Gravel fraction, %			53.83
7.	Natural humidity, %	9.00	33.30	18.53
8.	Filtration coefficient, m /day	-	-	-
9.	Natural slope angle, deg: Dry/Underwater	-	-	-
10.	Yield point*(for placeholder)	18.30	29.20	23.40
11.	Rolling border*(for placeholder)	11.60	21.30	16.03
12.	Plasticity number*(for aggregate)	6.70	7.90	7.37

Figure 5 shows a typical graph of the granulometric composition of loams.

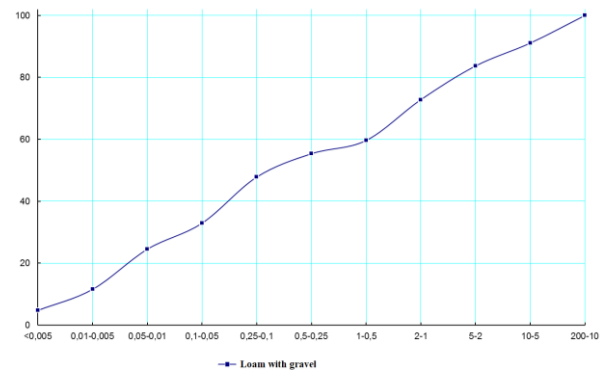


**Figure 5. Integral curve of the granulometric composition of modern lake sediments**

Stratigraphic-genetic complex of upper quaternary alluvial-proluvial deposits (apQIII). This complex extends across the foothill plain and the Alakol depression as a continuous cover. According to prior studies, deposit thickness varies from 8-20 m to 80-155 m and consists of boulder and gravel-pebble deposits interspersed with sand and loam (Table 6).

**Table 6. Physical and mechanical properties of loam with gravel IQIV**

N	Physical and mechanical properties	Minimum value	Maximum value	Arithmetic mean
1.	Soil density, g/cm <sup>3</sup>	-	-	-
2.	Volume density of soil, g/cm <sup>3</sup> : Loose/compacted	-	-	-
3.	Clay fraction, %			4.75
4.	Dust fraction, %			19.74
5.	Sand fraction, %			45.35
6.	Gravel fraction, %			30.16
7.	Natural humidity, %	13.30	30.80	23.43
8.	Yield point	18.50	40.00	27.50
9.	Rolling border	12.10	22.80	18.58
10.	Plasticity number	6.40	17.20	8.92
11.	Flow rate	0.47	1.21	0.82
12.	Water saturation coefficient	-	-	-
13.	Filtration coefficient, m/day	-	-	-

Fieldwork indicates that underground water in this area is mainly non-pressurized or low-pressure, with a pressure range of 1.7-5.0 m, and is encountered in wells at depths of 5-8 m to 11-25 m. Loam with gravel appears from the surface, occurring as interlayers throughout the section, alternating with sand, clay, and silt [11, 12].

This region, part of Kazakhstan's largest drainless basin, includes three artesian groundwater basins. Underground water associated with terrigenous coal-bearing (T3-J1J1) and terrigenous red-colored (K-N11) formations exists locally at great depths and does not significantly impact the region's engineering-geological conditions.

The Neogene pressure waters sometimes emerge through clay «windows», interacting with overlying aquifers. Local groundwater is found in eluvial-deluvial and deluvial-proluvial deposits [13, 14]. The boulder-gravel deposits contain fresh water, which transitions to gravel-sand and loam as the distance from foothills increases. Aquifer stratification results in pressurized lower horizons, with water-bearing interlayers reaching thicknesses of 180 m in foothill zones, but reducing to  $\leq 50$  m in depressions.

In the direction of the center of depressions, it decreases sharply and usually does not exceed 50 m. The depth of groundwater near the mountains reaches 100 m. Towards the center of the depression, it gradually decreases, and at the border with the lacustrine-alluvial plain, water wedges in the form of springs and hollows are noted [15].

#### 4. Conclusions

The capacity of water supply points in the Alakolsky basin is 2.5-50 dm<sup>3</sup>/s. The flow rates of self-spilling wells reach 50 dm<sup>3</sup>/s. The waters are mainly sodium and calcium bicarbonate, with mineralization not exceeding 0.7 g/dm<sup>3</sup>. Sediments of stratigraphic-genetic complexes associated with accumulative hummocky-ridge and flat concave plains are linked to groundwater with a level depth (depending on the relief) ranging from 0 to 20 m or more. The mineralization and chemical composition of groundwater are highly diverse. As the groundwater flows toward the center of the depressions, an increase in water salinity is observed, ranging from 1 to 10 g/dm<sup>3</sup>. Accordingly, the composition changes from calcium bicarbonate to magnesium-sodium sulfate-chloride.

Groundwater, mostly occurring at shallow depths (1-5 m), is associated with alluvial deposits. In floodplains and river deltas, the groundwater level depth is no more than 1 m. The thickness of alluvial aquifers does not exceed 30 m. The water content of rocks varies widely. Flow rates of tenths of a liter per second prevail, and only in the upper reaches of rivers, where the water-bearing rocks are pebbles, do well flow rates reach 3 dm<sup>3</sup>/s. The mineralization of the waters reaches 5-10 g/dm<sup>3</sup> and, in some cases, even 50 g/dm<sup>3</sup>. The composition of the water is sulfate and sodium chloride [16, 17].

The natural regime of groundwater is characterized by smooth, shallow-amplitude (0.5-1.0 m) fluctuations in levels throughout the year, with weakly expressed spring maxima and summer minima. The main autumn-winter maximum is due to the filtration flow of irrigation and wastewater from irrigated areas. The level rise is 1.8-2.2 m, and in areas of rice crop rotations, it reaches 5 m. An irrigation-type groundwater regime has developed over a large area.

Modern geological processes and phenomena in the region are mainly associated with human engineering and

economic activities, particularly land reclamation construction. Until the 1960s, the development of a number of DGPs was episodic. The erosive activity of water flows was observed only during spring floods and heavy rains, leading to bank erosion and collapse. Deflation was evident in the eolian processing of alluvial-lacustrine sediments, resulting in the formation of blow basins, sand dunes, wind ripples, and other microrelief forms [18, 19]. Salinization and waterlogging occurred in the form of extensive development of salt marshes, sores, and puffs in areas with a shallow groundwater level.

Abrasion was intensely observed on the southern and eastern shores of Lake Alakol. The southern shore of the lake (near the village of Koktum) has moved more than 200 m over 20 years. As a result of the washout and collapse of the coastal ledge, part of the village was destroyed. The shoreline of the lake has advanced very close to the railway track. The activation of abrasion processes is caused by frequently recurring hurricane winds and an increase in the lake's water area. According to measurements from 1862 and 1931, the lake's size increased in length and width by 5 km. Even more intensive growth of the water area was established by the 1951 measurements. Over 20 years, the lake's length increased by 15 km, its width by 5 km, and its depth significantly as well [20].

#### Author contributions

Conceptualization: M.M.A., M.R.Z.; Data curation: M.M.A., E.S.A.; Formal analysis: M.R.Z., E.S.A., E.M.K.; Funding acquisition: M.M.A., M.R.Z.; Investigation: E.S.A., E.M.K.; Methodology: M.M.A., M.R.Z.; Project administration: M.M.A., M.R.Z.; Resources: E.S.A., E.M.K.; Software: E.S.A., E.M.K.; Supervision: M.R.A., E.S.A.; Validation: M.M., E.S.; Visualization: E.S., E.M.; Writing – original draft: M.M.A., M.R.Z.; Writing – review & editing: E.S.A., E.M.K. All authors have read and agreed to the published version of the manuscript.

#### Funding

This research received no external funding.

#### Acknowledgements

This work was conducted as part of the report on the hydrogeological survey with engineering and geological investigations of sheets L-44-XXIII.

#### Conflicts of interests

The authors declare no conflict of interest.

#### Data availability statement

The original contributions presented in this study are included in the article. Further inquiries can be directed to the corresponding author.

#### References

- [1] Sanatbekov, M.E., Zholtaev, G., Tileuberdi, N., Auelkhan, E.S. & Imanskipova, Z.B. (2024). Study of geodynamic and hydrogeological criteria for assessing the hydrocarbon potential of the alakol depression. *Naukovyi Visnyk Natsionalnoho Hirnychoho Universytetu*, (4), 5-10. <https://doi.org/10.33271/nvngu/2024-4/005>

- [2] Alzhigitova, M.M., Zapparov, M.R. & Mirlas, V.M. (2021). Impact of anthropogenic activity on the condition of lake Alakol. *Engineering Journal of Satbayev University*, 143(2), 44-51. <https://doi.org/10.51301/vest.su.2021.i2.06>
- [3] Alzhigitova, M.M., Zapparov, M.R. (2020). Engineering and hydrogeological features of the Alakol depression. *Engineering Journal of Satbayev University*, 142(6), 33-41. <https://doi.org/10.51301/vest.su.2020.v142.i6.06>
- [4] Baibatsha, A.B., Kurkina, L.A. (2003). General Engineering Geology. Almaty, Scientific and Publishing Center «Gylym»
- [5] Barinov, A.V. (2003). Emergency Situations of Natural Character and Protection from Them. Moscow: Publishing House «Vladost-Press».
- [6] Tarikhazer, S.A., Karimova, E.J. & Kuchinskaya, I.Y. (2022). Quantitative assessment of mudflow risk in the Greater Caucasus of Azerbaijan (on the example of the northeastern slope). *Journal of Geology, Geography and Geoecology*, 31(4), 722-735. <https://doi.org/10.15421/112268>
- [7] Valeev, A., Karatayev, M., Abitbayeva, A., Uxukbayeva, S., Bektursynova, A. & Sharapkhanova, Z. (2019). Monitoring Coastline Dynamics of Alakol Lake in Kazakhstan Using Remote Sensing Data. *Geosciences*, 9(9), 404. <https://doi.org/10.3390/geosciences9090404>
- [8] Zaripov, A.S. & Luchnikov, A.I. (2021). Investigation of the dynamics of bank failure of the Kama and Votkinskoye reservoirs as a result of abrasion using aerial photography materials. *Georisk*, 15(1), 58-66. <https://doi.org/10.25296/1997-8669-2021-15-1-58-66>
- [9] Khalykov, E.E., Ly, Y.F., Abitbaeva, A.D., Togys, M.M. & Valeev, A.G. (2021). Determination of the dynamics of reworking the shore escarpment of Lake Alakol using a laser scanner. *Geography and Water Resources*, (4), 23-34.
- [10] Valeev, A.G., Akiyanova, F.J. & Sagintaev, J. (2020). Modern relief-forming processes of the shore zone of lake alakol. *Hydro-meteorology and ecology*, 2(97), 125-145.
- [11] Chaklikov, A.Y., Korobkin, V.V., Ismailov, A.A., Buslov, M.M., Tulemissova, Z.S. (2024). Specifics of the Geological Structure of the Alakol Basin and the Choice of Drilling Well Design. *Kazakhstan Journal for Oil & Gas Industry*, 6(1), 18-34. <https://doi.org/10.54859/kjoi108695>
- [12] Zhiyembayeva, J.A., Zhanakova, R.K., Sarybayev, M.A., Nurtay, G. & Yelzhanov, E.A. (2024). Investigation of hazardous geologic processes at the Kaskelen-Talgar polygon by geodetic methods. *Bulletin of Kazgasa*, 1(91), 108-121. <https://doi.org/10.51488/1680-080X/2024.1-08>
- [13] Kozhnazarov, A.D. (2004). Engineering Geodynamics. Almaty: KazNTU
- [14] Maltseva, K.A. & Maltsev, A.V. (2023, October). Efficiency of application of geophysical methods of soil investigation of landslide massifs. *XLIX Samara Regional Student Scientific Conference*, 1(S), 155-156
- [15] Gulkayyr, T. & Rakhmedinov, E.E. (2023). Large landslides in active structures of southwestern tien shan (batken oblast). *Bulletin of the Institute of Seismology of the National Academy of Sciences of the Kyrgyz Republic*, (1), 21
- [16] Zakirova, D.A., Satybaev, A.D. & Satybaldiev, B.S. (2024). Analysis of Causes of the origin of the sinkhole movement process (on the example of Nookat district of Osh oblast). *Bulletin of Science and Practice*, 10(9), 80-89. <https://doi.org/10.33619/2414-2948/106/08>
- [17] Semyachkov, A.I., Pochechun, V.A. & Semyachkov, K.A. (2023). Hydrogeoecological conditions of technogenic groundwater in waste disposal sites. *Notes of the Mining Institute*, (260), 168-179. <https://doi.org/10.31897/PMI.2023.24>
- [18] Bielova, N., Mykytyn, T. & Dolyenko, N. (2023). Monitoring of Modern Exogenous Processes in Precarpathia. *17th International Conference Monitoring of Geological Processes and Ecological Condition of the Environment*, (1), 1-5. <https://doi.org/10.3997/2214-4609.2023520165>
- [19] Hablovskiy, B., Hablovskaya, N., Shtohryn, L., Kasiyanchuk, D. & Kononenko, M. (2023). The Long-Term Prediction of Landslide Processes within the Precarpathian Depression of the Cernivtsi Region of Ukraine. *Journal of Ecological Engineering*, 24(7). <https://doi.org/10.12911/22998993/164753>
- [20] Cascini, L., Scoppettuolo, M.R. & Babilio, E. (2022). Forecasting the landslide evolution: from theory to practice. *Landslides*, 19(12), 2839-2851. <https://doi.org/10.1007/s10346-022-01934-3>

## Алакөл ойпатының делювиалды-пролювиалды (Q<sub>II-III</sub>) және аллювиалды (Q<sub>III-IV</sub>) шөгінділер кешендерінің байланысқан топырақтарының физика-механикалық қасиеттерін зерттеу

М.М. Альжигитова\*, М.Р. Заппаров, Е.С. Әуелхан, Е.М. Кульдеева

Satbayev University, Алматы, Қазақстан

\*Корреспонденция үшін автор: [m.alzhigitova@satbayev.university](mailto:m.alzhigitova@satbayev.university)

**Андатпа.** Инженерлік-геологиялық зерттеулер жүргізу кезінде ең маңызды міндеттердің бірі топырақтың физика-механикалық қасиеттерін анықтау болып табылады. Топырақтың физикалық қасиеттері Топырақтың атауын дәл анықтау үшін қажет, механикалық қасиеттері Іргетастардың, ғимараттар мен құрылыстардың негіздерінің тұрақтылығын есептеу үшін қажет мақалада Алакөл ойпатының делювиалды-пролювиалды және аллювиалды шөгінділер кешендерінің біртұтас топырақтарының физикалық-механикалық қасиеттері келтірілген. Аймақ аумағындағы қазіргі геологиялық процестер мен құбылыстар негізінен адамның инженерлік-шаруашылық қызметімен, атап айтқанда мелиорациялық құрылыспен байланысты. 60-шы жылдарға дейін бірқатар КПП-дың дамуы эпизодтық сипатта болды. Су ағындарының эрозиялық белсенділігі тек көктемгі су тасқыны кезінде және жағалаулардың шайылуы мен құлауында жаңбыр жауған кезде пайда болды. Дефляция аллювиалды көл шөгінділерін эолдық өңдеуде үрлеу бассейндерін, құмды қопсытқыштарды, жел толқындарын және микрорельефтің басқа түрлерін қалыптастыруда көрінді. Тұздану және батпақтану жер асты сулары деңгейінің таяз жатқан жерлерінде тұзды батпақтардың, қопсытқыштар мен қопсытқыштардың кең дамуы түрінде болды. Түйінді сөздер: абсолютті белгілер, ойпат, кешен, аллювиалды, делювиалды, физика-механикалық қасиеттері.

**Негізгі сөздер:** абсолютті белгілер, ойпат, кешен, аллювиалды, делювиалды, физика-механикалық қасиеттер.

## Изучение физико-механических свойств связных грунтов комплексов делювиально-пролювиальных (Q<sub>II-III</sub>) и аллювиальных (Q<sub>III-IV</sub>) отложений Алакольской впадины

М.М. Альжигитова\*, М.Р. Заппаров, Е.С. Ауелхан, Е.М. Кульдеева

Satbayev University, Алматы, Казахстан

\*Автор для корреспонденции: [m.alzhigitova@satbayev.university](mailto:m.alzhigitova@satbayev.university)

**Аннотация.** При проведении инженерно-геологических изысканий одной из главнейших задач является определение физико-механических свойств грунтов. Физические свойства грунтов необходимы для точного определения наименования грунта, механические свойства необходимы для расчета устойчивости фундаментов, оснований зданий и сооружений. В статье представлены результаты физико-механические свойства связных грунтов комплексов делювиально-пролювиальных и аллювиальных отложений Алакольской впадины. Современные геологические процессы и явления на территории региона связаны преимущественно с инженерно-хозяйственной деятельностью человека и, в частности, с мелиоративным строительством. До 60-х годов развитие ряда ОГП носило эпизодический характер. Эрозионная деятельность водных потоков проявлялась только в период весенних половодий и выпадения ливневых дождей в подмыве и обрушении берегов. Дефляция проявлялась в эоловой переработке аллювиально-озерных отложений с образованием котловин выдувания, песчаных барханов, ветровой ряби и других форм микрорельефа. Засоление и заболачивание происходило в форме широкого развития солончаков, соров и пухляков на участках неглубокого залегания уровня грунтовых вод.

**Ключевые слова:** абсолютные отметки, впадина, комплекс, аллювиальный, делювиальный, физико-механические свойства.

### Publisher's note

All claims expressed in this manuscript are solely those of the authors and do not necessarily represent those of their affiliated organizations, or those of the publisher, the editors and the reviewers.

<https://doi.org/10.51301/ejsu.2025.i1.05>

## Substantiating applicability of Western Donbas coal seams (Ukraine) for underground coal gasification

V.S. Falshtynskiy<sup>1</sup>, R.O. Dychkovskiy<sup>2</sup>, V.H. Lozynskiy<sup>1\*</sup>, P.B. Saik<sup>1</sup>, M.I. Lozynska<sup>3</sup>

<sup>1</sup>Dnipro University of Technology, Dnipro, Ukraine

<sup>2</sup>AGH University of Krakow, Krakow, Poland

<sup>3</sup>Geological Concern «Geobit», Chrzanow, Poland

\*Corresponding author: [lozynskiy.v.h@nmu.one](mailto:lozynskiy.v.h@nmu.one)

**Abstract.** The paper studies areas of coal seams in the Western Donbass (Ukraine), which can potentially be suitable for underground coal gasification (UCG) technology, which, in the conditions of the difficult energy situation in Ukraine, can significantly affect the consumer market of energy carriers. On the basis of a detailed research on the mining-geological and mining-technical conditions of ten sites according to the criteria for their suitability for UCG, the optimal site and coal seam have been chosen. The structures of coal seams, side rocks (roof, bottom), the location and size of tectonic disturbances, hydrogeological conditions, as well as the technical and elemental composition of coal have been analyzed. Based on the conducted research, it has been determined that it is recommended to place the experimental underground gas generator on the C<sub>5</sub> coal seam of # 4 site, located on the territory with the most developed infrastructure and optimal criteria for gasification suitability. The practical significance of the research is in the fact that the experience of mining the UCG # 4 site of the experimental gas generator allows adjusting the technology parameters for subsequent industrial replication. The proposed approach to the selection of a site and a coal seam can also be tested in other coal deposits with similar mining-geological and mining-technical conditions.

**Keywords:** underground coal gasification, coal seam, gas generator, coal, deposits.

Received: 10 August 2024

Accepted: 14 February 2025

Available online: 28 February 2025

### 1. Introduction

According to the prospected resources, Ukraine ranks seventh in the world (34.2 milliard ton; total reserves are estimated as 117 milliard tons). In this context, crude oil and gas reserves are 2.4% of coal ones [1-4]. Due to the limited resources of crude oil and natural gas (currently, output is 8-9.3% of the required production) coal importance for the national industrial complex growth and economic development of Ukraine is closely connected with the progress of coal sector [5-7].

Underground coal gasification (UCG) with further extraction and use of gasification products, which basic combustible components are CO, CH<sub>4</sub>, H<sub>2</sub>, is one of the ways to solve the problems of clean coal technologies [8, 9]. However, no unified theory of complex underground processing of coal and mine gases is available [10]. Consequently, the development of complex environmentally friendly methods to transform coal into new energy sources, liquid motor oils, olefins, and paraffin is actual mission [11[11], 12].

School of underground coal gasification was founded within the verge of Artem Dnipropetrovsk Mining Institute (the Dnipro University of Technology today) in the 1920s. Famous scientist, Professor O.M. Terpigoriev proposed the basic principles of underground gas generator operation.

Moreover, he participated actively in the industrial implementation of the first Pidzemgaz stations in Ukraine [13-15]. The suggested technology provides not only economical but also ecological benefits [16-19].

Starting from 1968, a number of scientists and researchers from the Department of Underground Mining of the Dnipro University of Technology (Artem Dnipropetrovsk Mining Institute) took active part in studies and developments of UCG methods at Pidzemgaz stations in the Russian Federation (Shatskaya and South-Abinsk stations); in Uzbekistan (Angren station); within lignite deposit of Synelnykove experimental site in Ukraine; with the Russian Federation research institutes (Skochinsky Institute of Mining; Uglegaz of MMI; Uzbekistan (Tashkent Polytechnic Institute); in Ukraine (Institute of Geology and Geochemistry of Combustible Minerals in Lviv, Donetsk Research & Development Institute, Dniprodiproshakht, Kryvyi Rih Mining Institute); in Poland (Central Mining Institute in Katowice, AGH University of Science and Technology in Krakow, Research Institute of Radical Technologies in Warsaw) etc. Design institute Dniprodiproshakht has developed four production projects of Pidzemgaz station for coal and lignite with the participation of the Dnipro University of Technology employees [13, 20-22].

Taking into consideration the criteria of coal seam applicability for UCG, mining and geological, hydrogeological, and mining conditions of the seam occurrence are analyzed to substantiate the selection of an experimental gasification site [23-26]. Thickness of a coal seam, its ultimate composition and rank, physical and mechanical characteristics, structure, texture and ultimate composition of rocks, enclosing the coal seam, water inflow, disjunctive and plicative disturbances are the basic criteria in terms of which the coal seam is applicable/inapplicable for UCG [27-30]. The required design capacity of a site for underground coal gasification as well as its service life is calculated basing upon the coal reserves and taking into consideration the payback for the construction and operation of gas generators [31-34]. Ultimate composition (output of combustibles  $V = 27-36\%$ ), structure and texture of coal seams, make them maximally applicable for UCG [35].

The aim of this study is to conduct an investigation of coal seams in the Western Donbass (Ukraine), which can potentially be suitable for underground coal gasification (UCG) technology.

## 2. Materials and methods

It should be noted that there are no unified criteria to evaluate the expediency of underground coal gasification use within the coal deposits [36, 37]. The Dnipro University of Technology has applied author's approach to determine the expediency of UCG use for the specific mining and geological conditions. The approach was tested industrially and supported as an efficient one while developing technical documentation of the underground gasification project as well as feasibility study (FS #3858) within Synelnykivske lignite deposit. Calculation of the document was supplemented by the data taking into consideration the current approaches concerning applicability of lignite and coal deposits for UCG [38, 39].

As practices have shown, the methods are rather efficient while determining UCG applicability in terms of manufacturability and in terms of economic indices. To evaluate potential gasification, a deposit is divided into patterns. Their applicability for underground gasification is identified with the help of general coefficient  $K$  which depends upon the natural parameters of gasification area occurrence relying upon the relevant coefficients [40, 41].

Carbonous content of Western Donbas is associated with Lower Carboniferous deposits of  $C_1$  series [42-44]. The coal seams occur at  $3-12^\circ$  north-eastwardly. Rock occurrence is linear one with northern and north-eastern dip at a  $3-4^\circ$  angle. The angle increases up to  $5-8^\circ$  in the neighbourhood of tectonic fault zones [45, 46]. The coal field contains three geological and industrial areas: Petrykivka, Novomoskovsk, and Petropavlivka. The coal is mined by DTEK Pavlohradvuhillia established in 1974. It involves 11 mines, Pavlohrad Preparation Plant, and other enterprises [47-49].

Further thorough study of Western Donbas deposits is required since their traditional mining is neither efficient nor expedient [50-52]. Moreover, sites of coal seams (both balance and off-balance ones), left in the process of mine operation, should also be analyzed since according to their criteria they may be applicable for UCG. In the next section we will discuss the characteristics of the selected sites.

In summary, our methodology offers a comprehensive framework that synergizes innovative evaluation techniques

with practical industrial insights. This approach systematically dissects the coal deposit into distinct patterns, facilitating a nuanced analysis of each zone's gasification potential based on geological and economic parameters. By employing a unique general coefficient and integrating current best practices, we enhance the feasibility and efficiency of underground coal gasification projects.

## 3. Results and discussion

### 3.1. Geological investigation of selected sites

Sites #1, 2, and 3 are located within a field of Pavlohradaska mine in Pavlohrad District of Dnipropetrovsk Region. It is a north-eastern slope of Ukrainian crystalline rock mass, stretching along the south-western boundary of the Dnieper-Donets Rift. Pavlohrad Town is at 8.0 km distance south-westwardly. Donetsk-Kyiv highway and Pavlohrad-Lozova and Krasnoarmiisk railway are nearby.

Site #1 is within the eastern mine-take wing. Its dimensions are: 2000 m along the strike and 350 m down-dip. The site area is 700000 m<sup>2</sup>. Pivdenno-Ternivskiy fault limits it in the north ( $H$  is 30-130 m). The fault has a small branch line in the central share of the site (i.e. fault #11 where  $H$  is 1.5 m) (Fig. 1).

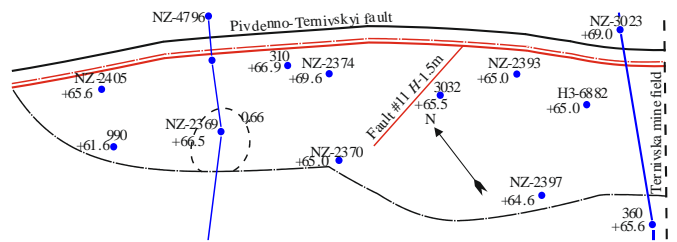


Figure 1. Site #1 plan

Site #2 is within a slope share of the western field of Pavlohradaska mine. Its dimensions are: 1500 m along the strike and 1400 m down-dip. The site area is 610000 m<sup>2</sup>. In the north, it is limited by Pivdenno-Ternivskiy fault #11 ( $H$  is 30-130 m; and  $58-68^\circ$ ). In the west, the site borders on Blahodatna mine field (Fig. 2).

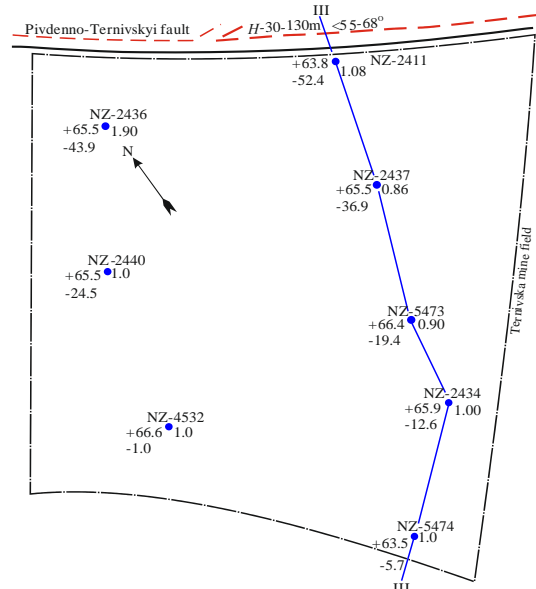


Figure 2. Site #2 plan

Site #3 is within the eastern mine-take wing. Its dimensions are: 900 m along the strike and 850 m down-dip. The site area is 765000 m<sup>2</sup>. In the west, it is limited by fault #12 ( $H$  is 0-35 m;  $<55^\circ$ ). In the east, it borders on Ternivska mine field (Fig. 3).

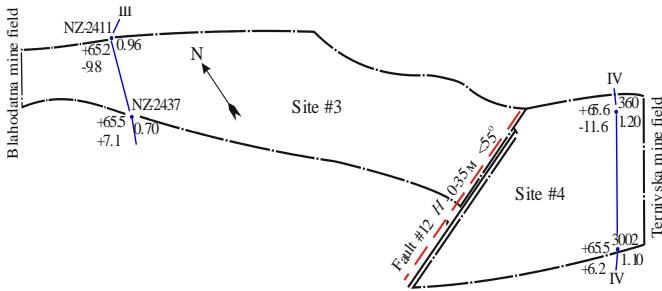


Figure 3. Site #3 plan

Up to 50 coal seams occur within the mine field. Only 9 of them are of working thickness ( $m \geq 0.45$  m).

The coal belongs to gas rank. In terms of one of the basic thickness criteria,  $C_4$  and  $C_5$  seams are applicable for UCG. Below you can find characteristics of the seams in accordance with all the criteria to identify their suitability for underground coal gasification.

The coal seam  $C_4^1$  is of simple structure; its occurrence is linear at  $3-4^\circ$  angle northerly and north-easterly increasing up to  $5-8^\circ$  within the zone of tectonic disturbances. Average thickness of the seam is 0.77 m; it varies from 0.54 to 1.1 m. The seam coal is low-ash and low-sulfur. Combustion heat varies from 21.4 to 23.1 MJ/kg; average value is 22.1 MJ/kg. The lowest calorific value is 17.3 kcal/kg.

The main roof of the seam and its floor is coal formation ( $C_1$ ) represented by the alternation of argillite, aleurite, and sandstone strata. The immediate roof of the seam is represented mainly by tough massive argillites. The argillite may be replaced with horizontally layered mica aleurite. Aleurite roof stability is somewhat higher than the argillite one. The main roof of the seam is represented mainly by horizontally layered monolith aleurite of moderate stability.

Usually, horizontally layered tough aleurite of medium stability is both the immediate and the main floor of the seam. Its upper thickness is 0.9-1.2 m. In water, the aleurite has a tendency to slaking and disintegration. Argillite of “curly” type may occur in the immediate floor. The mineral is unstable while watering. Hence, the rocks can be characterized as weakly stable and moderately stable ones exclusive of excessive fissuring zones in the neighbourhood of tectonic disturbances. Water level is associated with coal deposits. Pressure height is 54 m and more. Specific water output is 0.0036-0.073 m/s and  $K_f$  is 0.0056-1.72 m/day.

The coal seam  $C_5$  is of simple structure; its thickness is continuous; occurrence is linear at  $3-4^\circ$  angle northerly and north-easterly increasing up to  $5-8^\circ$  within the zone of tectonic disturbances. The coal is of medium ash and sulfur content. Combustion heat varies from 24.5 to 25.7 MJ/kg; average value is 4.9 MJ/kg. The lowest combustion heat is 19.1 MJ/kg. Coal deposits, represented by the alternation of argillite, aleurite, and sandstone layers, are the seam main roof and floor. The immediate roof is represented mainly by aleurite and argillite. The main roof is of medium caving features ( $A_2$ ). The immediate roof is represented mainly by aleurites and argillites. Aleurite of an upper layer is of

“curly” type of 0.6-1 m thickness. Lower, it is with sandstones interlayers. The mineral is of medium stability. Argillite of an upper layer (0.8-1.0 m) is of “curly” type. It is more compact lower along the seam. It is moderately stable. It becomes unstable if watering takes place. Figures 4-7 show geological sections in terms of the sites.

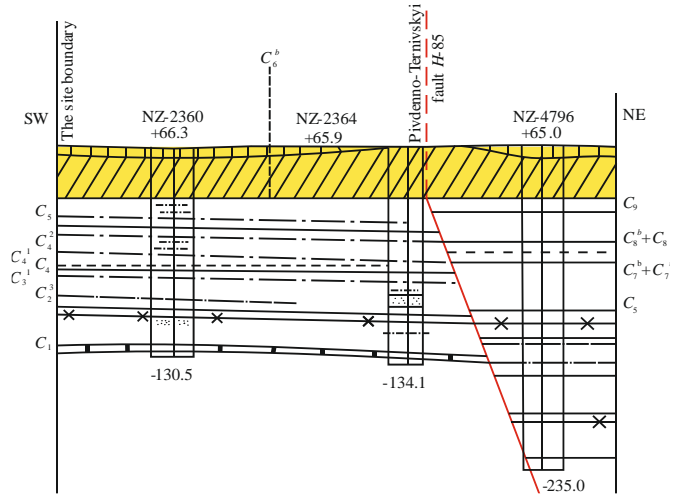


Figure 4. Geological section I-I

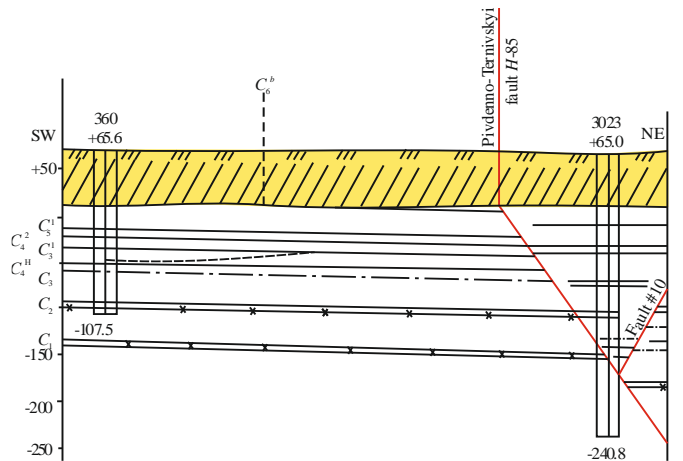


Figure 5. Geological section II-II

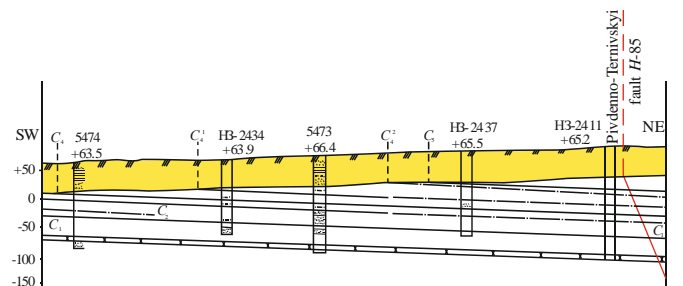


Figure 6. Geological section III-III

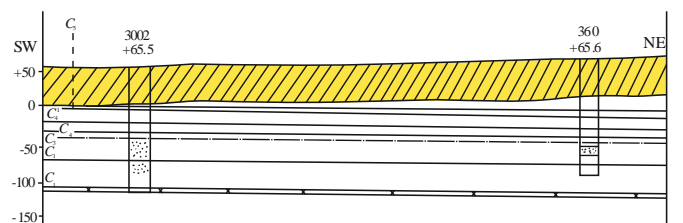


Figure 7. Geological section IV-IV



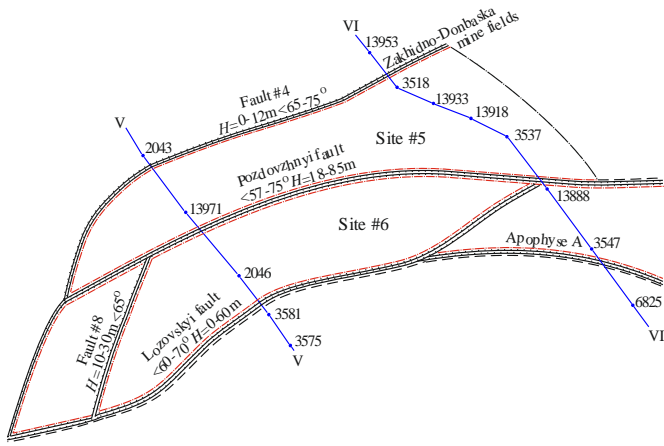


Figure 10. Plan of sites #5 and 6

Site #6 is in an incline share of the mine field. Its dimensions are as follows: 3600 m along the strike and 400 m down-dip. The site area is 1440000 m<sup>2</sup>. On the rise, it is limited by Lozovskiy fault. (*H* is 0-60 m; <60-70°); Pozdovzhnyi fault #1 limits it down-dip (*H* is 18-85 m; <57-75°) (Fig. 10). Up to 40 coal seams and layers have been penetrated; 13 of them are of working thickness (*m* ≥ 0.45 m). The coal is of gas and fat rank. In terms of a thickness criterion, being one of the basic ones, C<sub>6</sub>+C<sub>6</sub>' seam is of interest from the viewpoint of gasification. Below, you can find characteristics of the seam.

In terms of site #5, average occurrence depth of C<sub>6</sub>+C<sub>6</sub>' seam is 240 m; it is 285 m in terms of site #6. Its thickness varies from 1.14 to 1.18 m with average 1.15 m value in terms of site #5, and 1.00 to 1.40 m with average 1.12 m value in terms of site #6. C<sub>6</sub>+C<sub>6</sub>' seam is a continuous formation with a simple structure. Its occurrence is flat with 2-5° of rock inclination angle. The coal is of ash and sulfur content. Its combustion heat varies from 23.9 up to 26.2 MJ/kg; average value is 25.1 MJ/kg. The lowest combustion value is 17.8 MJ/kg.

Argillite (60%) and aleurite (39%) are the immediate roof of the seam. Very rarely, sandstone (1%) is available. Aleurite and argillite are fissured with flora remnants. The deposited minerals are from slightly stable to unstable and very unstable ones. The main roof is unstable and easily caved. Sandstone contains minor capacity of static water. Expectable water inflow is 9 m<sup>3</sup>/hour.

The immediate floor is represented by aleurite (65.5%), argillite (34%), and sandstone (0.5%) in some cases. The aleurite and argillite are of cloddy texture; a layer of “curly” type with up to 1-1.5 m thickness occurs over them. It contains phytollems. Water-bearing levels are associated with the seams of coal, sandstone, and limestone. The layer is of moderate stability; it becomes unstable while moistening. Figures 11 and 12 show geological sections of the sites.

Sand of Buchak Paleogene series is the roof. The water-bearing system is of sheet-like and fissured type with a subartesian surface. Average filtration coefficient is 0.68 m/day. The upper share of the section is of higher filtration characteristics. Carbon aquifers are connected hydraulically with Neogene-Paleogene and Quaternary deposits.

In view of the fact that the sites are isolated from the hydraulic connection by means of the abovementioned water-bearing levels, the seam inundation will take place owing to the water reserves available within the coal stratum.

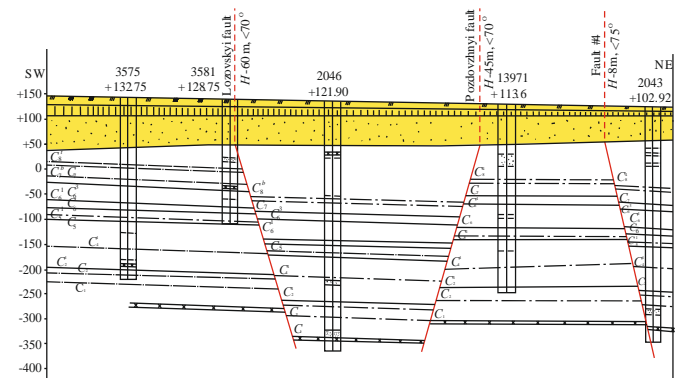


Figure 11. Geological section V-V

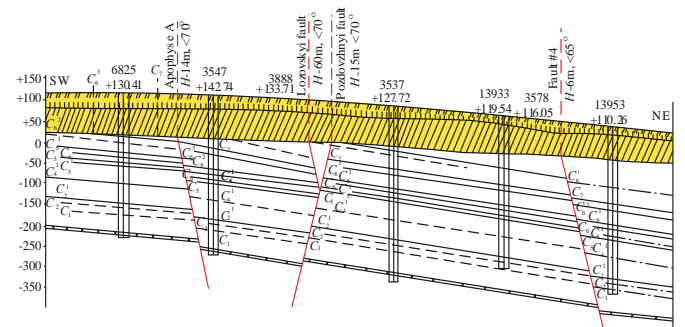


Figure 12. Geological section VI-VI

The sites #7 and 8 are within Blahodatna mine field in Pavlohrad District of Dnipropetrovsk Region. The mine field area is 32 km<sup>2</sup>. Its northern boundary passes through Verbskiy fault; false one passes through Pavlohradskiy-Viazivskiy fault.

The settlement of Blahodatna is at the mine field territory. Pavlohrad Town is at 8.0 km distance south-westwardly. Donetsk-Kyiv highway as well as Pavlohrad-Lozova and Pavlohrad-Krasnoarmiisk railway is nearby. The major one Samara River, being a left feeder of the Dnieper River, flows in the southern part of the mine field.

The analyzed site #7 is in the incline part of the mine field. Its dimensions are: 850 m along the strike and 1350 m down-dip. The site area is 1147500 m<sup>2</sup>. In the north, it is limited by Pivdenno-Ternivskiy fault; in the south, apophyse A-A (*H* is 2.5 m, <55°) limits it (Fig. 13).

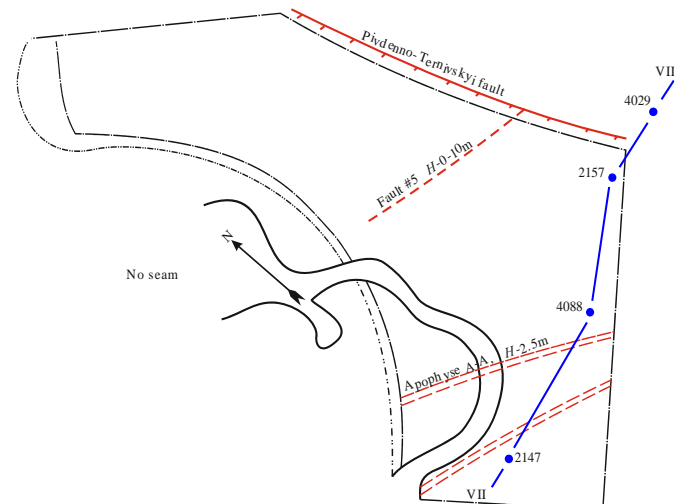


Figure 13. Site #7 plan

Tectonic disjunctive fault isolate site #7 from the upper water-bearing levels. Water will inflow from sandstone and the seam itself. Expectable water influx is up to 8 m<sup>3</sup>/hour.

Site #8 is within the incline part of the field. Its dimensions are: 2300 m along the strike and 1000 m down-dip. The site area is 2300000 m<sup>2</sup>. In the north, the site is limited by Pivdenno-Ternivskiyi fault (*H* is 30-130 m, <55-65°); and in the east it borders on Pavlohradskaya mine field (Fig. 14).

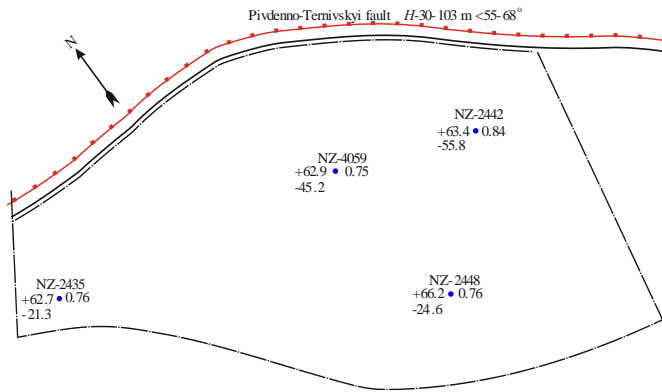


Figure 14. Site #8 plan

There are 12 seams on the mine balance. The coal is of gas ranks. In terms of thickness, being one of the basic criteria, C<sub>5</sub>-C<sub>5</sub><sup>l</sup> seams of site #7 are of interest for UCG. Site #8 is represented by C<sub>4</sub>-C<sub>4</sub><sup>b</sup> coal seams. Below you can find characteristics of the seams.

The seam is of simple structure; its thickness is stable; occurrence is continuous; rock inclination is at a 3-4° angle northwardly and north-eastwardly. The seam is separated by disjunctive disturbances. The coal is of medium ash and sulfur content. Combustion heat varies from 24.4 to 25.2 MJ/kg; average value is 24.8 MJ/kg. The lowest combustion heat is 18.9 MJ/kg.

The immediate roof of the seam is represented mainly by aleurite and argillite. Aleurite is horizontally layered; its hardness is medium, varying from low stable to unstable one. Argillite is layered with the insignificant amount of open-type fissures; it is of moderate hardness.

Argillite, aleurite, and sandstone are the seam main roof and floor. The main roof is easily caved. The immediate floor is represented mainly by aleurite and argillite. Aleurite is slightly fissured; on the top, it is of “curly” type with 0.6-1.0 m thickness. Argillite is horizontally layered; on the top, it is of “curly” type (*m* = 0.8-1.0 m). Figure 15 demonstrates its geological section. The seam is of simple structure; its occurrence is continuous; rock inclination is at 3-5° angle north-eastwardly.

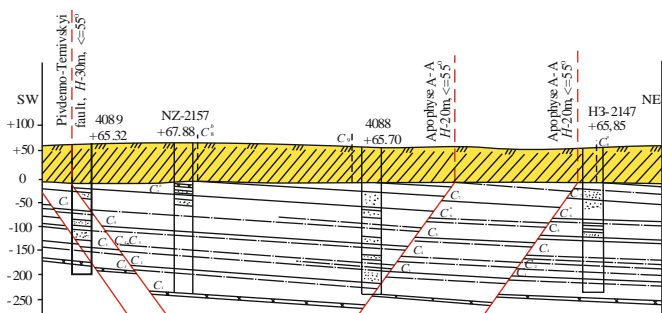


Figure 15. Geological section VII-VII

Occurrence depth varies from 84.0 to 122.0 m. Its thickness varies from 0.75 to 1.10 m. Average value is 0.85 m. The coal is of medium ash and sulfur content. Combustion heat is within the range of 24.05-26.6 MJ/kg. The lowest combustion heat is 17.4 MJ/kg. In terms of site #8, the seam reserves are 2.2 million tons. Geological conditions are similar to those within site #2.

The immediate roof of the seam is represented mainly by tight and massive argillite replaced in some cases with horizontally layered aleurite. Aleurite roof stability is somewhat higher to compare with the argillite one. Argillite, aleurite, and sandstone layers are the main roof and floor of the seam. The main roof is represented mainly by horizontally layered, monolith, and stable aleurite. The immediate floor of the seam is represented by mainly horizontally layered, dense, and medium-stable aleurolite; at the top, it is 0.6-1.4 m thick of “curly” type. In water, the aleurolite is prone to swelling and breaking. Argillite may occur within the immediate floor. In case of watering, it is not stable. The enclosing rocks of seam C<sub>4</sub>-C<sub>4</sub><sup>b</sup> belong to the unstable ones except the zones of increased fissility near the tectonic disturbances.

Aquifer is of layered-fissured type with pressure surface. Specific output is 0.0036-0.073 l/s, *K<sub>f</sub>* is 0.0056-1.72 m/day. Basing on the fact that there is no structural barrier from the side of seam outcrop, one can expect water influx of up to 30 m<sup>3</sup>/hour.

Site #9 is located within the field of Ternivska mine. The mine is located in Pavlograd District. There are such settlements as Blahodatne and Ternivka near the mine; the town of Pavlohrad is located north-westward at the distance of 13 km. Donetsk-Kyiv highway as well as the railway connecting Donetsk and Dnipro is nearby. The site is located within the eastern flank of the incline area of the mine field. The site dimensions are as follows: along the strike – 1150 m and to the dip – 1500 m. The site area is 740000 m<sup>2</sup> (Fig. 16).

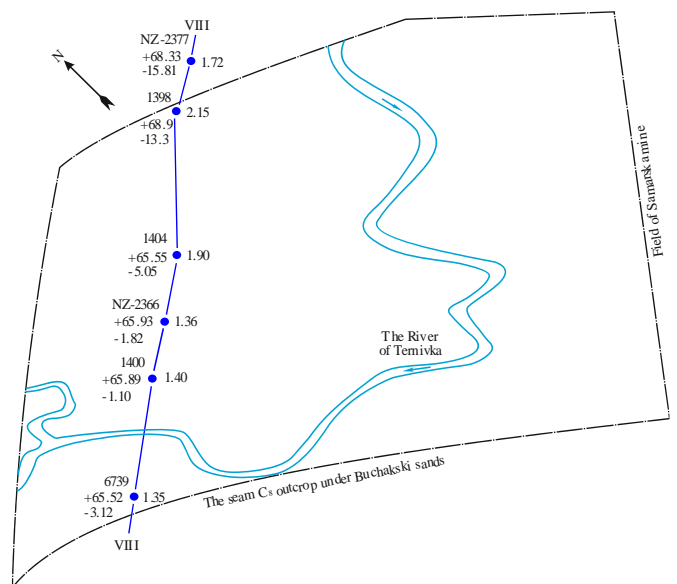


Figure 16. Plan of site #9

The coal within the area is of gas rank. Coal-bearing thickness contains 9 seams of working thickness (*m* ≥ 0.45 m). Among them, seam C<sub>8</sub>-C<sub>8</sub><sup>b</sup> is suitable for gasification in terms of its thickness. The seam characteristics are given below.

Depth of the seams  $C_8+C_8^b$  occurrence varies from 65.0 to 85.0 m. Average seam thickness is 1.4 m. Rock occurrence is linear and stable. Seam structure is complex; interlayer thickness in the middle of the seam is 0.1-0.5 m. Rock inclination is northward at the angle of 3-5°. Coal is of low ash content and mid-sulfur. Combustion heat varies within the range of 22.9-25.6 kkal/kg; average value is 23.8 kkal/kg. Lower combustion heat is 18.2 kkal/kg.

The dividing rock layering, represented by massive, slightly micaceous argillite broken by rare fissures, is the immediate roof of  $C_8^b$  seam. In terms of thickness being less than 1 m, that is a “false” roof. The argillite is of lumpy texture with the vegetation remains.

It is prone to caving and sloughing. The aleurolite is slightly micaceous, horizontally layered, and unstable with the thickness of 3-15.5 m; it is broken by fissures. The main roof is represented mainly by aleurolite and sandstone. Mining conditions are complex due to the neighbouring Buchak-skiy aquifer.

Homogenous and massive argillite ( $m = 1-17$  m) prevails within the immediate floor; within the upper share (0.6-1 m) it is of lumpy texture and of “curly” type. It is unstable. The main and immediate floor rocks are characterized by low stability; they are prone to swelling while watering. Figure 17 shows the geological section.

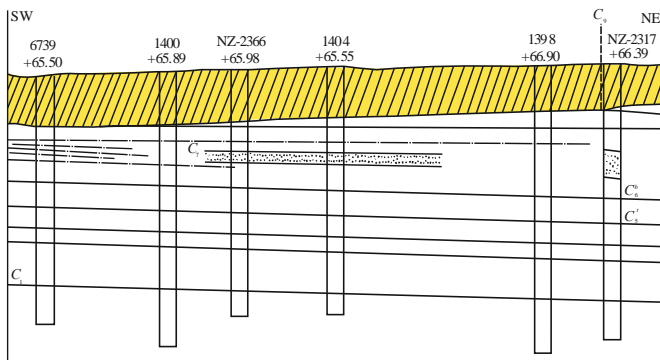


Figure 17. Geological section VIII-VIII

Permeability of the enclosing rocks is lower than the one of coal. Coal reserves in terms of the seam within the site boundaries are 3.1 million tons.

Sandstones, limestones, and coal seams are aqueous among the Carbon deposits. A weathering zone developed down to the depth of 150-200 m as well as the sites of coal seam and sandstone outcrops under the sands of Buchak-ska series are the most watered ones in the Carbon thickness. Aquifer is of strata and fissured type with the pressure surface. Pressure head is 54 m and higher. Specific output is 0.0036-0.073 l/s,  $K_f$  is 0.0056-1.72 m/day. Buchak-ski sands and the seam occurring by 25-30 m higher are involved in the seam watering. Paying attention to the shallow depth of the seam occurrence and its considerable watering, water influx is expected to be up to 20-26 m<sup>3</sup>/hour.

Site #10 is located within the field of Yuvileina mine in Pavlohrad-Petropavlivka district of Western Donbas. Following settlements are right near the site: Pershotravensk (town), Petropavlivka (settlement) located 12 km north-eastwardly, and Pavlohrad (town) to the north-east at the distance of 45 km. Regional centre of Petropavlivka includes bast plant, flour milling plant, and butter making factory. Villages of Rosynky and Mykolayivka as well as Brahynivka railway

station are located near the mine. Railway main line Yasyn-uvata-Pavlohrad-Dnipro passes at the distance of 5 km from the site boundary, it is connected with Yuvileina mine by the rail access through Mykolayivka station.

Site #10 is within the inclined mine field. It is limited by the following faults: Podovzhnyi #3 in the north ( $H - 6-10$  m,  $<70^\circ$ ) and Podovzhnyi in the south ( $H - 40-125$  m,  $<60-70^\circ$ ). The site dimensions are as follows: along the strike – 2000 m and to the dip – 300 m. The site area is 600000 m<sup>2</sup> (Fig. 18).

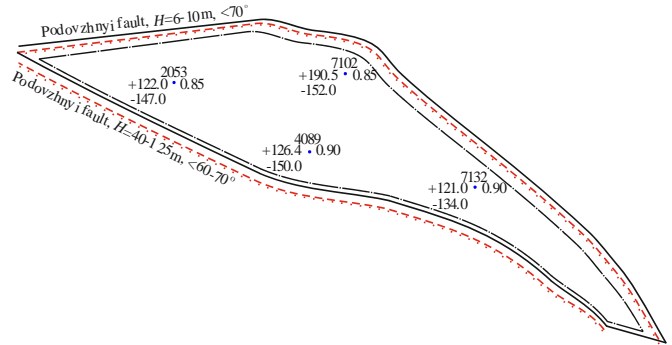


Figure 18. Plan of site #10

The coal rank within the site under analysis is gas. Coal-bearing thickness contains 10 seams of working thickness ( $m \geq 0.45$  m). Among them,  $C_6$  seam is suitable for UCG in terms of one of the main criteria. The seam characteristics are given below. Depth of the seam  $C_6$  occurrence varies from 250 to 280 m. The thickness is within the range of 0.85-1.2 m in terms of the average value of 0.9 m. The seam is of simple structure; the rock occurrence is linear and stable. Rock dip is south-eastward at the angle of 3-5°.

Coal is with medium ash and sulfur content. Combustion heat is within the range of 22.3-25.4 MJ/kg in terms of average value of 23.1 MJ/kg. The lowest fuel combustion heat is 17.7 MJ/kg.

Argillite is the immediate roof of the seam (60%); aleurolite occurs rarely (40%). The argillite is dark gray; its thickness varies from 1.2 to 1.7 m; it is of low stability. The aleurite is gray; it alternates with sandstone. Its thickness is 0.75-1.1 m. It is of low stability. In turn, it becomes unstable within the excessive fissuring zones. The immediate roof consists of aleurite (70%), argillite (29%), and sandstone (1%). The aleurite is gray and white mica-schist with plant remains; it is “curly” type in the upper share of the layer. Its thickness is 0.35-15 m. It has a tendency for slacking. Its stability is of medium value; it becomes unstable while watering.

The main roof is easily caving. It is represented by dark gray argillite with plant remains; it is of “curly” type in the upper share of the layer. Its thickness is 0.5-12 m. It has a tendency for slacking and for intensive heaving. It is unstable mineral. Sandstone, limestone, and coal seams are the watered rocks. Water content depends upon the fissuring degree. Aquifer is of sheet-like and fissured type. Well outputs penetrate the coal levels. In terms of maximum decrease, being 3.6-79.5 m, they vary from 0.052 to 1.8 l/sec; specific output varies from 0.0013 to 0.178 l/sec. In view of the fact that the faults protect the site from the upper aquifers, the expected water inflow may be 3 m<sup>3</sup>/hour. The seam reserves are 1.2 million tons within the site.

### 3.2. Substantiated applicability coefficients for the selected sites

A comprehensive review of the site's geological and operational characteristics was first undertaken to ensure the selected locations meet all technical and safety requirements. Detailed field observations, combined with in-depth laboratory analyses and numerical modeling, have provided critical

insights into the variability and reliability of key parameters. Relying upon the practices of Pidzembgaz stations, field experiments, bench tests, laboratory studies, and analytical research, and taking into consideration the factors, influencing gasification of DTEK Pavlohradvuhillia coal seams, applicability coefficients, shown in Tables 1-4 have been substantiated.

Table 1. Basic expediency criteria of underground gasification as for the coal seams of Western Donbas (Part 1)

Coal seams	m, m	A, %	Structure of the coal seam		Wall rocks (roof, floor); total			Sulfur content in the seam; S, %
			Ratio between the thickness of interlayers and the seam thickness; $m_{pp}/m$	Expansion of the interlayers over the site area; $S_{pp}/S$	Thickness of clays or other low-permeable rocks within the roof; $h^1$ , m $h^1/m > H_{obv}$ ;	Thickness of clays or other low-permeable rocks within the floor; $h$ , m $H \geq 2.0$ m	Distance from the seam roof to certain high-permeable layers or undrained water-bearing levels ( $h_2$ ); $h_2 > h_m$ , $h_m$ – height of fractured zone, m	
C4 <sup>1</sup>	0.77	8.2 – 23	–	–	6.2 > 4	3.2 > 2	8.0 > 6.9	1.4
C5	1.05	10.2 – 12	–	–	8.8 > 5.3	4.0 > 2	10.2 > 8.8	1.5
C6	1.15	9.2 – 21	–	–	8.1 > 5.9	3.5 > 2	9.5 > 9.2	1.7
C4	0.85	11.2 – 28	–	–	7.7 > 4.3	2.5 > 2	11.3 > 7.8	2.3
C8	1.40	8.8 – 30	0.36	0.68	9.8 > 7.3	3.6 > 2	12.0 > 11.2	2.8
C6	0.9	10 – 26	–	–	14.5 > 4.6	2.2 > 2	10.6 > 8.5	2.2

Table 2. Basic expediency criteria of underground gasification as for the coal seams of Western Donbas (Part 2)

Coal seams	Minimum safe mining depth ( $H_b$ , m) and angle of seam dip $\alpha = 0$ up to 45°; $H/m \geq 15$ , where $n = 15$ , $H_b = m \cdot n$	Tectonic disturbances $L_H \geq L_T$	$Q_{air}$ , MJ/m <sup>3</sup>	$Q_{oxygen}$ , MJ/m <sup>3</sup>	$Q_{air}$ , MJ/m <sup>3</sup>	$Q_{oxygen}$ , MJ/m <sup>3</sup>	Ratio between the gas permeability of coal and rocks
			Water influx in the channel, m <sup>3</sup> /hour		Humidity of UCG gas, g/m <sup>3</sup>		
C4 <sup>1</sup>	29.6 m > 11.5; $H_b = 11.5$ m	The site boundaries; disjunctive disturbances	3.2	7.14	3.2	7.14	17 – 28
C5	96.8 m > 15.8; $H_b = 15.8$ m	The site boundaries; disjunctive disturbances	1.3 – 2.4	421	265		16 – 24
			3.48	7.5	3.48	7.5	
C6	72.5 m > 17.3; $H_b = 17.3$ m	The site boundaries; disjunctive disturbances	0.86 – 1.2	308	226		19 – 29
			2.94	6.68	2.94	6.68	
C4	44.7 m > 12.8; $H_b = 12.8$ m	The site boundaries; disjunctive disturbances	1.0 – 1.45	375	254		18 – 30
			2.4	5.42	2.4	5.42	
C8	25.4 m > 21; $H_b = 21$ m	The site boundaries; disjunctive disturbances	2.12 – 3.07	505	378		17 – 32
			2.6	5.5	3.63	7.66	
C6	17.5 m > 9.7; $H_b = 9.7$ m	The site boundaries; disjunctive disturbances	2.2 – 3.24	493	365		19 – 28
			2.71	5.65	3.31	7.34	
			1.8 – 2.52	476	334		

Table 3. Coefficient of suitability of Western Donbas coal seam sites for UCG (Part 1)

Coal seam	Geological factor						Hydrogeological factor					
	Coal reserves and coal rank	Thickness of coal seam	Structure and texture of seam	Ash content of coal	Mining depth	Disturbance of UCG site	Lithology of wall rocks		Watering and permeability of rocks	Water influx into the gas generator	Seam watering	Seam permeability
							roof	floor				
C4 <sup>1</sup>	0.66	0.54	0.61	0.82	0.64	0.65	0.71	0.6	0.62	0.64	0.82	0.76
C5	0.65	0.65	0.82	0.84	0.85	0.74	0.76	0.71	0.74	0.72	0.85	0.84
C6	0.68	0.66	0.8	0.82	0.81	0.63	0.7	0.55	0.70	0.66	0.82	0.84
C4	0.73	0.56	0.66	0.76	0.64	0.67	0.72	0.56	0.61	0.58	0.80	0.76
C8	0.74	0.68	0.55	0.67	0.62	0.64	0.68	0.50	0.63	0.61	0.8	0.78
C6	0.67	0.6	0.65	0.72	0.83	0.74	0.69	0.52	0.65	0.64	0.78	0.80

Table 4. Coefficient of suitability of Western Donbas coal seam sites for UCG (Part 2)

Coal seam	Mining and technical factor						Available consumers of the gasification products	Coefficient of coal seams suitability for UCG
	Rock pressure	Coal losses in situ	Blowing and gas losses	Environmental protection	Heat losses			
C4 <sup>1</sup>	0.82	0.78	0.80	0.77	0.52	0.83	0.64	
C5	0.80	0.88	0.90	0.87	0.62	0.85	0.70	
C6	0.80	0.86	0.88	0.85	0.63	0.80	0.71	
C4	0.83	0.78	0.80	0.78	0.54	0.84	0.67	
C8	0.85	0.74	0.77	0.74	0.64	0.80	0.68	
C6	0.80	0.84	0.86	0.82	0.57	0.85	0.66	

The coefficients represent the possibility to mine coal seams of the sites using underground coal gasification method involving the implementation of operational parameters, providing success of the technique. It is recommended to place an experimental gas generator within coal seam  $C_5$  of UCG site #4 where there is the most developed infrastructure, and criteria of applicability for gasification are optimal. Development practices of UCG site #4 will help correct the technological parameters for further industrial expansion.

Building on these coefficients, the next step is to conduct pilot-scale experiments that will help us validate and fine-tune the UCG process under controlled conditions. We believe that the insights gained during this trial will allow us to adjust our gasification methodology more accurately and enhance the simulation models we use for similar geological settings. Continuous monitoring, along with close collaboration with field experts, will be crucial to ensuring both the efficiency and safety of the operation as we advance toward industrial-scale applications.

#### 4. Conclusions

The following was taken into consideration while determining applicability for UCG of the sites of Western Donbas coal seams at the territory of DTEK Pavlohradvuhillia:

- operation analysis of Ukrainian Pidzemgaz stations in the process of coal gasification;
- pursuance of the research using underground experimental gas generator and bench units;
- geological, hydrogeological, and structural conditions of the coal seams occurrence; and
- surface topography as well as infrastructural development.

The determined coefficient of changes in the applicability of coal seams for gasification depends upon the availability of natural protective layers (i.e. disjunctive disturbances) at the boundaries of the strata. The layers provide tightness of underground gas generators in terms of stratification. Occurrences depths, being 65-390 m, and 26-45 m distances between the coal seams make their underground gasification safe, taking into consideration 0.77-1.4 m gasification thickness. Water inflow into an underground gas generator is 0.86-3.24 m<sup>3</sup>/hour involving extra expenditures connected with the preparation and operation of the underground gas generators within such UCG sites as #1, 7, 8, and 9.

It is recommended to place an experimental gas generator within coal seam  $C_5$  of UCG site #4 where there is the most developed infrastructure, and criteria of applicability for gasification are optimal. Development practices of UCG site #4 will help correct the technological parameters for further industrial expansion.

The practical significance of the research is in the fact that the experience of mining the UCG #4 site of the experimental gas generator allows adjusting the technology parameters for subsequent industrial replication. The proposed approach to the selection of a site and a coal seam can also be tested in other coal deposits with similar mining-geological and mining-technical conditions.

#### Author contributions

Conceptualization: VSF, ROD; Data curation: PBS, MIL; Formal analysis: PBS, VHL, MIL; Funding acquisition: ROD, VHL; Investigation: VSF, VHL; Methodology: VSF;

Project administration: ROD; Resources: PBS, MIL; Supervision: ROD; Validation: PBS, MIL; Visualization: VSF, VHL; Writing – original draft: VSF, ROD, VHL, PBS, MIL; Writing – review & editing: ROD, VHL. All authors have read and agreed to the published version of the manuscript.

#### Funding

The presented results have been obtained within the framework of the research projects GP-516 “Scientific and practical principles of low-rank coal gasification technology” and GP-512 «Co-gasification of carbon-containing raw materials during ultrathin coal seams gasification with a focus on hydrogen production» supported by the Ministry of Education and Science of Ukraine, No. of State registration 0122U001301 and 0123U100985.

#### Acknowledgements

The authors express their gratitude to the editor and the anonymous reviewers for their valuable suggestions and recommendations, which were taken into consideration during the revision.

#### Conflicts of interests

Author VHL declared that he was an editorial board member of the *Engineering Journal of Satbayev University* at the time of submission. This had no impact on the peer review process and the final decision. The remaining authors declare no conflict of interest.

#### Data availability statement

The original contributions presented in this study are included in the article. Further inquiries can be directed to the corresponding author.

#### References

- [1] Salieiev, I. (2024). Organization of processes for complex mining and processing of mineral raw materials from coal mines in the context of the concept of sustainable development. *Mining of Mineral Deposits*, 18(1), 54-66. <https://doi.org/10.33271/mining18.01.054>
- [2] Starodubets, K.M., Dubosarskyi, V.R., & Mamyshev, I.Y. (2023). The state of reserves and prospective resources of the Southern oil and gas region of Ukraine. *Mineral Resources of Ukraine*, (2), 36-41. <https://doi.org/10.31996/mru.2023.2.36-41>
- [3] Astrof, V., Ghodsi, M., Grieveson, R., & Holzner, M. (2022). Russia’s invasion of Ukraine: assessment of the humanitarian, economic, and financial impact in the short and medium term. *International Economics and Economic Policy*, 19(2), 331-381. <https://doi.org/10.1007/s10368-022-00546-5>
- [4] Lytvyniuk, S.F., & Kurylo, M.M. (2024). Substantiation of condition parameters for the calculation of reserves of iron ore deposits to optimize development systems. *Mineral Resources of Ukraine*, (2), 16-20. <https://doi.org/10.31996/mru.2024.2.16-20>
- [5] Bielov, O.P., & Adamchuk, A.A. (2018). Substantiation of the ways to use lignite concerning the integrated development of lignite deposits of Ukraine. *Naukovi Visnyk Natsionalnoho Hirnychoho Universytetu*, (3), 5-13. <https://doi.org/10.29202/nvngu/2018-3/6>
- [6] Bondarenko, V., Salieiev, I., Kovalevska, I., Chervatiuk, V., Malashkevych, D., Shyshov, M., & Chernyak, V. (2023). A new concept for complex mining of mineral raw material resources from DTEK coal mines based on sustainable development and

- ESG strategy. *Mining of Mineral Deposits*, 17(1), 1-16. <https://doi.org/10.33271/mining17.01.001>
- [7] Makarov, V., Perov, M., Bilan, T., Novoseltsev, O., & Zapozhzhets, A. (2024). Technological State of Coal Mining in Ukraine. *Geominig: Systems and Decision-Oriented Perspective*, 31-41. [https://doi.org/10.1007/978-3-031-70725-4\\_2](https://doi.org/10.1007/978-3-031-70725-4_2)
- [8] Lozynskiy, V. (2023). Critical review of methods for intensifying the gas generation process in the reaction channel during underground coal gasification (UCG). *Mining of Mineral Deposits*, 17(3), 67-85. <https://doi.org/10.33271/mining17.03.067>
- [9] Saik, P., Petlevanyi, M., Lozynskiy, V., Sai, K., & Merzlikin, A. (2018). Innovative approach to the integrated use of energy resources of underground coal gasification. *Solid State Phenomena*, (277), 221-231. <https://doi.org/10.4028/www.scientific.net/SSP.277.221>
- [10] Koval, V., Kryshstal, H., Udovychenko, V., Soloviova, O., Froter, O., Kokorina, V., & Veretin, L. (2023). Review of mineral resource management in a circular economy infrastructure. *Mining of Mineral Deposits*, 17(2), 61-70. <https://doi.org/10.33271/mining17.02.061>
- [11] Abbas, Q., Yaqoob, H., Sajjad, U., Ali, H. M., & Jamil, M. M. (2025). Utilization of Local Coal in Pakistan Oil-Fired Power Plants and Future Clean Technologies for Power Generation. *Case Studies in Chemical and Environmental Engineering*, 101132. <https://doi.org/10.1016/j.cscee.2025.101132>
- [12] Keboletse, K.P., Ntuli, F., & Oladijo, O.P. (2021). Influence of coal properties on coal conversion processes-coal carbonization, carbon fiber production, gasification and liquefaction technologies: a review. *International Journal of Coal Science & Technology*, 8(5), 817-843. <https://doi.org/10.1007/s40789-020-00401-5>
- [13] Dychkovskiy, R., Falshtynskiy, V., Lozynskiy, V., & Saik, P. (2015). Development the concept of borehole underground coal gasification technology in Ukraine. *New Developments in Mining Engineering*, 91-95. <https://doi.org/10.1201/b19901-18>
- [14] Lozynskiy, V. (2024). Numerical simulation of carbonaceous raw material combustion in a coal seam channel. *Mining of Mineral Deposits*, 18(4), 109-124. <https://doi.org/10.33271/mining18.04.109>
- [15] Falshtynskiy, V., Dychkovskiy, R., Lozynskiy, V., & Saik, P. (2015). Analytical, laboratory and bench test researches of underground coal gasification technology in National Mining University. *New Developments in Mining Engineering*, 97-106. <https://doi.org/10.1201/b19901-19>
- [16] Feng, Y., Chen, J., & Luo, J. (2024). Life cycle cost analysis of power generation from underground coal gasification with carbon capture and storage (CCS) to measure the economic feasibility. *Resources Policy*, 92, 104996. <https://doi.org/10.1016/j.resourpol.2024.104996>
- [17] Wiatowski, M., Basa, W., Pankiewicz-Sperka, M., Szyja, M., Thomas, H. R., Zagorscak, R., & Kapusta, K. (2024). Experimental study on tar formation during underground coal gasification: Effect of coal rank and gasification pressure on tar yield and chemical composition. *Fuel*, 357, 130034. <https://doi.org/10.1016/j.fuel.2023.130034>
- [18] Su, F.Q., He, X.L., Dai, M.J., Yang, J.N., Hamanaka, A., Yu, Y.H., & Li, J.Y. (2023). Estimation of the cavity volume in the gasification zone for underground coal gasification under different oxygen flow conditions. *Energy*, 285, 129309. <https://doi.org/10.1016/j.energy.2023.129309>
- [19] Yin, Z., Xu, H., Chen, Y., Zhao, T., & Wu, J. (2023). Experimental simulate on hydrogen production of different coals in underground coal gasification. *International Journal of Hydrogen Energy*, 48(19), 6975-6985. <https://doi.org/10.1016/j.ijhydene.2022.03.205>
- [20] Borgulat, J., Ponikiewska, K., Jałowicki, Ł., Strugała-Wilczek, A., & Plaza, G. (2022). Are Wetlands as an Integrated Bioremediation System Applicable for the Treatment of Wastewater from Underground Coal Gasification Processes?. *Energies*, 15(12), 4419. <https://doi.org/10.3390/en15124419>
- [21] Wiatowski, M., Muzyka, R., Kapusta, K., & Chrubasik, M. (2021). Changes in properties of tar obtained during underground coal gasification process. *International Journal of Coal Science & Technology*, 8(5), 1054-1066. <https://doi.org/10.1007/s40789-021-00440-6>
- [22] Grabowski, J., Korczak, K., & Tokarz, A. (2021). Aquatic risk assessment based on the results of research on mine waters as a part of a pilot underground coal gasification process. *Process Safety and Environmental Protection*, (148), 548-558. <https://doi.org/10.1016/j.psep.2020.10.003>
- [23] Laciak, M., Kačur, J., & Durdán, M. (2022). Modeling and Control of Energy Conversion during Underground Coal Gasification Process. *Energies*, 15(7), 2494. <https://doi.org/10.3390/en15072494>
- [24] Gao, W., Zagorščak, R., & Thomas, H. R. (2022). Insights into ground response during underground coal gasification through thermo-mechanical modeling. *International Journal for Numerical and Analytical Methods in Geomechanics*, 46(1), 3-22. <https://doi.org/10.1002/nag.3287>
- [25] Kačur, J., Laciak, M., Durdán, M., & Flegner, P. (2023). Investigation of underground coal gasification in laboratory conditions: A review of recent research. *Energies*, 16(17), 6250. <https://doi.org/10.3390/en16176250>
- [26] An, N., Zagorščak, R., Thomas, H. R., & Gao, W. (2021). A numerical investigation into the environmental impact of underground coal gasification technology based on a coupled thermal-hydro-chemical model. *Journal of Cleaner Production*, (290), 125181. <https://doi.org/10.1016/j.jclepro.2020.125181>
- [27] Biswas, A. K., Islam, M. R., & Habib, M. A. (2023). An analytical investigation of critical factors to prioritize coalfields for Underground Coal Gasification–Bangladesh case. *Heliyon*, 9(7). <https://doi.org/10.1016/j.heliyon.2023.e18416>
- [28] Bazaluk, O., Lozynskiy, V., Falshtynskiy, V., Saik, P., Dychkovskiy, R., & Cabana, E. (2021). Experimental studies of the effect of design and technological solutions on the intensification of an underground coal gasification process. *Energies*, 14(14), 4369. <https://doi.org/10.3390/en14144369>
- [29] Mandal, R., & Maity, T. (2023). Operational process parameters of underground coal gasification technique and its control. *Journal of Process Control*, 129, 103031. <https://doi.org/10.1016/j.jprocont.2023.103031>
- [30] Saik, P., & Berdnyk, M. (2022). Mathematical model and methods for solving heat-transfer problem during underground coal gasification. *Mining of Mineral Deposits*, 16(2), 87-94. <https://doi.org/10.33271/mining16.02.087>
- [31] Gu, Y., Li, H., Dou, L., Wu, M., Guo, H., Huang, W., & Feng, L. (2024). Advance in detection and management for underground coal fires: A global technological overview. *Combustion Science and Technology*, 1-38. <https://doi.org/10.1080/00102202.2024.2365260>
- [32] Qin, B., Li, H., Wang, Z., Jiang, Y., Lu, D., Du, X., & Qian, Q. (2024). New framework of low-carbon city development of China: Underground space based integrated energy systems. *Underground Space*, 14, 300-318. <https://doi.org/10.1016/j.undsp.2023.06.008>
- [33] Wei, Z., Jiang, L., Chen, S., Dong, Z., Chen, Y., Liu, B., ... & Ali, S. F. (2024). Towards A hydrogen economy: Understanding pore alterations in the context of underground coal gasification. *Journal of Cleaner Production*, 484, 144325. <https://doi.org/10.1016/j.jclepro.2024.144325>
- [34] Zou, C., Chen, Y., Kong, L., Fenjin, S., Shanshan, C., & Zhen, D. (2019). Underground coal gasification and its strategic significance to the development of natural gas industry in China. *Petroleum Exploration and Development*, 46(2), 205-215. [https://doi.org/10.1016/S1876-3804\(19\)60002-9](https://doi.org/10.1016/S1876-3804(19)60002-9)
- [35] Tabachenko, M., Saik, P., Lozynskiy, V., Falshtynskiy, V., & Dychkovskiy R. (2016). Features of setting up a complex, combined and zero-waste gasifier plant. *Mining of Mineral Deposits*, 10(3), 37-45. <http://dx.doi.org/10.15407/mining10.03.037>

- [36] Pivnyak, G., Dychkovskiy, R., Bobyliov, O., Cabana, E. C., & Smoliński, A. (2018). Mathematical and Geomechanical Model in Physical and Chemical Processes of Underground Coal Gasification. *Solid State Phenomena*, (277), 1-16. <https://doi.org/10.4028/www.scientific.net/ssp.277.1>
- [37] Falshtynskiy, V., Dychkovskiy, V., Lozynskiy, V., & Saik, P. (2012). New method for justification the technological parameters of coal gasification in the test setting. *Geomechanical Processes During Underground Mining – Proceedings of the School of Underground Mining*, 201-208. <https://doi.org/10.1201/b13157-35>
- [38] Falshtynskiy, V., Dychkovskiy, R., & Iliashov, M. (2011). Engineering support of BUCG process in Solonovsk coal deposits. *Technical and Geoinformational Systems in Mining*, 47-56. <https://doi.org/10.1201/b11586>
- [39] Saik, P.B., Dychkovskiy, R.O., Lozynskiy, V.H., Malanchuk, Z.R., & Malanchuk, Ye.Z. (2016). Revisiting the underground gasification of coal reserves from contiguous seams. *Naukovyi Visnyk Natsionalnoho Hirnychoho Universytetu*, (6), 60-66.
- [40] Pivnyak, G., Falshtynskiy, V., Dychkovskiy, R., Saik, P., Lozynskiy, V., Cabana, E., & Koshka, O. (2020). Conditions of Suitability of Coal Seams for Underground Coal Gasification. *Key Engineering Materials*, (844), 38-48. <https://doi.org/10.4028/www.scientific.net/kem.844.38>
- [41] Lozynskiy V. (2025). Multi-Criteria Assessment of Coal Seams Suitability for Co-Gasification Using the Preference Selection Index. *Heliyon*. Preprint.
- [42] Stovba, S.M., & Stephenson, R.A. (1999). The Donbas Foldbelt: its relationships with the uninverted Donets segment of the Dniepr-Donets Basin, Ukraine. *Tectonophysics*, 313(1-2), 59-83. [https://doi.org/10.1016/S0040-1951\(99\)00190-0](https://doi.org/10.1016/S0040-1951(99)00190-0)
- [43] Stovba, S., Khriashchevska, O., Mazur, S., Stephenson, R., Vengrovych, D., & Drachev, S. (2024). Hydrocarbon prospects in the Dniepr-Donets Basin, Ukraine, and the Ukrainian Carpathians: an overview. *Annales Societatis Geologorum Poloniae*, 94. <https://doi.org/10.14241/asgp.2024.07>
- [44] Van Hinsbergen, D.J., Abels, H.A., Bosch, W., Boekhout, F., Kitchka, A., Hamers, M., & Stephenson, R.A. (2015). Sedimentary geology of the middle Carboniferous of the Donbas region (Dniepr-Donets basin, Ukraine). *Scientific Reports*, 5(1), 1-8. <https://doi.org/10.1038/srep09099>
- [45] Sachsenhofer, R.F., Privalov, V.A., & Panova, E.A. (2012). Basin evolution and coal geology of the Donets Basin. *International Journal of Coal Geology*, (89), 26-40. <https://doi.org/10.1016/j.coal.2011.05.002>
- [46] Haidai, O., Ruskykh, V., Ulanova, N., Prykhodko, V., Cabana, E.C., Dychkovskiy, R., & Smolinski, A. (2022). Mine Field Preparation and Coal Mining in Western Donbas: Energy Security of Ukraine – Case Study. *Energies*, 15(13), 4653. <https://doi.org/10.3390/en15134653>
- [47] Saik, P., Maksymova, E., Lozynskiy, V., Cabana, E., & Petlovanyi, M. (2021). Synergistic approach as an innovative basis for obtaining a natural gas substitute. *E3S Web of Conference*, (230), 01022. <https://doi.org/10.1051/e3sconf/202123001022>
- [48] Nehrii, S., Nehrii, T., Bachurin, L., & Piskurska, H. (2019). Problems of mining the prospective coal-bearing areas in Donbas. *E3S Web of Conferences*, (123), 01011. <https://doi.org/10.1051/e3sconf/201912301011>
- [49] Symanovych, H., Lisovytska, I., Odnovol, M., Ahaiev, R., & Poimanov, S. (2024). Rationale and modeling of technology for complex bottom-hole zone de-stressing of gas-dynamically active rock mass. *Mining of Mineral Deposits*, 18(2), 83-92. <https://doi.org/10.33271/mining18.02.083>
- [50] Sdvizhkova, Ye.A., Babets, D.V., & Smirnov, A.V. (2014). Support loading of assembly chamber in terms of Western Donbas plough longwall. *Naukovyi Visnyk Natsionalnoho Hirnychoho Universytetu*, (5), 26-32.
- [51] Law, B.E., Ulmishek, G.F., Clayton, J.L., Kabyshev, B.P., Pashova, N.T., & Krivosheya, V.A. (1998). Basin-centered gas evaluated in Dnieper-Donets basin, Donbas foldbelt, Ukraine. *Oil and Gas Journal*, 96(47), 74-78.
- [52] Bondarenko, B., Kovalevska, I., Krasnyk, V., Chernyak, V., Haidai, O., Sachko, R., & Vivcharenko, I. (2024). Methodical principles of experimental-analytical research into the influence of pre-drilled wells on the intensity of gas-dynamic phenomena manifestations. *Mining of Mineral Deposits*, 18(1), 67-81. <https://doi.org/10.33271/mining18.01.067>

## Батыс Донбасс (Украина) көмір қабаттарының көмірді жерасты газдандыруға жарамдылығының негіздемесі

В.С. Фальштинский<sup>1</sup>, Р.Е. Дичковский<sup>2</sup>, В.Г. Лозинский<sup>1\*</sup>, П.Б. Саик<sup>1</sup>, М.И. Лозинская<sup>3</sup>

<sup>1</sup>«Днепр политехникасы» ұлттық техникалық университеті, Днепр, Украина

<sup>2</sup>Краковтағы тау-кен металлургия академиясы (AGH), Краков, Польша

<sup>3</sup>«Геобит» геологиялық концерні, Хианув, Польша

\*Корреспонденция үшін автор: [lozynskiy.v.h@nmu.one](mailto:lozynskiy.v.h@nmu.one)

**Андатпа.** Мақалада көмірді жерасты газдандыру технологиясына (ПГВ) жарамды болуы мүмкін Батыс Донбасс (Украина) көмір қабаттарының учаскелері қарастырылған. Бұл технология Украинаның күрделі энергетикалық жағдайы жағдайында энергия тұтынушыларының нарығына айтарлықтай әсер етуі мүмкін. Он учаскенің тау-кен-геологиялық және тау-кен техникалық жағдайларын егжей-тегжейлі зерделеу негізінде олардың ПГВ-ға жарамдылық критерийлері бойынша оңтайлы учаске мен көмір қабатын таңдау жүзеге асырылды. Көмір қабаттарының, бүйірлік жыныстардың (шатыр, табан) құрылымдары, тектоникалық бұзылулардың орналасуы мен мөлшері, гидрогеологиялық жағдайлар, сондай-ақ көмірдің техникалық және элементтік құрамы талданады. Жүргізілген зерттеу негізінде эксперименттік жерасты газ генераторын ең дамыған инфрақұрылымы және газдандыруға жарамдылығының оңтайлы критерийлері бар аумақта орналасқан №4 учаскенің С5 көмір қабатына орналастыру ұсынылады. Зерттеудің практикалық маңыздылығы эксперименттік газ генераторының №4 пгв учаскесін пысықтау тәжірибесі кейінгі өнеркәсіптік таралым үшін технология параметрлерін түзетуге мүмкіндік береді. Учаске мен көмір қабатын таңдауға ұсынылған тәсілді тау-кен геологиялық және тау-кен техникалық жағдайлары ұқсас басқа көмір кен орындарында да тексеруге болады.

**Негізгі сөздер:** көмірді жерасты газдандыру, қабат, газ генераторы, тас көмір, кен орны.

## Обоснование пригодности угольных пластов Западного Донбасса (Украина) к подземной газификации угля

В.С. Фальштинский<sup>1</sup>, Р.Е. Дичковский<sup>2</sup>, В.Г. Лозинский<sup>1\*</sup>, П.Б. Саик<sup>1</sup>, М.И. Лозинская<sup>3</sup>

<sup>1</sup>Национальный технический университет «Днепропетровская политехника», Днепр, Украина

<sup>2</sup>Горно-Металлургическая Академия в Кракове (AGH), Краков, Польша

<sup>3</sup>Геологический концерн «Геобит», Хианув, Польша

\*Автор для корреспонденции: [lozynskiy.v.h@nmtu.one](mailto:lozynskiy.v.h@nmtu.one)

**Аннотация.** В статье рассмотрены участки угольных пластов Западного Донбасса (Украина), которые могут быть пригодны к технологии подземной газификации угля (ПГВ). Данная технология в условиях сложного энергетического положения Украины может существенно повлиять на потребительский рынок энергоносителей. На основе детального изучения горно-геологических и горнотехнических условий десяти участков по критериям их пригодности к ПГВ осуществлен выбор оптимального участка и угольного пласта. Проанализированы структуры угольных пластов, боковых пород (кровли, подошвы), расположение и размер тектонических нарушений, гидрогеологические условия, а также технический и элементный состав угля. На основе проведенного исследования установлено, что экспериментальный подземный газогенератор рекомендуется разместить на каменноугольном пласте  $C_5$  участка №4, расположенного на территории с наиболее развитой инфраструктурой и оптимальными критериями пригодности к газификации. Практическое значение исследования состоит в том, что опыт отработки участка ПГВ №4 экспериментального газогенератора позволит скорректировать параметры технологии для последующего промышленного тиражирования. Предложенный подход к выбору участка и угольного пласта может быть апробирован также на других угольных месторождениях с похожими горно-геологическими и горнотехническими условиями.

**Ключевые слова:** подземная газификация угля, пласт, газогенератор, каменный уголь, месторождение.

### Publisher's note

All claims expressed in this manuscript are solely those of the authors and do not necessarily represent those of their affiliated organizations, or those of the publisher, the editors and the reviewers.

<https://doi.org/10.51301/ejsu.2025.i1.06>

## Optimization of water resources use in agriculture of Yenbekshi-Kazakh District through artificial groundwater recharge

A.Zh. Ismagulova<sup>1\*</sup>, V.M. Mirlas<sup>2</sup>, N.A. Burshukov<sup>1</sup>

<sup>1</sup>Institute of Hydrogeology and Geoecology named after U.M. Akhmedsafin, Almaty, Kazakhstan

<sup>2</sup>Ariel University, Ariel, Israel

\*Corresponding author: [ismagulovaaida101@gmail.com](mailto:ismagulovaaida101@gmail.com)

**Abstract.** In the context of increasing water resource scarcity, the search for alternative irrigation sources has become a key factor in the sustainable development of agriculture. One of the effective solutions is the reconstruction and creation of cascades of water accumulation ponds, which significantly improve the reliability of the water reuse system. The implementation of this practice has notably enhanced irrigated farming conditions, especially during drought periods. In the villages of Baiterek, Alga, and Koishibek, the water supply issue has been largely mitigated, leading to the return of 1420 hectares of previously abandoned land to agricultural use. These lands are now actively used for growing crops, ensuring stable production. Over 300 farms now have access to a dependable irrigation water supply, which contributes to the development of the agricultural sector and reduces drought-related risks. Thus, the use of water accumulation systems demonstrates high efficiency and significance for food security and the resilience of agriculture in a changing climate.

**Keywords:** meltwater, aquifers, irrigation system, water supply system, irrigation.

Received: 21 November 2024

Accepted: 14 February 2025

Available online: 28 February 2025

### 1. Introduction

Existing uncertainties in water resource forecasts and the long-term (century-scale) accumulation of fresh water in aquifer reservoirs play an important role in setting and achieving sustainable development goals.

Climate change affects water management at all levels, including hydropower, drainage and irrigation systems, water supply, and wastewater management. This impact is primarily reflected in operational costs, which increase significantly [1]. During the transition from a planned to a market economy, investments in water management were nearly nonexistent, resulting in the deterioration of irrigation and drainage systems and the worsening of the ecological and reclamation conditions of lands [1-3]. Given the deterioration and decommissioning of these facilities, there is a risk of failing to maintain even the existing volumes of irrigated agriculture in the medium term. Rising water temperatures, combined with increased frequency of extreme weather events (such as floods and droughts), are expected to negatively impact water quality and increase contamination (e.g., higher concentrations of biogenic substances, dissolved organic carbon, pathogens, pesticides, salts, and thermal pollution), which will harm ecosystems [4] (Figures 1 and 2).

Research on water supply issues and the effective use of natural water resources has been conducted by scientists from the Institute of Hydrogeology and Geoecology of U.M. Akhmedsafin, as well as by structural units of the Ministry of

Agriculture of Kazakhstan. Technologies for using groundwater have been developed [5, 6].

The current state of irrigated agriculture and the growing water demand of rural producers highlight the need to use floodwaters, viewing them as a natural water resource for the agricultural sector. Floods in Kazakhstan are inevitable because rivers are primarily fed by precipitation. Thus, there is an urgent need to include the construction of reservoirs for river flow regulation in flood prevention measures, alongside the construction of protective ditches, dams, bypass channels, and other structures [7]. Ponds for collecting meltwater can subsequently be used for agriculture, energy production, and other industries. Additionally, extreme rainfall events, such as those that recently occurred in Astana and Atyrau, must be managed effectively. According to Deputy of the Mazhilis Andrey Begeneev, creating such lakes could significantly improve the operations of emergency services and other water-related organizations. The text was also signed by Mazhilis deputies A. Milyutin, Sh. Utemisov, N. Ashim, T. Berdongarov, Zh. Dyusengaliev, V. Kiyansky, A. Pepenin, A. Samakova, I. Umurzakov, O. Shishigina, A. Bazarbayev, M. Begentaev, A. Kozhakhmetov, E. Kappel, A. Muradov, B. Sorokin, and A. Turtaev.

Dostay Zh.D. et al. [8] clearly substantiated the priorities for ensuring the environmental safety of water bodies in transboundary basins and the foundations for interstate use of transboundary rivers based on the principles of integrated water resources management.

© 2025. A.Zh. Ismagulova, V.M. Mirlas, N.A. Burshukov

[ismagulovaaida101@gmail.com](mailto:ismagulovaaida101@gmail.com); [vladimirmster@gmail.com](mailto:vladimirmster@gmail.com); [nurbek.burshukov@gmail.com](mailto:nurbek.burshukov@gmail.com)

Engineering Journal of Satbayev University. eISSN 2959-2348. Published by Satbayev University

This is an Open Access article distributed under the terms of the Creative Commons Attribution License (<http://creativecommons.org/licenses/by/4.0/>), which permits unrestricted reuse, distribution, and reproduction in any medium, provided the original work is properly cited.

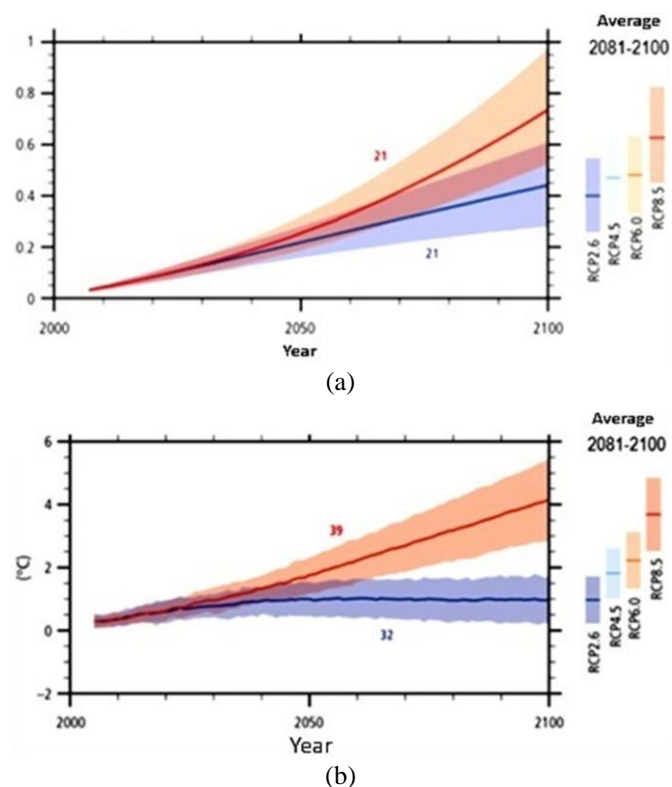


**Figure 1. Projected global climate change impacts; (a) – average change in land surface temperature (compared to 1986-2005), mean for 2081-2100; (b) – mean sea level rise (relative to the 1986-2005 period), average for 2081-2100**

Mirlash V.M. and Ismagulova argue that water scarcity in southeastern Kazakhstan, exacerbated by long distances from high-quality natural water sources, necessitates the combined use of surface and groundwater from local aquifers for irrigation, pasture watering, and decentralized drinking water supply for small rural settlements [9]. In arid conditions, this is the only way to prevent groundwater depletion, increase its storage capacity, and expand its natural filtration area. This approach ensures the availability of drinking water for the population [10-13].

## 2. Materials and methods

The natural and climatic conditions, terrain, and availability of temporary and floodwater sources in the lower parts of alluvial fans and the gently sloping erosion-denudation foothill plains of the arable lands in the Baiterek rural district enable the creation of a cascade of seasonal regulation reservoirs and offer vast prospects for their use as a primary source of irrigation. To address the main objective of the research program, extensive work has been carried out over the past several years to develop and subsequently implement the efficient utilization of local runoff and groundwater. Depending on soil, hydrological conditions, and terrain, seasonal regulation reservoirs are established to optimize water storage and use.

As a result of the project implementation, the reconstruction of the distribution irrigation canal was carried out, along with the repair of two seasonal regulation reservoirs. A unique cascade of seasonal regulation reservoirs was created, utilizing local temporary and floodwater sources.

The irrigation system incorporating accumulation ponds consists of distribution canals that follow the land's natural slope and flow into artificially created accumulation ponds. Once the water in these ponds has warmed and reached favorable irrigation conditions, it is directed into irrigation canals for watering crops. Any unused irrigation water is transported via canals to the next accumulation pond.

All irrigation canals are equipped with retention and regulation structures at their downstream ends, while the outflows of the seasonal regulation reservoirs are fitted with level regulators for the lower reach. Thus, the irrigation system ensures favorable conditions for plant growth during watering by incorporating seasonal regulation reservoirs and enables more efficient use of irrigation water through the structure of the irrigation system.

At the same time, the project tested innovative designs of sluice gates and spillways, which demonstrated positive results in water accounting and the prevention of vandalism by the local population.

The simplicity, durability, low cost, short production time, and guaranteed reliability of the proposed innovative sluice gate-featuring a manually operated movable spillway with an anti-vandal mechanism-allowed its successful implementation not only in this project but also in all hydro-melioration systems of the Yenbekshi-Kazakh district. It has been recommended for adoption in other regions of Kazakhstan.

In this regard, hydrological posts and hydrogeological wells have been installed at the site to study the quality and determine the suitability of accumulated irrigation water for cultivated agricultural crops, as well as the groundwater formed due to the backwater effect caused by infiltration between the seasonal regulation reservoirs.

During the project implementation and subsequently during the operation of the seasonal regulation reservoirs and the use of irrigated lands, regular ecological monitoring has been and will continue to be conducted to assess the hydrological regime of the local river flow and the quality of accumulated water sources-including meltwater, rainwater, floodwater, and emerging perched groundwater. The latter forms in higher-elevation areas of the terrain and is used by peasant and farming enterprises for irrigating cultivated agricultural crops.

To obtain initially crucial indicators of the quality of water accumulated in seasonal regulation reservoirs and groundwater for its subsequent use in irrigating cultivated agricultural crops, water samples were collected and analyzed in the accredited laboratory of Satbayev University.

To ensure a comprehensive assessment of irrigation water quality, we applied agronomic, technical, and environmental criteria [14-21].

Due to the absence of unified approved standards, the suitability of water for irrigation was determined based on its chemical analysis using irrigation coefficients, which were calculated by various methods (Table 1).

Internationally, the assessment of irrigation water for the risk of soil alkalization is conducted based on the calculation of the Sodium Adsorption Ratio (SAR, Table 1). This method is based on the principle that when sodium concentration exceeds that of divalent cations, there is a risk of sodium displacing calcium from the soil's exchange complex, replacing it with sodium. As a result, soil alkalization may occur, leading to a sharp deterioration in its water-physical properties.

**Table 1. Formulas for calculating irrigation coefficients**

Author	Calculation Formula
H. Stabler	$K_a = \frac{288}{5rCl^-}, \text{ at } rNa^+ < rCl^-$
	$K_a = \frac{288}{rNa^+ + 4rCl^-},$ at $rCl^- + rSO_4^{2-} > rNa^+ > rCl^-$
	$K_a = \frac{288}{10rNa^+ - 5rCl^- - 9rSO_4^{2-}},$ at $rNa^+ > rCl^- + rSO_4^{2-}$
A.M. Mozheyko, T.K. Vorotnik	$K_a = \frac{(rNa^+ + rK^+) \cdot 100\%}{rCa^{2+} + rMg^{2+} + rNa^+ + rK^+}$
I.N. Antipov-Karataev, G.M. Kader	$K_a = \frac{rCa^{2+} + rMg^{2+}}{rNa^+ + 0.238\sum u}$
M.F. Budanov	$K_2 = \frac{rNa^+}{rCa^{2+} + rMg^{2+}},$
	$K_3 = \frac{r\sum u}{rCa^{2+} + rMg^{2+}}$
SAR	$SAR = \frac{rNa^+}{\sqrt{\frac{rCa^2 rMg^{2+}}{2}}}$

**3. Results and discussion**

As part of the key objective of the project-focused on organizing, testing, and adapting a model site for water recycling systems under conditions of increasing river water shortages – the reconstruction and modernization of the on-farm irrigation network and two reservoirs were carried out in the Baiterek rural district of the Yenbekshi-Kazakh district in the Almaty region. This made it possible to create a unique cascade of seasonal regulation reservoirs that utilize local temporary and floodwater sources.

1. Seasonal regulation reservoir «Saimasay-1». Saimasay-1 seasonal regulation reservoir, located in the Almaty Region, Enbekshikazakh District, Baiterek Rural District, PC SPC "Margulan" (coordinates: 43°26'31" N, 77°16'42" E) (Table 2).

**Table 2. Technical specifications of the «Saimasay-1» storage pond before and after reconstruction and modernization**

Parameter	Saimasay-1 (before)	Saimasay-1 (after)	Change
Normal water level (NWL), m	635.0	637.0	+2.0
Maximum water level (MWL), m	635.5	637.5	+2.0
Total storage capacity, Mm <sup>3</sup>	0.912	1.482	+0.57
Usable storage capacity, Mm <sup>3</sup>	0.571	1.026	+0.455
Water surface area, ha	6.54	8.50	+1.96
Length, m	600	600	-
Width, m	380	380	-
Maximum depth, m	5.40	7.40	+2.0
Dam height, m	7.2	9.0	+2.0
Dam crest width, m	5.5	7.5	+2.0
Dam base width, m	8.5	12.5	+4.0

The dam height was increased to 9.0 m, and the crest width was expanded to 7.5 m. The normal water level (NWL) was set at an absolute elevation of 635.0 m, compared to the initial level of 637.0 m; the maximum flood level (MFL) was adjusted to 637.5 m from the previous 635.5 m.

The total storage capacity increased by +0.57 million m<sup>3</sup>, reaching 1.482 million m<sup>3</sup> (previously 0.912 million m<sup>3</sup>). The usable storage capacity improved by +0.455 million m<sup>3</sup>, reaching 1.026 million m<sup>3</sup>, compared to the previous average of 0.571 million m<sup>3</sup>.

The surface area of open water at the usable storage capacity expanded to 8.50 ha, an increase of +1.96 ha from the previous 6.54 ha. The serviced area increased from 2,433 ha to 3,503 ha, enabling the establishment of approximately 50 to 75 new farming enterprises by utilizing previously abandoned irrigated croplands.

2. Seasonal regulation reservoir "Saimasai-3"

The completed set of maintenance and operational works at the Saimasay-3 seasonal regulation reservoir has enhanced the dam, basin, and hydraulic structures to meet the requirements for optimizing water availability for existing irrigated lands. Additionally, it has facilitated the reclamation of at least 350 hectares of previously abandoned arable land for agricultural use.

The dam height has been increased to 3.5 meters, and the dam crest width has been extended to 5.0 meters. At this width, the crest of the dam will rise above both the normal water level (NWL) and the maximum water level (MWL). The dam slope steepness during its expansion, considering the physical and mechanical properties of the soil, the impact of self-weight, water influence, seismic and dynamic effects, as well as external loads on the crest and slopes, was set as follows: upstream (wet): 2.50, downstream (dry): 1.75 (Figure 3).

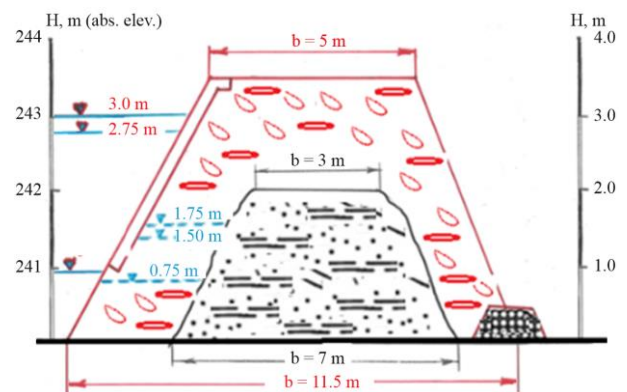


**Figure 3. Schematic nomogram of the longitudinal profile of the averaged parameters of the dam of the Sai-Masai-3 seasonal regulation reservoir before and after the completed work**

Saimasai-3 seasonal regulation reservoir, located in the Almaty Region, Enbekshikazakh District, Baiterek Rural District, PC "SPK Margulan" (coordinates: 43°27'40.8" N, 77°11'22.0" E), at an absolute elevation of 622 m (Table 3).

The Normal Water Level (NWL) was set at an absolute elevation of 621.0 m, compared to the initial level of 619.8 m. The Maximum Water Level (MWL) was adjusted to 621.5 m from the previous 620.2 m. The Dead Storage Level remains unchanged at 618.0 m.

**Table 3. Technical characteristics of the «Saimasai-3» seasonal regulation reservoir before and after reconstruction and modernization**

Parameter	Saimasai-1 (before)	Saimasai-1 (after)	Change
Normal water level (NWL), m	619.8	621.0	+1.2
Maximum water level (MWL), m	620.2	621.5	+1.3
Total storage capacity, Mm <sup>3</sup>	0.183	0.345	+0.162
Usable storage capacity, Mm <sup>3</sup>	0.153	0.305	+0.152
Water surface area, ha	7.35	11.42	+4.07
Serviced area, ha	962.9	1320	+357.1
Length, m	500	510	+10
Width, m	105	120	+15
Maximum depth, m	2.80	4.30	+1.5
Dam height, m	2.0	3.5	+1.5
Dam crest width, m	3.5	5.0	+1.5
Dam base width, m	7.0	11.5	+4.5

Total reservoir capacity increased by 0.162 million m<sup>3</sup>, reaching 0.345 million m<sup>3</sup> (previously 0.183 million m<sup>3</sup>). Usable capacity increased by 0.152 million m<sup>3</sup>, reaching 0.305 million m<sup>3</sup>, compared to the previous average value of 0.153 million m<sup>3</sup>.

Water surface area at full usable capacity reached 11.40 ha, which is 4.05 ha more than before (7.35 ha). Irrigated area expanded from 962.9 ha to 1320 ha, enabling the potential creation of 25-30 new farming households, utilizing previously abandoned irrigated cropland.

The social impact lies in improving the social environment and enhancing the quality of life of the population. This is reflected in indicators such as the rise in educational levels due to participation in the development and implementation of new technologies in irrigated agriculture in one of the major administrative districts of Almaty Region, Republic of Kazakhstan.

The primary beneficiaries involved in the research and implementation activities were members of local rural communities, as well as farmers and agricultural enterprises. On pilot and experimental sites, local community members took an active role in implementing the very technology of water reuse systems.

In the future, the ongoing efforts to establish water reuse systems will continue, with the formation of a management and coordination council involving farmers, local elders and aksakals, representatives of local akimats, and other stakeholders.

The work and training conducted during the project have increased awareness and self-consciousness within the local community. This has fostered greater engagement among community members in adopting water reuse systems, artificial aquifer technologies, and the reuse of drainage and discharge water.

#### 4. Conclusions

It is proposed to implement the most efficient integrated use of local runoff and groundwater, where seasonal regulation reservoirs are created based on soil, hydrological conditions, and terrain features. Additionally, agrotechnical measures are applied to retain local runoff directly in the fields.

The establishment of seasonal regulation reservoirs for more effective utilization of flood runoff is both economically viable and environmentally acceptable. The project has enabled the development of irrigated agriculture in areas distant from irrigation systems.

Repair and restoration work on seasonal regulation reservoirs, including the replacement of individual structural components and bringing parameters to their design forms and dimensions, will significantly extend the standard service life of water management and hydraulic structures. This will provide a 100% guarantee of accumulating the required water volume and subsequently ensuring irrigation water supply for an area of 1,400 hectares, including 350 hectares of previously unused arable land.

The utilization of local river runoff including meltwater, rainwater, floodwaters, and emerging groundwater (perched water) formed in higher-altitude areas through accumulation in seasonal regulation reservoirs for irrigation will lead to a sharp reduction and significant conservation of scarce water resources by 45-50%.

Thus, each water user will be provided with information on the quality of the water used and its compliance with national irrigation standards.

#### Author contributions

Conceptualization: A.Zh.I., V.M.M.; Data curation: A.Zh.I., N.A.B.; Formal analysis: A.Zh.I., V.M.M., N.A.B.; Funding acquisition: A.Zh.I.; Investigation: A.Zh.I.; Methodology: A.Zh.I., V.M.M.; Project administration: A.Zh.I., V.M.M.; Resources: A.Zh.I., V.M.M.; Software: A.Zh.I., N.A.B.; Supervision: A.Zh.I.; Validation: A.Zh.I.; Visualization: A.Zh.I., N.A.B.; Writing – original draft: A.Zh.I.; Writing – review & editing: V.M.M., N.A.B. All authors have read and agreed to the published version of the manuscript.

#### Funding

This research received no external funding.

#### Conflicts of interests

The authors declare no conflict of interest.

#### Data availability statement

The original contributions presented in this study are included in the article. Further inquiries can be directed to the corresponding author.

#### References

- [1] UN. (2009). *Water Resources and Climate Compliance Guidelines*; UN: New York, NY, USA; Geneva, Switzerland. Retrieved from: <https://www.un.org/water>
- [2] Central research institute for complex use of water resources. (2017). *Proceedings of the V-th International Water Forum*, Minsk, Belarus, Water Resources and Climate. Retrieved from: <http://www.cricuwr.by/>
- [3] UN. (2020). *Water Resources and Climate Change*. In UN World Water Development Report, Water Management of Kazakhstan. Retrieved from: <https://www.unesco.org/reports/wwdr>
- [4] Republican State Enterprise «Kazhydromet». (2023). *Review of Climate Features in Kazakhstan*; Astana, Kazakhstan. Retrieved from: <https://www.kazhydromet.kz/>
- [5] Institute of Hydrogeology and Geoecology named after U.M. Akhmedsafin. (2023). *Groundwater Resources as the Main Reserve of Irrigated Agriculture in Kazakhstan*. Almaty, Kazakhstan
- [6] Shakibaev, I.I. (2014). *Hydrogeological and Meliorative Aspects of the Problems of Irrigated Lands in the South of Kazakhstan*. LLP Kontur, Almaty, Kazakhstan

- [7] Reports for 2016–2023. Regional Hydrogeological and Meliorative Center of the Ministry of Agriculture of the Republic of Kazakhstan.
- [8] Mirlas, V., Kulagin, V., Ismagulova, A. & Anker, Y. (2022). MODFLOW and HYDRUS Modeling of Groundwater Supply Prospect Assessment for Distant Pastures in the Aksu River Middle Reaches. *Sustainability*, 14(24), 16783. <https://doi.org/10.3390/su142416783>
- [9] Mirlas, V., Kulagin, V., Ismagulova, A. & Anker, Y. (2022). Field Experimental Study on the Infiltration and Clogging Processes at Aksu Research Site, Kazakhstan. *Sustainability*, 14(23), 15645. <https://doi.org/10.3390/su142315645>
- [10] Ali, M. & Talukder, M.S.U. (2008). Increasing Water Productivity in Crop Production – A Synthesis. *Agricultural Water Management*, 95(11), 1201–1213. <https://doi.org/10.1016/j.agwat.2008.06.008>
- [11] Absametov, M.K. (2020). Rational Use and Protection of Groundwater in the Republic of Kazakhstan in the Context of Climatic and Anthropogenic Changes. *Almaty, Kazakhstan*
- [12] Absametov, M.K., Mukhamedzhanov, M.A., Sydykov, Z.S. & Murtazin, E.Z. (2017). Groundwater of Kazakhstan – A Strategic Resource for Water Security of the Country. *Almaty, Kazakhstan*
- [13] Dostai, Z.D., Romanova, S.M. & Tursunov, E.A. (2012). Quality of Surface Waters of Kazakhstan and Issues of International Water Allocation. In River Runoff Resources of Kazakhstan. *Almaty, Kazakhstan*
- [14] Ismagulova, A. & Mirlas, V. (2019). Study of Hydrodynamics of Infiltration and Colmatation Processes in Daily Regulation Basins During Artificial Replenishment of Groundwater Reserves. *News of the National Academy of Sciences of the Republic of Kazakhstan. Series of geology and technology sciences*, 3(435), 85–95. <https://doi.org/10.32014/2019.2518-170X.72>
- [15] Ibatullin, S.R., Balgabaev, N.N., Kalashnikov, A.A. & Kvan, R.A. (2012). Irrigation of Kazakhstan: Management and Water Conservation. Book 1: Complex of Measures for Management and Rational Use of Water Resources in Irrigated Agriculture. *Almaty, Kazakhstan*

## Жер асты суларын жасанды түрде толықтыру арқылы Еңбекші-Қазақ ауданының ауыл шаруашылығында су ресурстарын пайдалануды оңтайландыру

А.Ж. Исмагулова<sup>1\*</sup>, В.М. Мирлас<sup>2</sup>, Н.А. Буршуков<sup>1</sup>

<sup>1</sup>У.М.Ахмедсафин атындағы Гидрогеология және геоэкология институты, Алматы, Қазақстан

<sup>2</sup>Ариэль университеті, Ариэль, Израиль

\*Корреспонденция үшін автор: [ismagulovaaida101@gmail.com](mailto:ismagulovaaida101@gmail.com)

**Андатпа.** Су тапшылығының күшеюі жағдайында балама суару көздерін іздеу ауыл шаруашылығын тұрақты дамытудың негізгі факторына айналуға тиімді шешімдердің бірі суды қайта өңдеу жүйесінің сенімділігін айтарлықтай арттыруға мүмкіндік беретін су қоймаларының каскадтарын қайта құру және құру болып табылады. Осы тәжірибені енгізу нәтижесінде әсіресе құрғақшылық кезеңдерінде суармалы егіншіліктің жағдайы айтарлықтай жақсарды. Бәйте-рек, Алға және Қойшыбек ауылдарында сумен қамту мәселесі іс жүзінде шешіліп, бұрын қараусыз қалған 1420 гектар жер ауыл шаруашылығы айналымына қайтарылды. Бұл аумақтар тұрақты өнім өндіруді қамтамасыз ететін ауыл шаруашылығы дақылдарын өсіру үшін белсенді түрде пайдаланылады. 300-ден астам шаруа қожалығы суармалы судың сенімді көзіне қол жеткізді, бұл ауыл шаруашылығы саласының дамуына ықпал етіп, құрғақшылыққа байланысты тәуекелдерді азайтады. Осылайша, су сақтау жүйелерін пайдалану азық-түлік қауіпсіздігін қамтамасыз ету және өзгермелі климат жағдайында ауыл шаруашылығының тұрақтылығын арттыру үшін жоғары тиімділік пен маңыздылықты көрсетеді.

**Негізгі сөздер:** еріген сулар, сулы горизонттар, суару жүйесі, сумен жабдықтау жүйесі, суару.

## Оптимизация использования водных ресурсов в сельском хозяйстве Еңбекши-Казахского района посредством искусственного восполнения подземных вод

А.Ж. Исмагулова<sup>1\*</sup>, В.М. Мирлас<sup>2</sup>, Н.А. Буршуков<sup>1</sup>

<sup>1</sup>Институт гидрогеологии и геоэкологии имени У.М.Ахмедсафина, Алматы, Казахстан

<sup>2</sup>Университет Ариэль, Ариэль, Израиль

\*Автор для корреспонденции: [ismagulovaaida101@gmail.com](mailto:ismagulovaaida101@gmail.com)

**Аннотация.** In the context of increasing water shortages, the search for alternative irrigation sources is becoming a key factor in the sustainable development of agriculture. One effective solution is the reconstruction and creation of cascades of water storage ponds, which can significantly increase the reliability of the recycling water use system. As a result of the implementation of this practice, the conditions of irrigated agriculture have significantly improved, especially during dry periods.

In the villages of Baiterek, Alga and Koyshibek, it was possible to practically solve the water supply problem, which led to the return of 1420 hectares of previously abandoned land to agricultural circulation. These territories are actively used for growing crops, ensuring stable production. More than 300 farms have gained access to a reliable source of irrigation water, which contributes to the development of the agricultural sector and reduces the risks associated with droughts. Thus, the use of water storage systems demonstrates high efficiency and importance for ensuring food security and increasing the sustainability of agriculture in a changing climate.

**Ключевые слова:** талые воды, водоносные горизонты, оросительная система, система водоснабжения, ирригация.

#### **Publisher's note**

All claims expressed in this manuscript are solely those of the authors and do not necessarily represent those of their affiliated organizations, or those of the publisher, the editors and the reviewers.

## CONTENTS

<i>Sarsembekov T.K., Chepushtanova T.A., Merkibayev E.S.</i> ECONOMIC ANALYSIS OF THE PROCESSING OF VARIOUS TITANIUM-CONTAINING RAW MATERIALS TO OBTAIN TITANIUM, VANADIUM, AND NIOBIUM.....	1
<i>Kenzhaliyev B.K., Ultarakova A.A., Lokhova N.G., Kassymzhanov K.K., Mukangaliyeva A.O.</i> PRODUCTION OF IRON OXIDE PIGMENT FROM THE METALLIC COMPONENT OF ILMENITE SMELTING.....	8
<i>Myrzakhan A., Korosteleva E., G. Smailova, A. Uderbaeva</i> INVESTIGATION OF SELF-PROPAGATING HIGH-TEMPERATURE SYNTHESIS BASED ON TiB+Ti COMPOSITE POWDERS.....	16
<i>Alzhigitova M.M., Zapparov M.R., Auelkhan E.S., Kuldeyeva E.M.</i> INVESTIGATION OF THE PHYSICO-MECHANICAL PROPERTIES OF COHESIVE SOILS IN DELUVIAL-PROLUVIAL (QII-III) AND ALLUVIAL (QIII-IV) DEPOSITS OF THE ALAKOL DEPRESSION.....	24
<i>Falshtynskiy V.S., Dychkovskiy R.O., Lozynskiy V.H., Saik P.B., Lozynska M.I.</i> SUBSTANTIATING APPLICABILITY OF WESTERN DONBAS COAL SEAMS (UKRAINE) FOR UNDERGROUND COAL GASIFICATION.....	31
<i>Ismagulova A.Zh., Mirlas V.M., Burshukov N.A.</i> OPTIMIZATION OF WATER RESOURCES USE IN AGRICULTURE OF YENBEKSHI- KAZAKH DISTRICT THROUGH ARTIFICIAL GROUNDWATER RECHARGE.....	43

## МАЗМҰНЫ

<i>Сарсембеков Т.К., Чепуштанова Т.А., Меркибаев Е.С.</i> ТИТАН, ВАНАДИЙ ЖӘНЕ НИОБИЙ АЛУ АРҚЫЛЫ ҚҰРАМЫНДА ТИТАН БАР ӘР ТҮРЛІ ШИКІЗАТТЫ ӨНДЕУДІҢ ЭКОНОМИКАЛЫҚ ТАЛДАУЫ.....	1
<i>Кенжалиев Б.К., Ультаракова А.А., Лохова Н.Г., Касымжанов К.К., Мұқанғалиева А.Ө.</i> ИЛЬМЕНИТ БАЛҚЫМАСЫНЫҢ МЕТАЛЛ ҚҰРАМДАС БӨЛГІНЕН ТЕМІР ОКСИДТІ ПИГМЕНТ АЛУ.....	8
<i>Мырзахан А., Коростелева Е., Смаилова Г., Удербаева А.</i> TiB+Ti КОМПОЗИЦИЯЛЫҚ ҰНТАҚТАРЫНА НЕГІЗДЕЛГЕН ӨЗДІГІНЕН ТАРАЛАТЫН ЖОҒАРЫ ТЕМПЕРАТУРАЛЫ СИНТЕЗДІ ЗЕРТТЕУ.....	16
<i>Альжигитова М.М., Заппаров М.Р., Әуелхан Е.С., Кульдеева Е.М.</i> АЛАКӨЛ ОЙПАТЫНЫҢ ДЕЛЮВИАЛДЫ-ПРОЛЮВИАЛДЫ (QII-III) ЖӘНЕ АЛЛЮВИАЛДЫ (QIII-IV) ШӨГІНДІЛЕР КЕШЕНДЕРІНІҢ БАЙЛАНЫСҚАН ТОПЫРАҚТАРЫНЫҢ ФИЗИКА-МЕХАНИКАЛЫҚ ҚАСИЕТТЕРІН ЗЕРТТЕУ.....	24
<i>Фальштинский В.С., Дичковский Р.Е., Лозинский В.Г., Саик П.Б., Лозинская М.И.</i> БАТЫС ДОНБАСС (УКРАИНА) КӨМІР ҚАБАТТАРЫНЫҢ КӨМІРДІ ЖЕРАСТЫ ГАЗДАНДЫРУҒА ЖАРАМДЫЛЫҒЫНЫҢ НЕГІЗДЕМЕСІ.....	31
<i>Исмагулова А.Ж., Мирлас В.М., Буришуков Н.А.</i> ЖЕР АСТЫ СУЛАРЫН ЖАСАНДЫ ТҮРДЕ ТОЛЫҚТЫРУ АРҚЫЛЫ ЕҢБЕКШІ-ҚАЗАҚ АУДАНЫНЫҢ АУЫЛ ШАРУАШЫЛЫҒЫНДА СУ РЕСУРСТАРЫН ПАЙДАЛАНУДЫ ОҢТАЙЛАНДЫРУ.....	43

## СОДЕРЖАНИЕ

<i>Сарсембеков Т.К., Чепуштанова Т.А., Меркибаев Е.С.</i> ЭКОНОМИЧЕСКИЙ АНАЛИЗ ПЕРЕРАБОТКИ РАЗЛИЧНОГО ТИТАНСОДЕРЖАЩЕГО СЫРЬЯ С ПОЛУЧЕНИЕМ ТИТАНА, ВАНАДИЯ И НИОБИЯ.....	1
<i>Кенжалиев Б.К., Ультаракова А.А., Лохова Н.Г., Касымжанов К.К., Мукангалиева А.О.</i> ПОЛУЧЕНИЕ ЖЕЛЕЗООКСИДНОГО ПИГМЕНТА ИЗ МЕТАЛЛИЧЕСКОЙ СОСТАВЛЯЮЩЕЙ ПЛАВКИ ИЛЬМЕНИТА.....	8
<i>Мырзахан А., Коростелева Е., Смаилова Г., Удербаета А.</i> ИССЛЕДОВАНИЕ САМОРАСПРОСТРАНЯЮЩЕГОСЯ ВЫСОКОТЕМПЕРАТУРНОГО СИНТЕЗА НА ОСНОВЕ КОМПОЗИЦИОННЫХ ПОРОШКОВ TiV+Ti.....	16
<i>Альжигитова М.М., Заптаров М.Р., Ауелхан Е.С., Кульдеева Е.М.</i> ИЗУЧЕНИЕ ФИЗИКО-МЕХАНИЧЕСКИХ СВОЙСТВ СВЯЗНЫХ ГРУНТОВ КОМПЛЕКСОВ ДЕЛЮВИАЛЬНО-ПРОЛЮВИАЛЬНЫХ (Q <sub>II-III</sub> ) И АЛЛЮВИАЛЬНЫХ (Q <sub>III-IV</sub> ) ОТЛОЖЕНИЙ АЛАКОЛЬСКОЙ ВПАДИНЫ.....	24
<i>Фальшитинский В.С., Дичковский Р.Е., Лозинский В.Г., Саик П.Б., Лозинская М.И.</i> ОБОСНОВАНИЕ ПРИГОДНОСТИ УГОЛЬНЫХ ПЛАСТОВ ЗАПАДНОГО ДОНБАССА (УКРАИНА) К ПОДЗЕМНОЙ ГАЗИФИКАЦИИ УГЛЯ.....	31
<i>Исмагулова А.Ж., Мирлас В.М., Буриуков Н.А.</i> ОПТИМИЗАЦИЯ ИСПОЛЬЗОВАНИЯ ВОДНЫХ РЕСУРСОВ В СЕЛЬСКОМ ХОЗЯЙСТВЕ ЕНБЕКШИ-КАЗАХСКОГО РАЙОНА ПОСРЕДСТВОМ ИСКУССТВЕННОГО ВОСПОЛНЕНИЯ ПОДЗЕМНЫХ ВОД.....	43

***Учредитель:*** Satbayev University

***Регистрация:***

Министерство информации и общественного развития Республики Казахстан  
№ KZ19VPY00056529 от 30.09.2022

**Официальный сайт:** <https://vestnik.satbayev.university/index.php/journal/>

**Основан в августе 1994 г. Выходит 6 раз в год**

***Адрес редакции:***

г. Алматы, ул. Сатпаева,  
22 тел.: 292-63-46